

Title: The PAMELA excess in the light of cosmic ray propagation

Date: Jun 11, 2009 02:00 PM

URL: <http://pirsa.org/09060037>

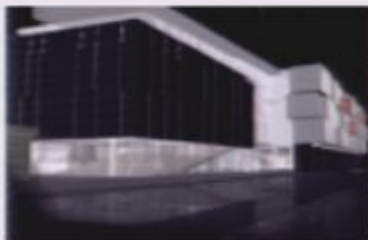
Abstract: The positron excess measured by PAMELA may be the long waited hint of the presence of dark matter particles in the Milky Way halo. But before we rejoice, we need to examine the other Possible astrophysical explanations. Whatever the sources -- DM or conventional -- a crucial ingredient is the transport of cosmic rays in the magnetic fields of the Galaxy to which I will pay particular attention in this presentation.

The PAMELA excess & cosmic ray propagation

Pierre Salati – Université de Savoie & LAPTH

The Menu

- 1) Cosmic ray propagation in the Milky Way
- 2) Antiprotons or the revenge of orthodoxy
- 3) Secondary positron uncertainties
- 4) Astrophysical explanations of the PAMELA excess



The PAMELA excess & cosmic ray propagation

Pierre Salati – Université de Savoie & LAPTH

The Menu

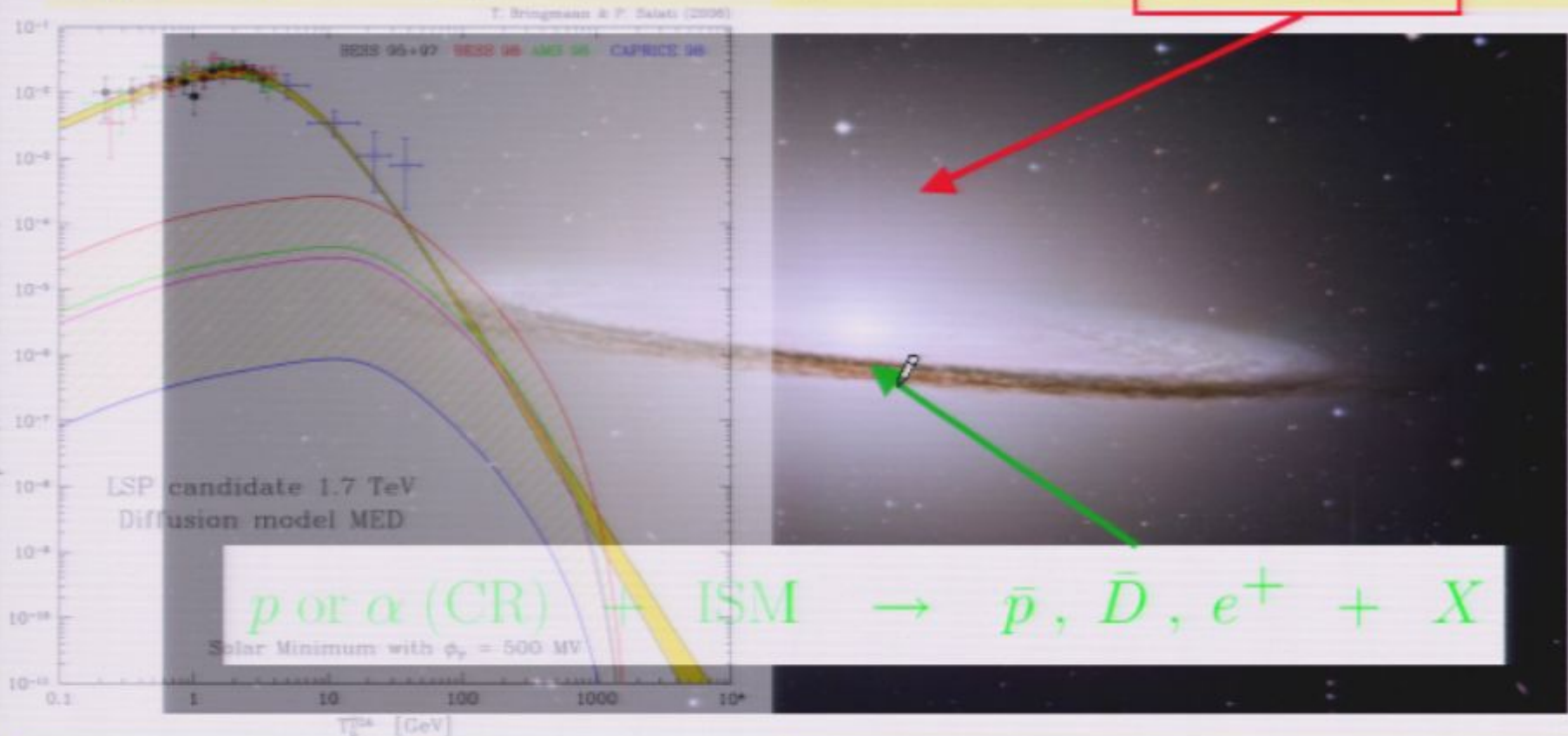
- 1) Cosmic ray propagation in the Milky Way
- 2) Antiprotons or the revenge of orthodoxy
- 3) Secondary positron uncertainties
- 4) Astrophysical explanations of the PAMELA excess



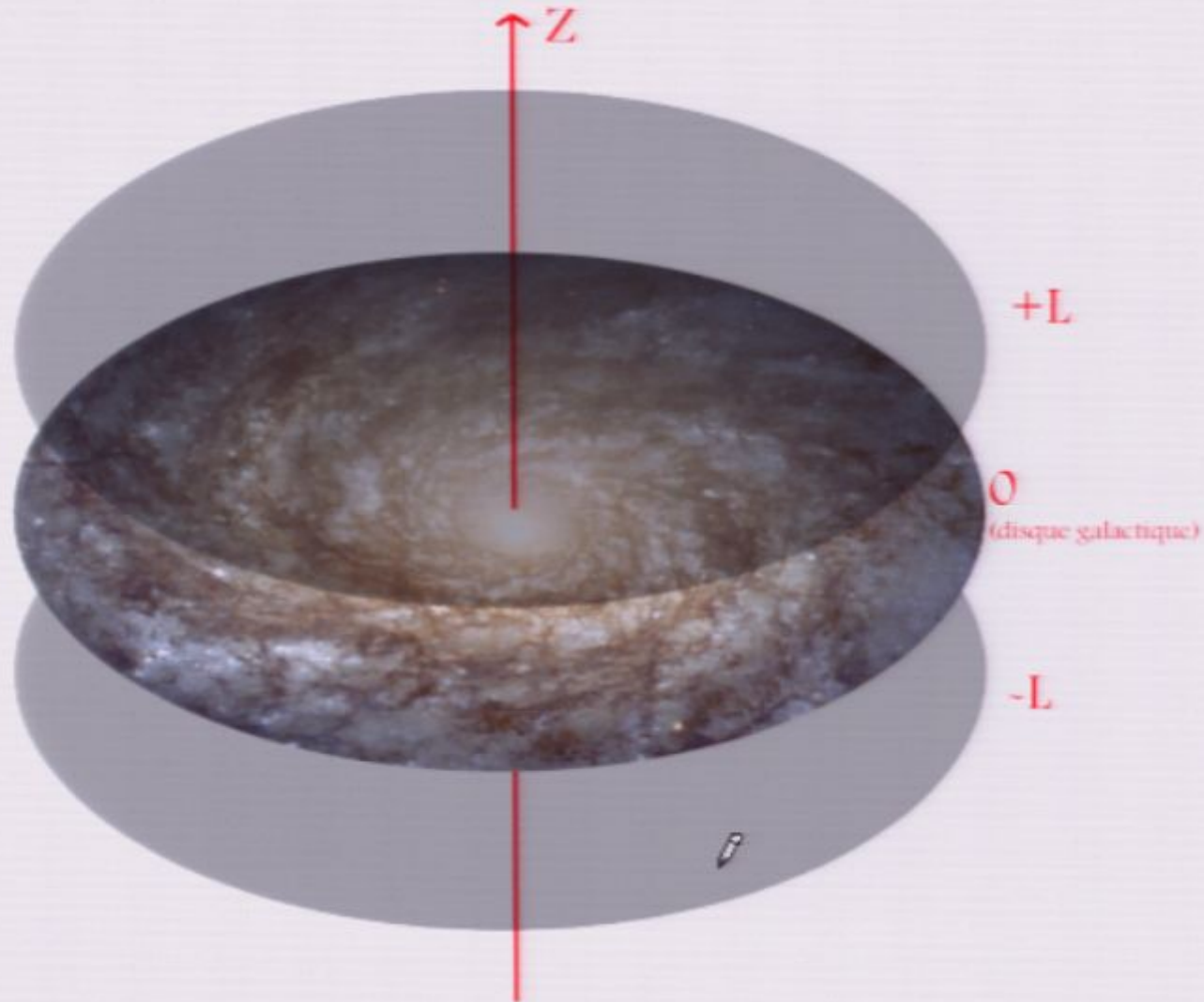
Indirect signatures of DM species

Weakly Interacting Massive particles – WIMPs – may be the major component of the haloes of galaxies. Their mutual annihilations would produce an indirect signature of high-energy cosmic rays :

$$\chi + \chi \rightarrow q\bar{q}, W^+W^-, \dots \rightarrow \gamma, \bar{p}, \bar{D}, e^+ \text{ \& } \nu's$$



1) Cosmic ray propagation in the Milky Way



Transport of Cosmic Rays in Chaotic Magnetic Fields

F. Casse, M. Lemoine & G. Pelletier, PRD **D65** (2002) 023002

Magnetic turbulence $\delta\mathbf{B}(\mathbf{x}) = \int \frac{d\mathbf{k}}{(2\pi)^3} e^{-i\mathbf{k}\cdot\mathbf{x}} \delta\mathbf{B}(\mathbf{k})$ whose power spectrum is defined by

$$\langle \delta\mathbf{B}(\mathbf{k}) \delta\mathbf{B}^\dagger(\mathbf{k}') \rangle = (2\pi)^3 \delta(\mathbf{k} - \mathbf{k}') S_{3d}(\mathbf{k})$$

and follows between k_{\min} and k_{\max} the power law

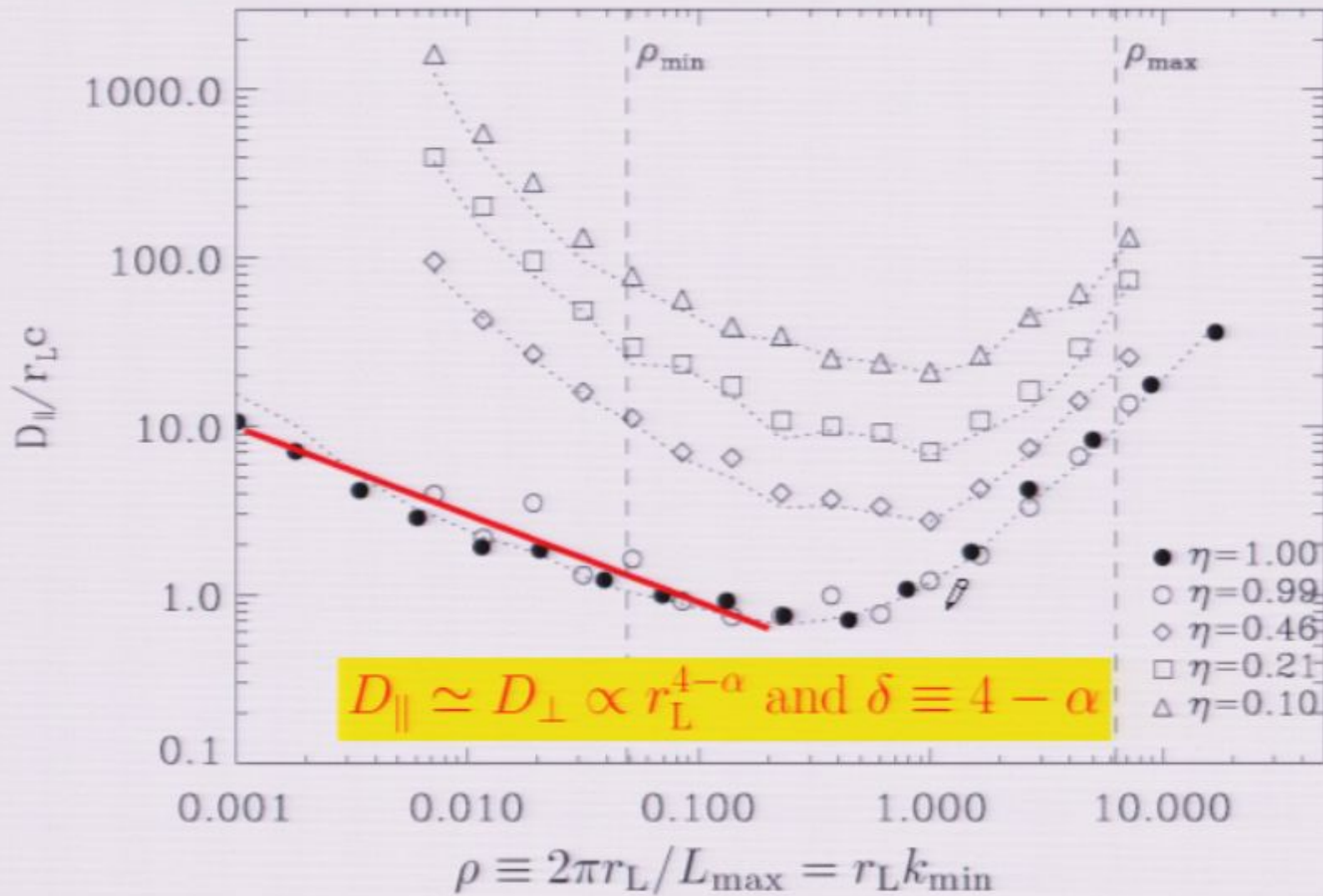
$$S_{3d}(\mathbf{k}) \propto k^{-\alpha}$$

The level of turbulence wrt to the homogeneous field \mathbf{B}_0 is defined by

$$\eta = \frac{\langle \delta\mathbf{B}^2 \rangle}{\mathbf{B}_0^2 + \langle \delta\mathbf{B}^2 \rangle}$$

Transport of Cosmic Rays in Chaotic Magnetic Fields

F. Casse, M. Lemoine & G. Pelletier, PRD **65** (2002) 023002



$\delta = 1/3$ (Kolmogorov) or $\delta = 1/2$ (Iroshnikov, Kraichnan)

Transport of Cosmic Rays in Chaotic Magnetic Fields

F. Casse, M. Lemoine & G. Pelletier, PRD **D65** (2002) 023002

Magnetic turbulence $\delta\mathbf{B}(\mathbf{x}) = \int \frac{d\mathbf{k}}{(2\pi)^3} e^{-i\mathbf{k}\cdot\mathbf{x}} \delta\mathbf{B}(\mathbf{k})$ whose power spectrum is defined by

$$\langle \delta\mathbf{B}(\mathbf{k}) \delta\mathbf{B}^\dagger(\mathbf{k}') \rangle = (2\pi)^3 \delta(\mathbf{k} - \mathbf{k}') S_{3d}(\mathbf{k})$$

and follows between k_{\min} and k_{\max} the power law

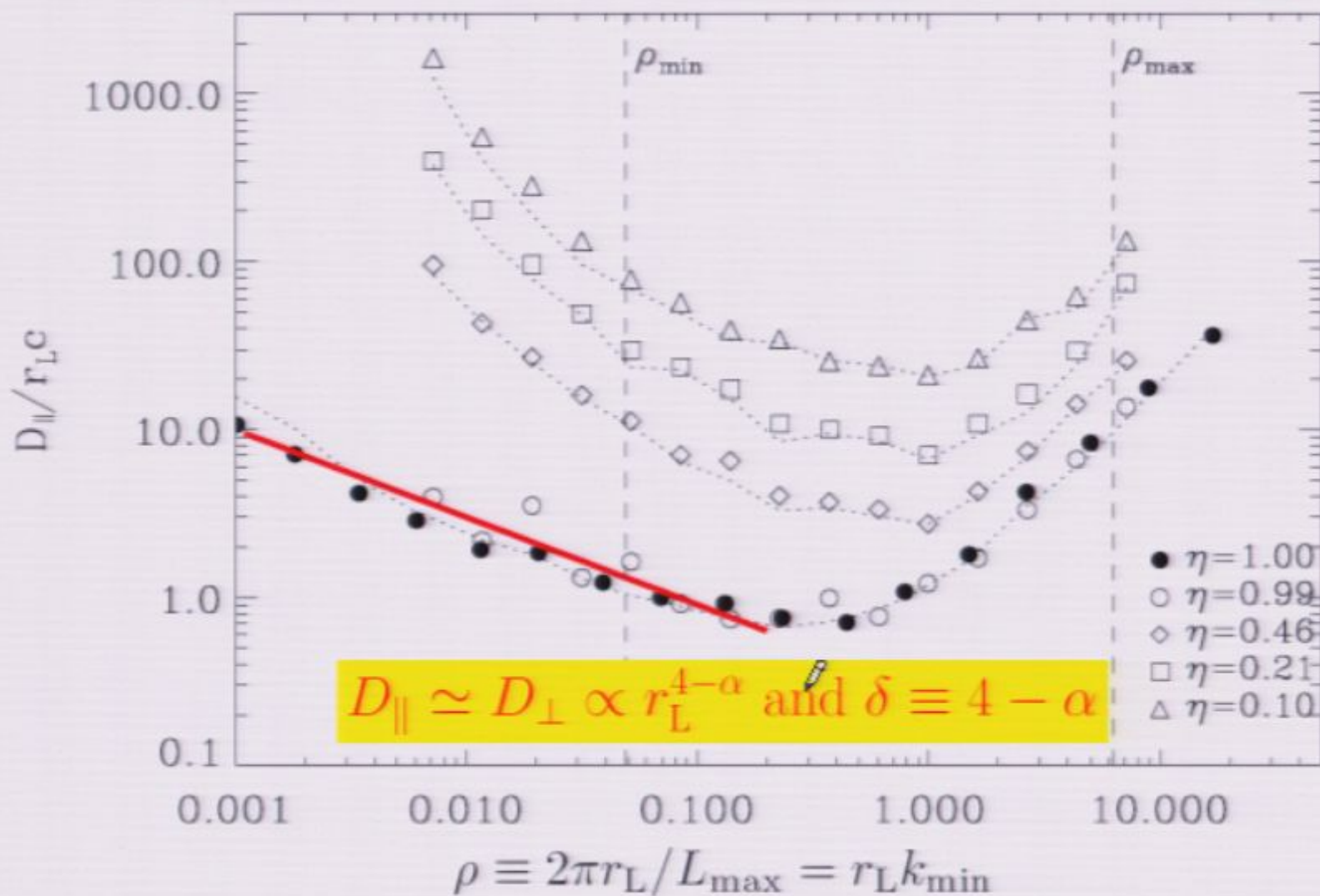
$$S_{3d}(\mathbf{k}) \propto k^{-\alpha}$$

The level of turbulence wrt to the homogeneous field \mathbf{B}_0 is defined by

$$\eta = \frac{\langle \delta\mathbf{B}^2 \rangle}{\mathbf{B}_0^2 + \langle \delta\mathbf{B}^2 \rangle}$$

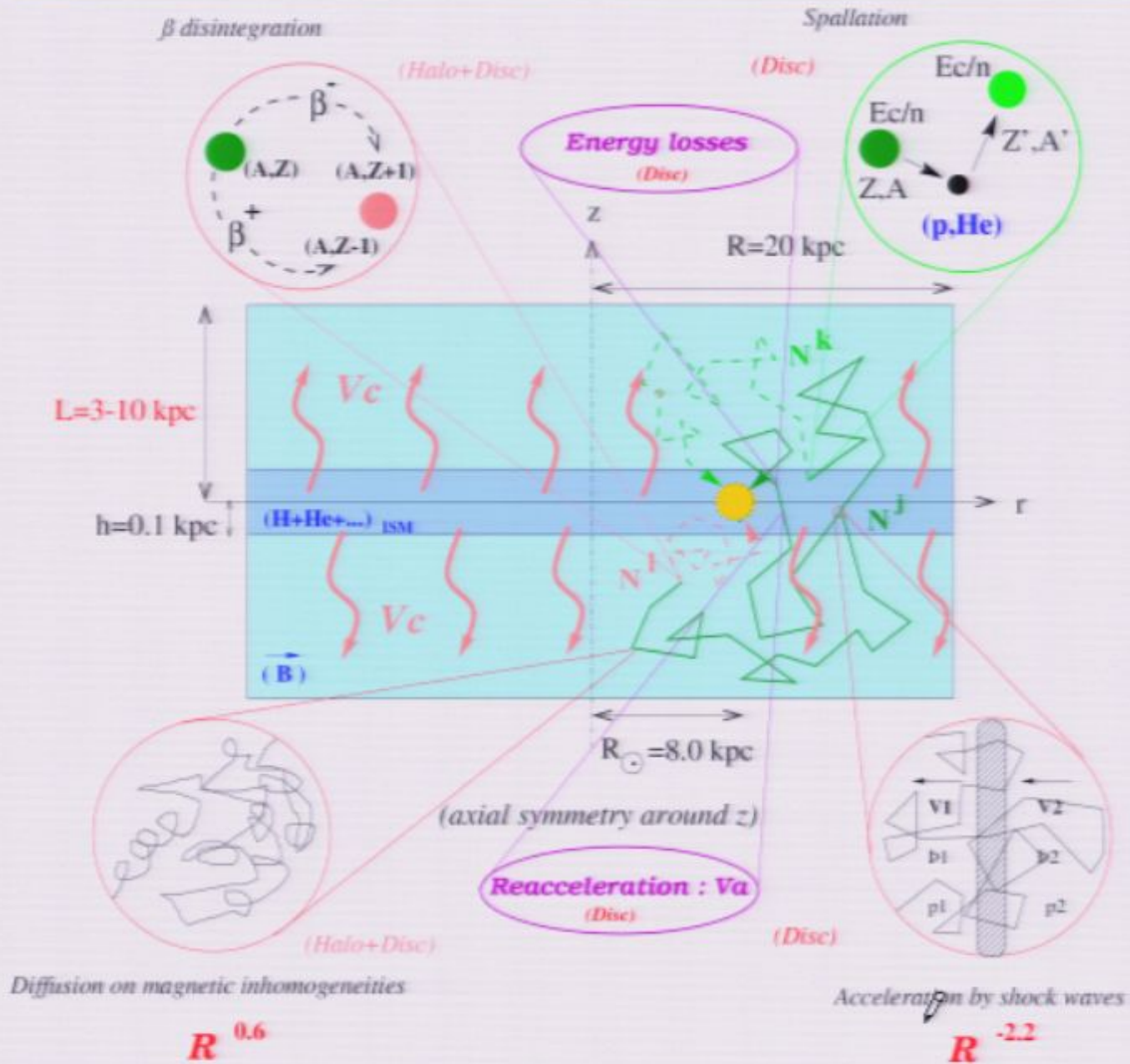
Transport of Cosmic Rays in Chaotic Magnetic Fields

F. Casse, M. Lemoine & G. Pelletier, PRD **65** (2002) 023002



$\delta = 1/3$ (Kolmogorov) or $\delta = 1/2$ (Iroshnikov, Kraichnan)

Milky-Way seen by a cosmic-ray physicist



Cosmic-rays diffuse in space and energy

The master equation for the CR density $\Psi(\vec{x}, E) = dn/dE$ is

$$\partial_M J^M = \partial_t \Psi + \vec{\nabla} \cdot \vec{J} + \partial_E J_E = Q$$

∅

Cosmic-rays diffuse in space and energy

- Diffusion and convection in space

$$\vec{J} = -K \vec{\nabla} \Psi + \Psi \vec{V}_C$$

- Second order Fermi mechanism

$$J_E = b^{\text{loss}}(E) \Psi - K_{EE}(E) \partial_E \Psi$$

- Steady state holds with $\partial_t \Psi = 0$



$$V_C \partial_z \Psi - K \Delta \Psi + \partial_E \{ b^{\text{loss}}(E) \Psi - K_{EE}(E) \partial_E \Psi \} = Q$$

Cosmic-rays diffuse in space and energy

The master equation for the CR density $\Psi(\vec{x}, E) = dn/dE$ is

$$\partial_M J^M = \partial_t \Psi + \vec{\nabla} \cdot \vec{J} + \partial_E J_E = Q$$

Cosmic-rays diffuse in space and energy

- Diffusion and convection in space

$$\vec{J} = -K \vec{\nabla} \Psi \neq \Psi \vec{V}_C$$

- Second order Fermi mechanism

$$J_E = b^{\text{loss}}(E) \Psi - K_{EE}(E) \partial_E \Psi$$

- Steady state holds with $\partial_t \Psi = 0$



$$V_C \partial_z \Psi - K \Delta \Psi + \partial_E \{ b^{\text{loss}}(E) \Psi - K_{EE}(E) \partial_E \Psi \} = Q$$

Cosmic-rays diffuse in space and energy

The master equation for the CR density $\Psi(\vec{x}, E) = dn/dE$ is

$$\partial_M J^M = \partial_t \Psi + \vec{\nabla} \cdot \vec{J} + \partial_E J_E = Q$$

Cosmic-rays diffuse in space and energy

- Diffusion and convection in space

$$\vec{J} = -K \vec{\nabla} \Psi + \Psi \vec{V}_C$$

- Second order Fermi mechanism

$$J_E = \underbrace{b^{\text{loss}}(E)}_{\text{loss}} \Psi - K_{EE}(E) \partial_E \Psi$$

- Steady state holds with $\partial_t \Psi = 0$



$$V_C \partial_z \Psi - K \Delta \Psi + \partial_E \{ b^{\text{loss}}(E) \Psi - K_{EE}(E) \partial_E \Psi \} = Q$$

Cosmic-rays diffuse in space and energy

- Diffusion and convection in space

$$\vec{J} = -K \vec{\nabla} \Psi + \Psi \vec{V}_C$$

- Second order Fermi mechanism

$$J_E = b^{\text{loss}}(E) \Psi - K_{EE}(E) \partial_E \Psi$$

- Steady state holds with $\partial_t \Psi = 0$

$$K(E) = K_0 \beta \times \mathcal{R}^\delta \quad \Downarrow \quad K_{EE} = \frac{2}{9} V_a^2 \frac{E^2 \beta^4}{K(E)}$$

$$V_C \partial_z \Psi - K \Delta \Psi + \partial_E \{ b^{\text{loss}}(E) \Psi - K_{EE}(E) \partial_E \Psi \} = Q$$

Cosmic-rays diffuse in space and energy

- Diffusion and convection in space

$$\vec{J} = -K \vec{\nabla} \Psi + \Psi \vec{V}_C$$

- Second order Fermi mechanism

$$J_E = b^{\text{loss}}(E) \Psi - K_{EE}(E) \partial_E \Psi$$

- Steady state holds with $\partial_t \Psi = 0$

Thickness (L)

$$K(E) = K_0 \beta \times \mathcal{R}^\delta \quad \Downarrow$$

$$K_{EE} = \frac{2}{9} V_a^2 \frac{E^2 \beta^4}{K(E)}$$

$$V_C \partial_z \Psi - K \Delta \Psi + \partial_E \{ b^{\text{loss}}(E) \Psi - K_{EE}(E) \partial_E \Psi \} = Q$$

Cosmic-rays diffuse in space and energy

- A propagation model is characterized by the set δ, K_0, L, V_C, V_a

Case	δ	K_0 [kpc ² /Myr]	L [kpc]	V_C [km/s]	V_a [km/s]
max	0.46	0.0765	15	5	117.6
med	0.70	0.0112	4	12	52.9
min	0.85	0.0016	1	13.5	22.4

- Different methods to solve the CR diffusion equation

The semi-analytic approach – radial Bessel expansion & Green functions

The numerical Galprop code – Crank–Nicholson semi-implicit scheme

- Constraints from the typical secondary to primary B/C ratio

$$V_C \partial_z \Psi - K \Delta \Psi + \partial_E \{ b^{\text{loss}}(E) \Psi - K_{EE}(E) \partial_E \Psi \} = Q$$

Cosmic-rays diffuse in space and energy

- A propagation model is characterized by the set δ, K_0, L, V_C, V_a

Case	δ	K_0 [kpc ² /Myr]	L [kpc]	V_C [km/s]	V_a [km/s]
max	0.46	0.0765	15	5	117.6
med	0.70	0.0112	4	12	52.9
min	0.85	0.0016	1	13.5	22.4

- Different methods to solve the CR diffusion equation

The semi-analytic approach – radial Bessel expansion & Green functions

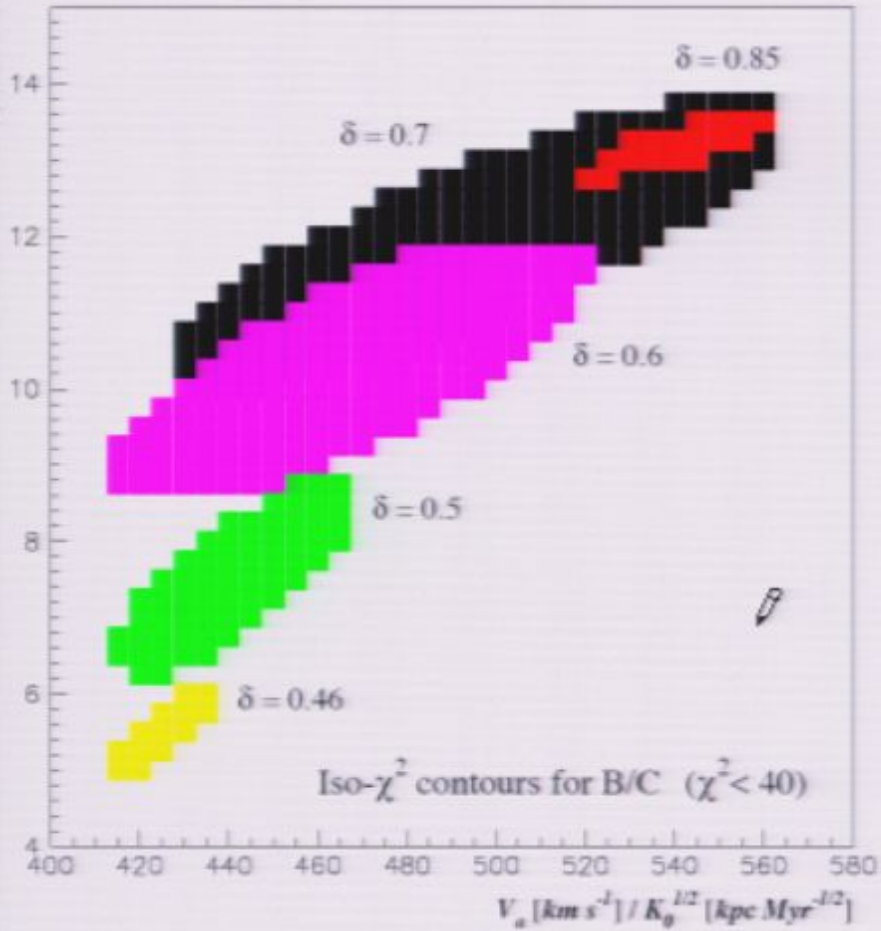
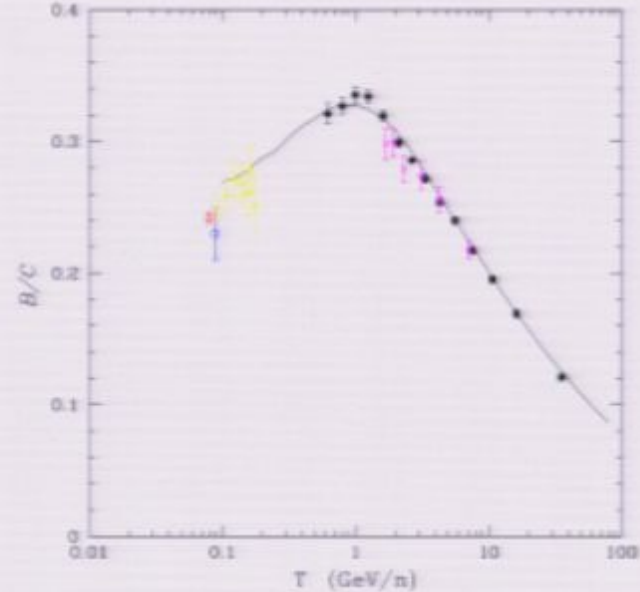
The numerical Galprop code – Crank–Nicholson semi-implicit scheme

- Constraints from the typical secondary to primary B/C ratio

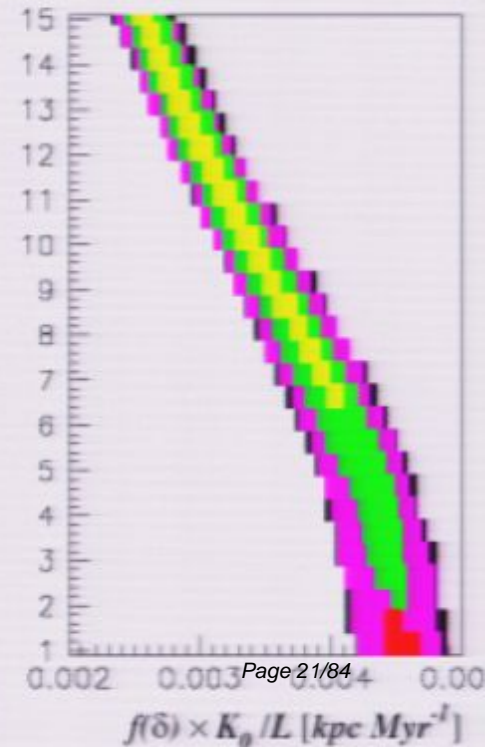
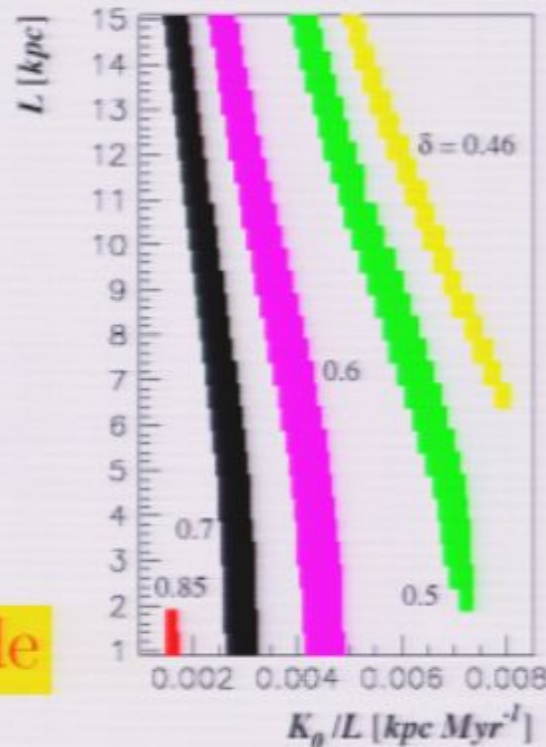
$$V_C \partial_z \Psi - K \Delta \Psi + \partial_E \{ b^{\text{loss}}(E) \Psi - K_{EE}(E) \partial_E \Psi \} = Q$$

B/C ratio analysis – D. Maurin et al.

THE ASTROPHYSICAL JOURNAL, 555:585–596, 2001 July 10
 © 2001. The American Astronomical Society. All rights reserved. Printed in U.S.A.



Iso- χ^2 contours for B/C ($\chi^2 < 40$)



~ 1,600 models are compatible

Cosmic-rays diffuse in space and energy

- A propagation model is characterized by the set δ, K_0, L, V_C, V_a

Case	δ	K_0 [kpc ² /Myr]	L [kpc]	V_C [km/s]	V_a [km/s]
max	0.46	0.0765	15	5	117.6
med	0.70	0.0112	4	12	52.9
min	0.85	0.0016	1	13.5	22.4

- Different methods to solve the CR diffusion equation

The semi-analytic approach – radial Bessel expansion & Green functions

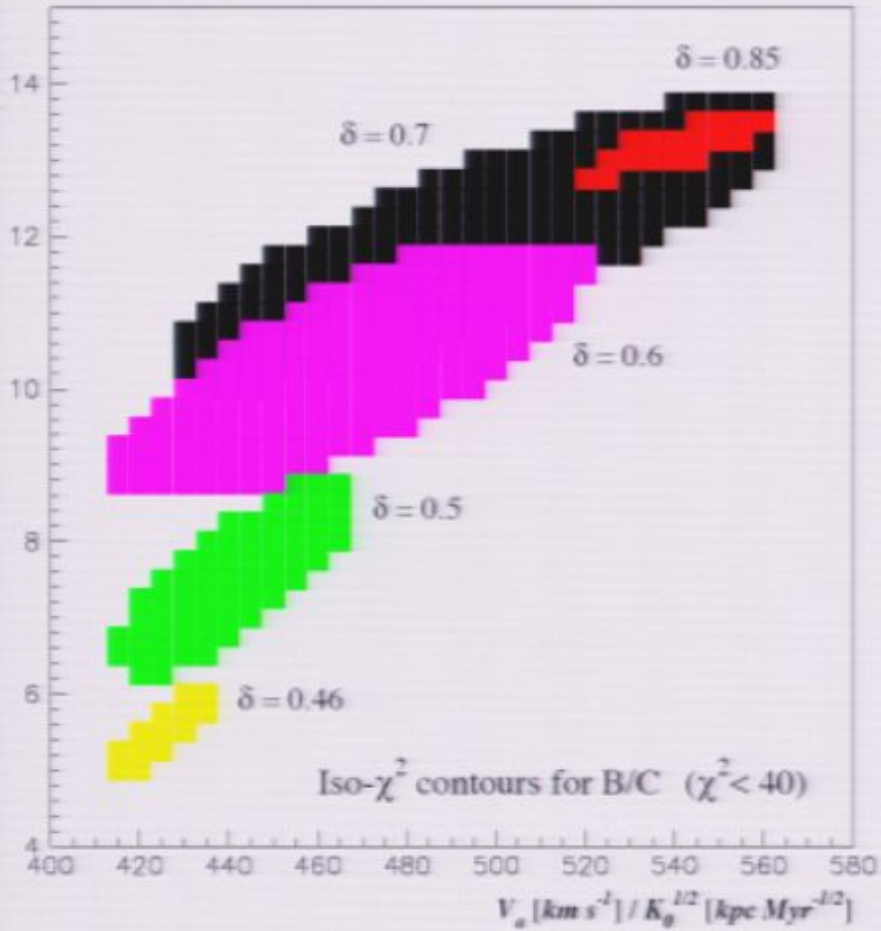
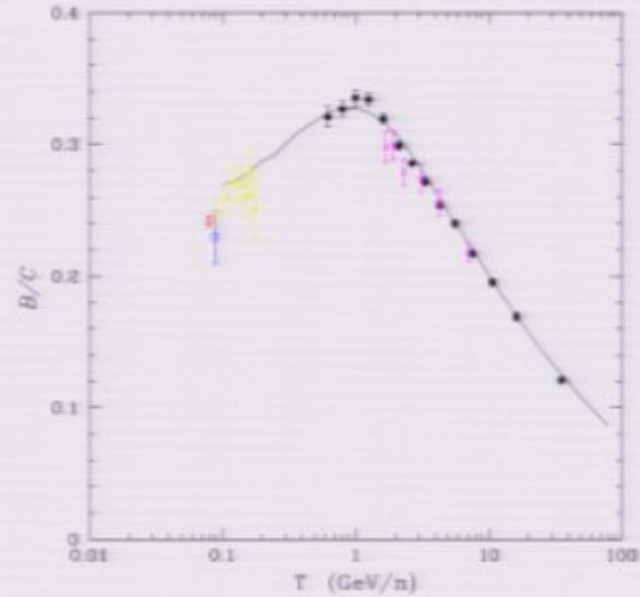
The numerical Galprop code – Crank–Nicholson semi-implicit scheme

- Constraints from the typical secondary to primary B/C ratio

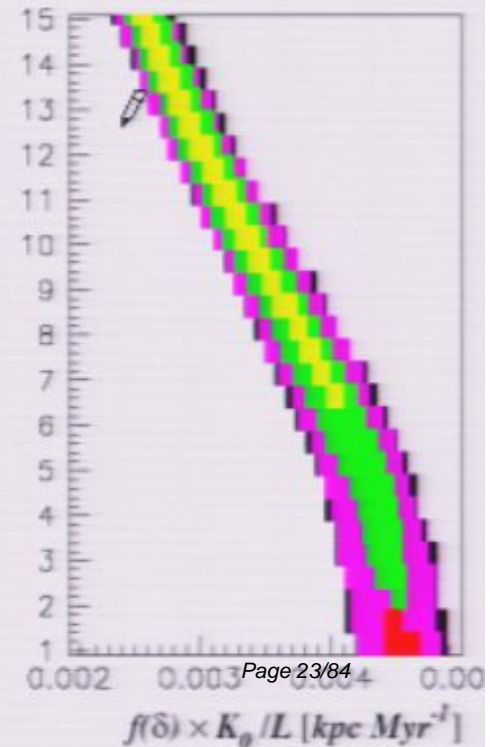
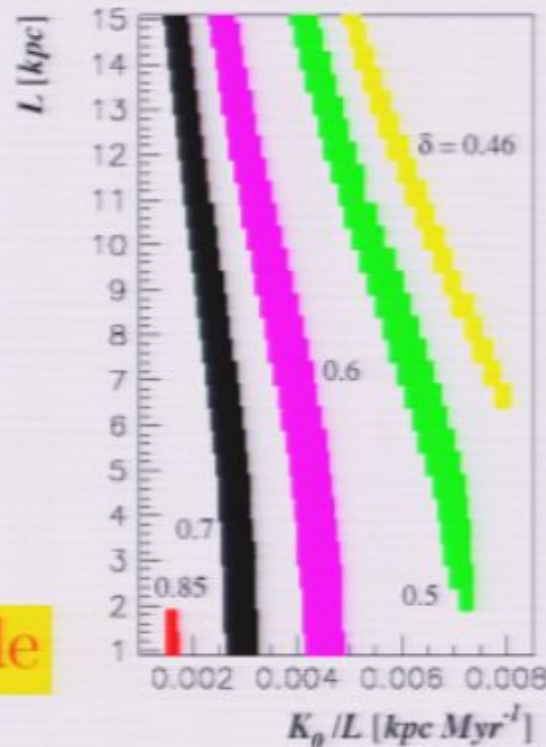
$$V_C \partial_z \Psi - K \Delta \Psi + \partial_E \{ b^{\text{loss}}(E) \Psi - K_{EE}(E) \partial_E \Psi \} = Q$$

B/C ratio analysis – D. Maurin et al.

THE ASTROPHYSICAL JOURNAL, 555:585–596, 2001 July 10
 © 2001. The American Astronomical Society. All rights reserved. Printed in U.S.A.



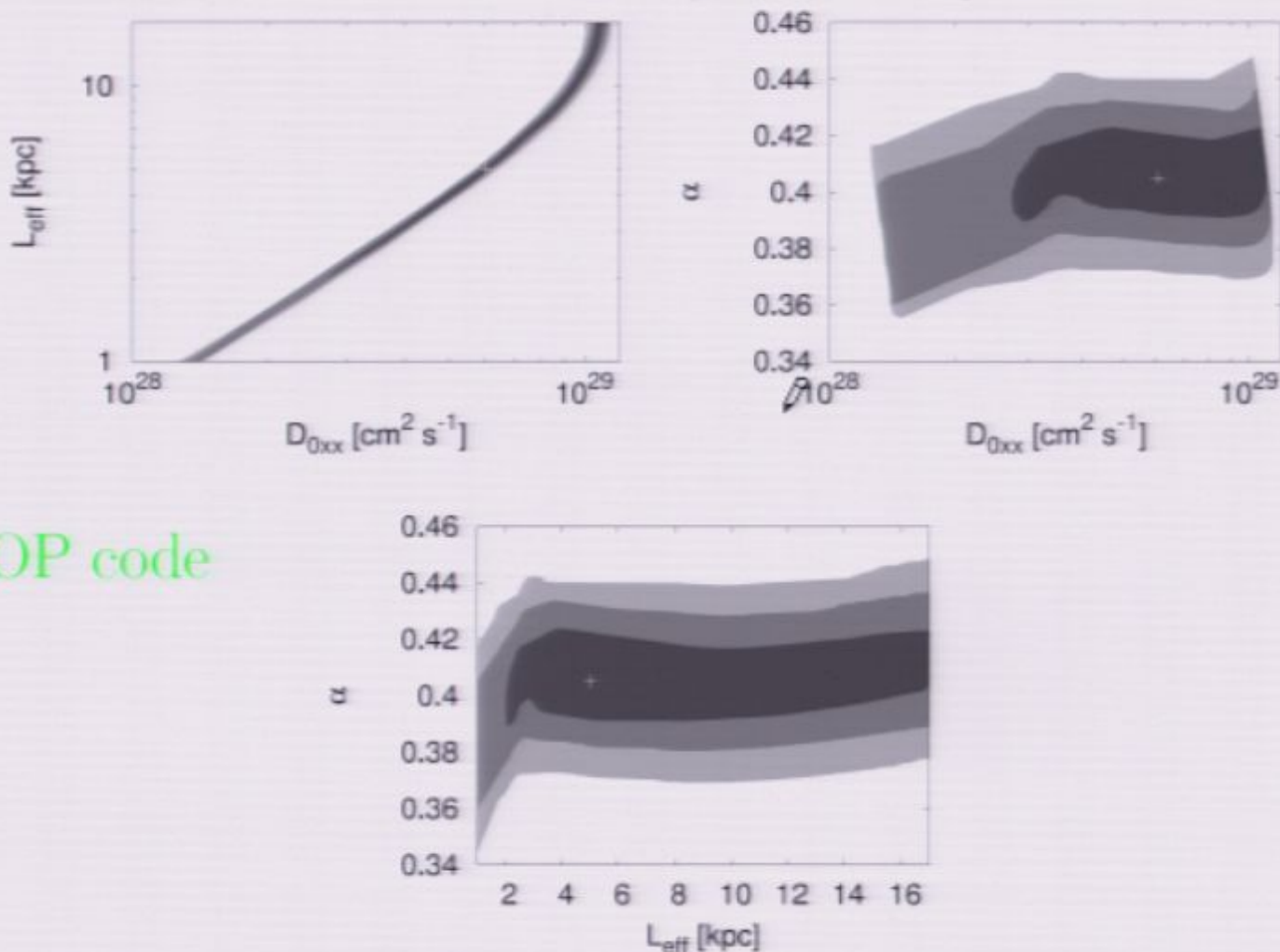
Iso- χ^2 contours for B/C ($\chi^2 < 40$)



~ 1,600 models are compatible

Melanie Simet¹ and Dan Hooper^{1,2}

arXiv:0904.2398v1 [astro-ph.HE] 15 Apr 2009

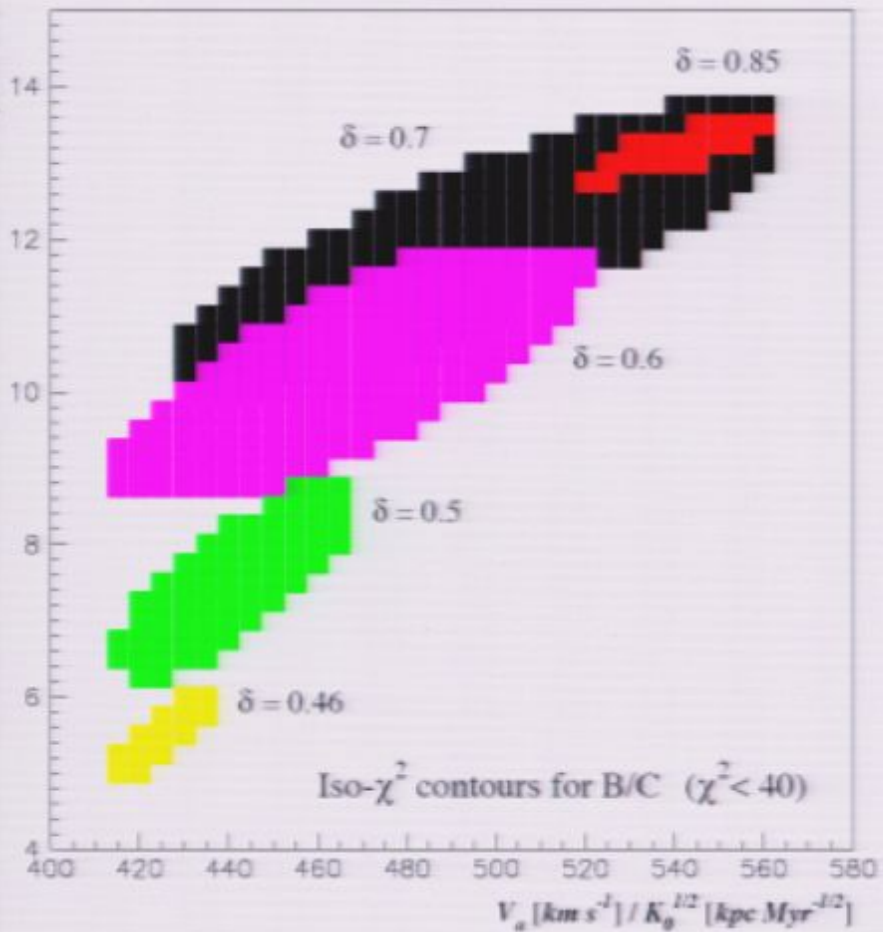
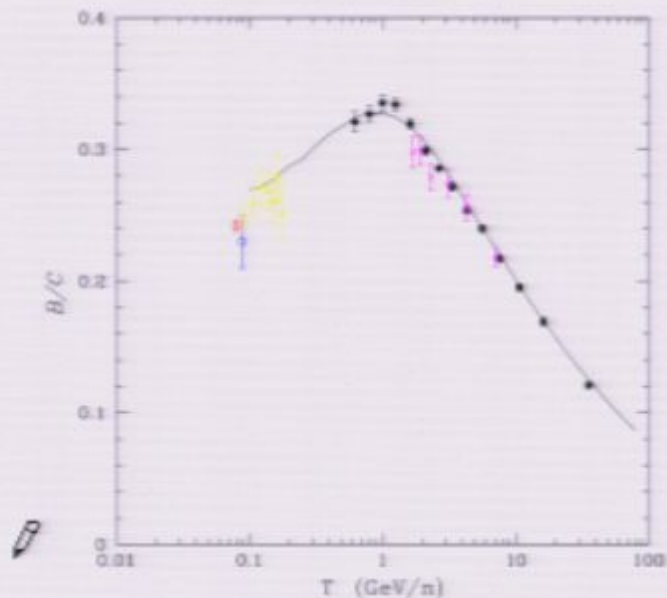


GALPROP code

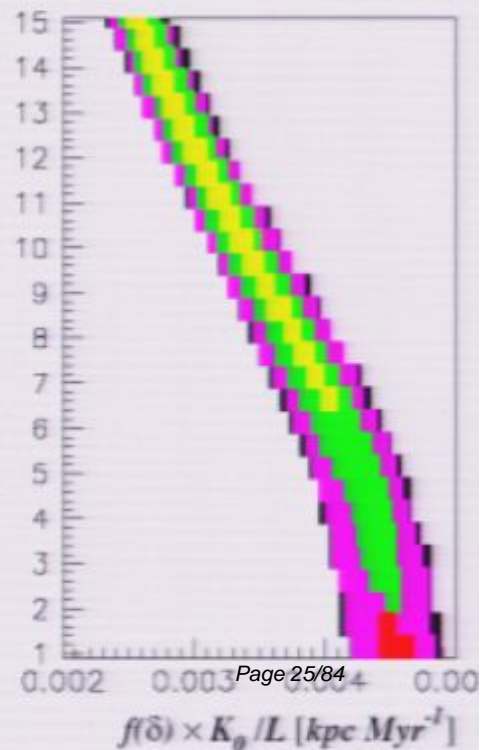
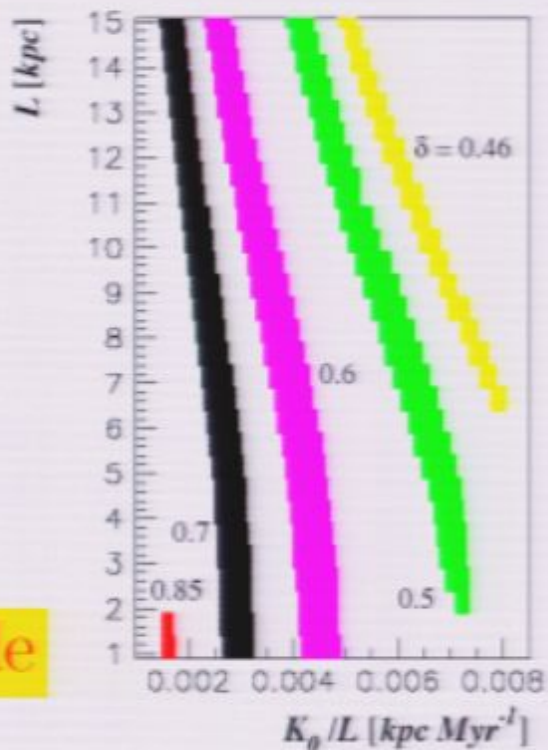
In Fig. 1, we plot the acceptable ranges of the propagation model parameters, based on our χ^2 calculation. Neglecting the effects of convection for the time being, we find the overall best fit for the following set of propagation parameters: $D_{0xx} = 6.04 \times 10^{28} \text{ cm}^2 \text{ s}^{-1}$, $L_{\text{eff}} = 5.0$ kpc, and $\alpha = 0.41$, which yields a χ^2 per degree-of-freedom of 1.37. Although the acceptable parameter regions are well constrained in D_{0xx} and α , the allowed values for L_{eff} extend beyond the range we considered (1-17 kpc). For physical reasons, however, we do not consider values outside of this range. We find that the data prefer values of α which lie between those predicted for Kolmogorov-type ($\alpha = 1/3$) [20] and Kraichnan-type ($\alpha = 1/2$) [21] turbulence.

B/C ratio analysis – D. Maurin et al.

THE ASTROPHYSICAL JOURNAL, 555:585–596, 2001 July 10
 © 2001. The American Astronomical Society. All rights reserved. Printed in U.S.A.



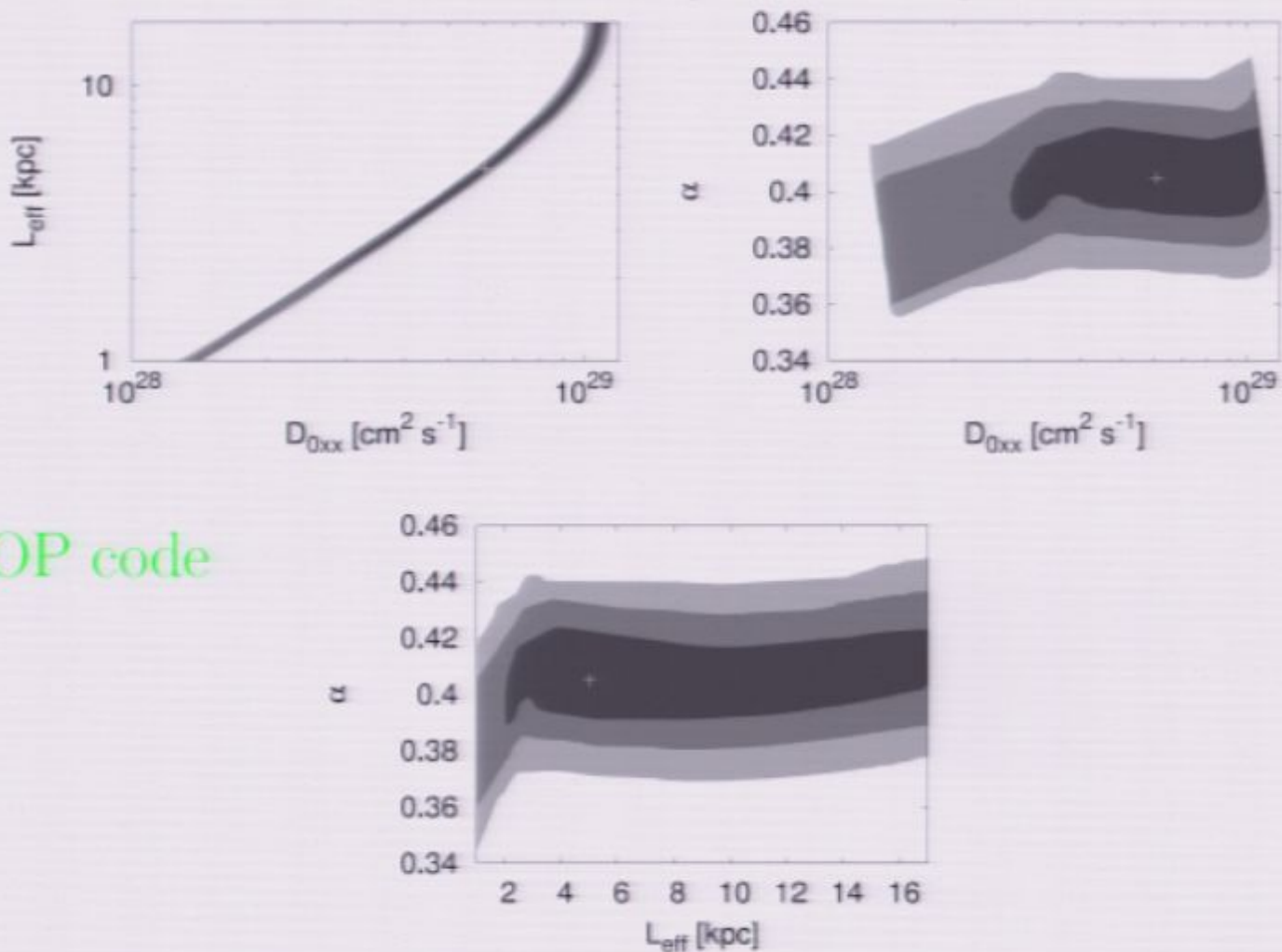
Iso- χ^2 contours for B/C ($\chi^2 < 40$)



~ 1,600 models are compatible

Melanie Simet¹ and Dan Hooper^{1,2}

arXiv:0904.2398v1 [astro-ph.HE] 15 Apr 2009

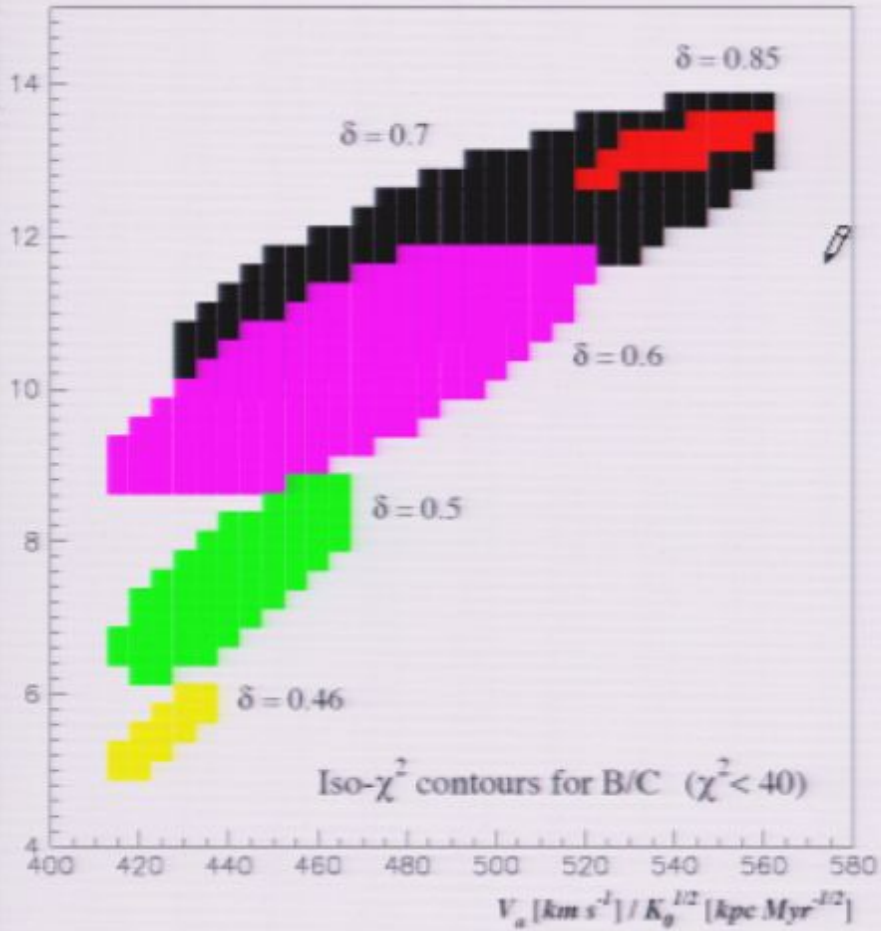
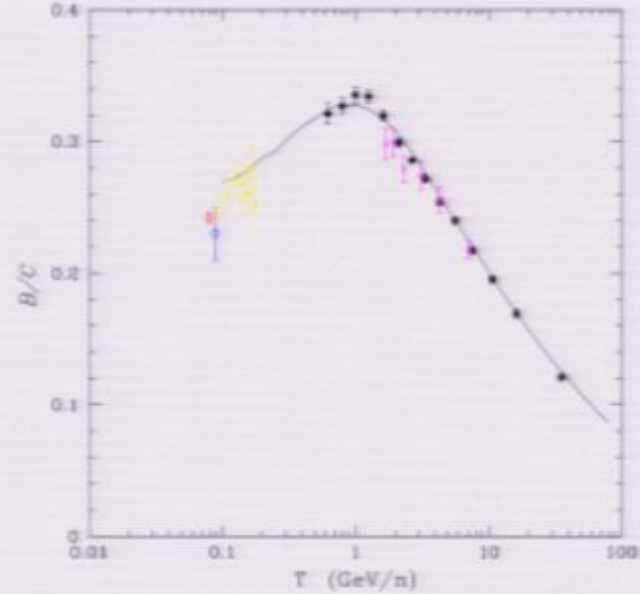


GALPROP code

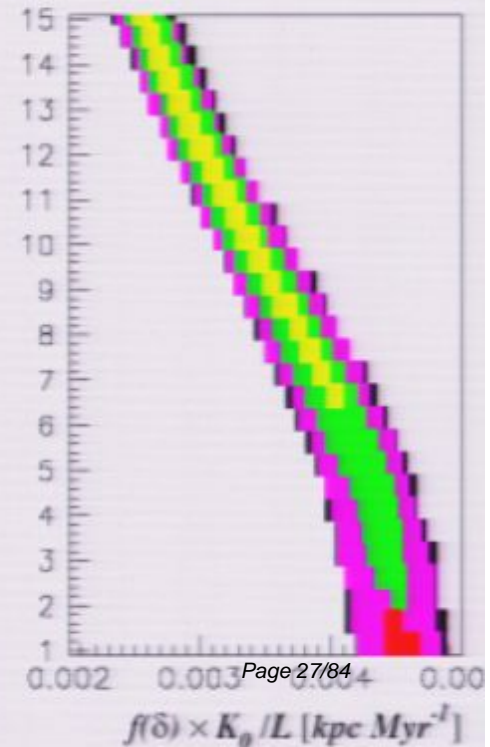
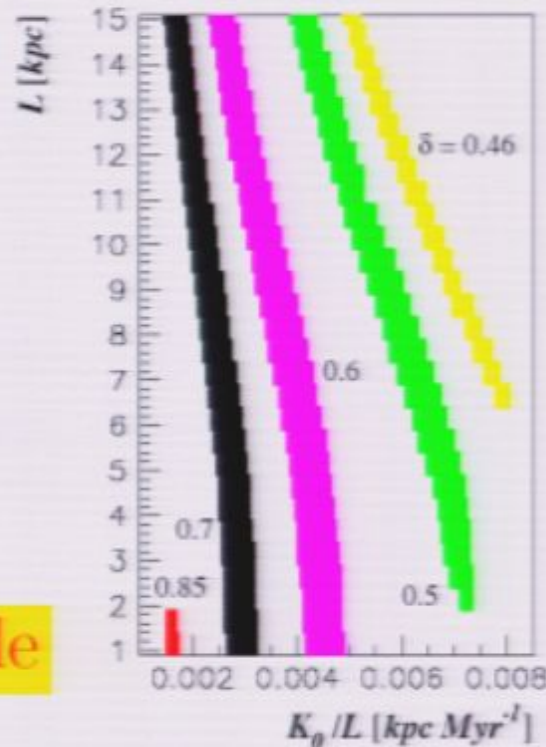
In Fig. 1, we plot the acceptable ranges of the propagation model parameters, based on our χ^2 calculation. Neglecting the effects of convection for the time being, we find the overall best fit for the following set of propagation parameters: $D_{0xx} = 6.04 \times 10^{28} \text{ cm}^2 \text{ s}^{-1}$, $L_{\text{eff}} = 5.0$ kpc, and $\alpha = 0.41$, which yields a χ^2 per degree-of-freedom of 1.37. Although the acceptable parameter regions are well constrained in D_{0xx} and α , the allowed values for L_{eff} extend beyond the range we considered (1-17 kpc). For physical reasons, however, we do not consider values outside of this range. We find that the data prefer values of α which lie between those predicted for Kolmogorov-type ($\alpha = 1/3$) [20] and Kraichnan-type ($\alpha = 1/2$) [21] turbulence.

B/C ratio analysis – D. Maurin et al.

THE ASTROPHYSICAL JOURNAL, 555:585–596, 2001 July 10
 © 2001. The American Astronomical Society. All rights reserved. Printed in U.S.A.



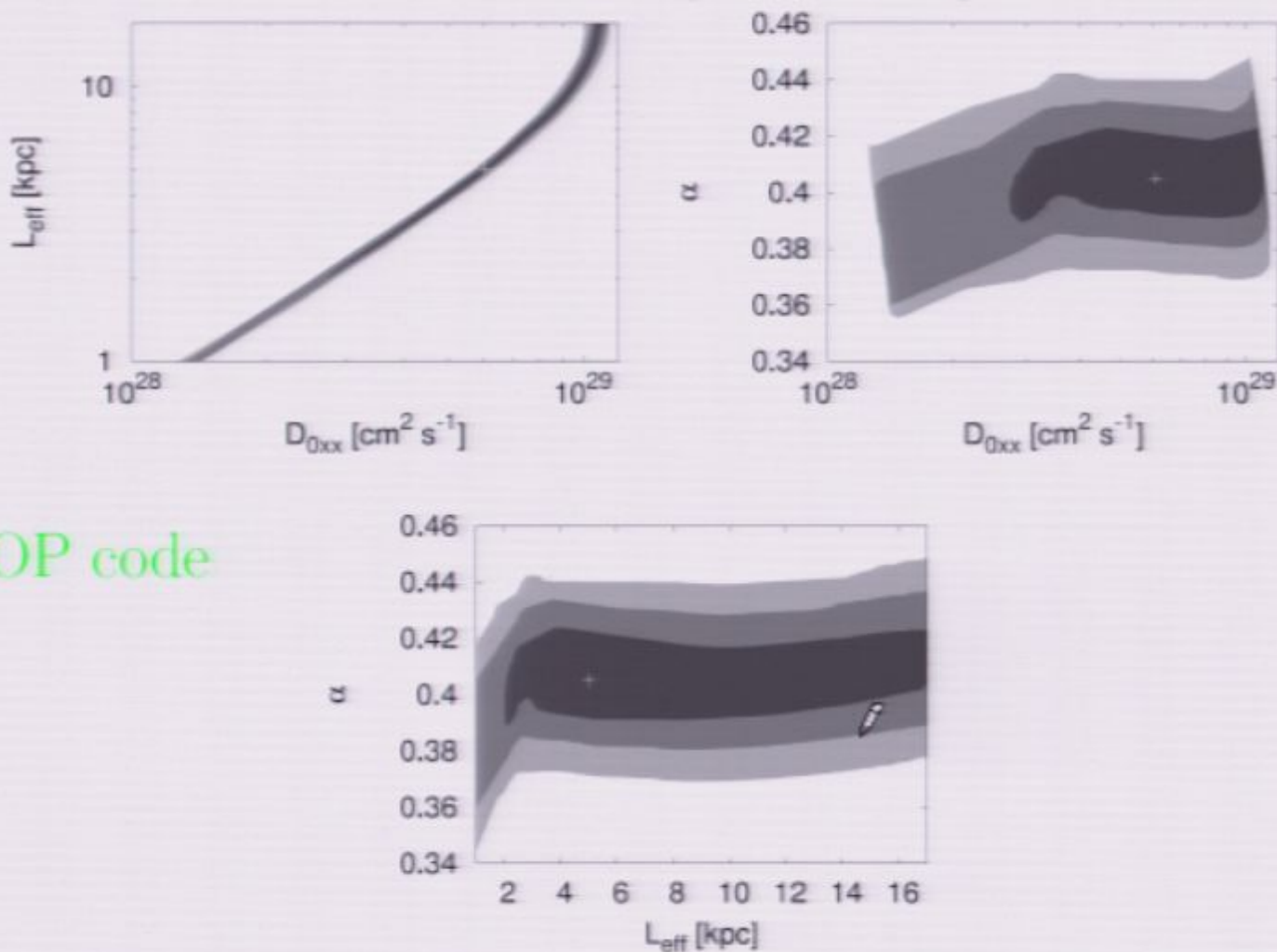
Iso- χ^2 contours for B/C ($\chi^2 < 40$)



~ 1 600 models are compatible

Melanie Simet¹ and Dan Hooper^{1,2}

arXiv:0904.2398v1 [astro-ph.HE] 15 Apr 2009

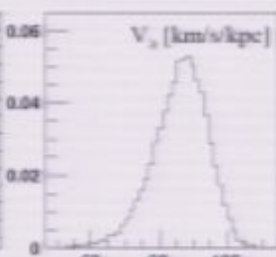
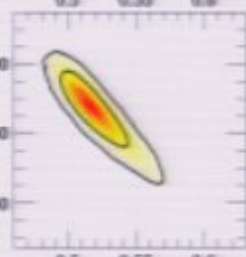
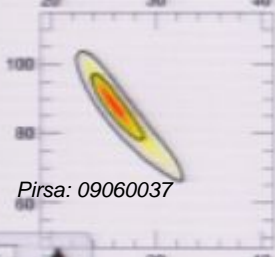
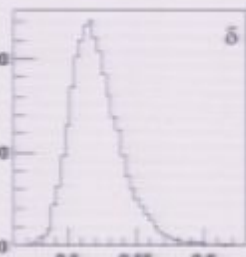
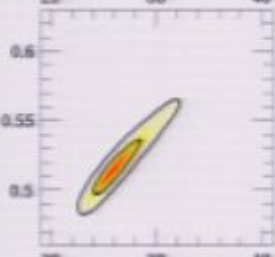
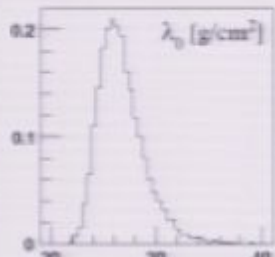
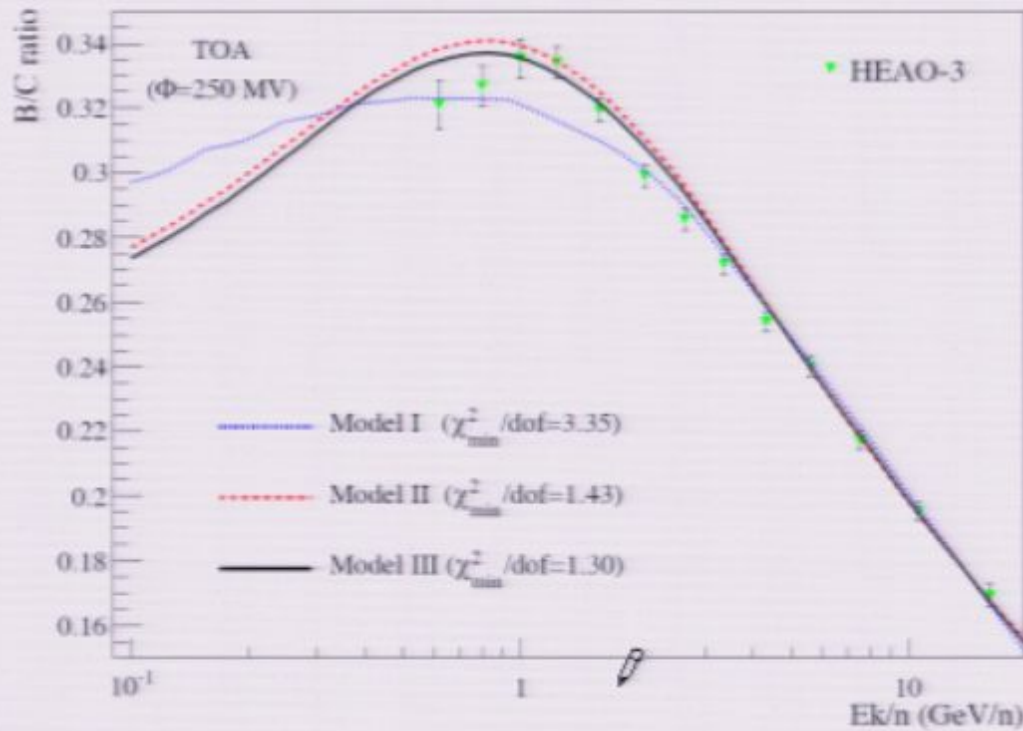


GALPROP code

In Fig. 1, we plot the acceptable ranges of the propagation model parameters, based on our χ^2 calculation. Neglecting the effects of convection for the time being, we find the overall best fit for the following set of propagation parameters: $D_{0xx} = 6.04 \times 10^{28} \text{ cm}^2 \text{ s}^{-1}$, $L_{\text{eff}} = 5.0$ kpc, and $\alpha = 0.41$, which yields a χ^2 per degree-of-freedom of 1.37. Although the acceptable parameter regions are well constrained in D_{0xx} and α , the allowed values for L_{eff} extend beyond the range we considered (1-17 kpc). For physical reasons, however, we do not consider values outside of this range. We find that the data prefer values of α which lie between those predicted for Kolmogorov-type ($\alpha = 1/3$) [20] and Kraichnan-type ($\alpha = 1/2$) [21] turbulence.

A Markov Chain Monte Carlo for Galactic Cosmic Ray physics

A. Putze¹, L. Derome¹, D. Maurin², L. Perotto³, and R. Taillet^{4,5}



$$\lambda_{\text{esc}}(R) = \begin{cases} \lambda_0 \beta R_0^{-(\delta-\delta_0)} R^{-\delta_0} & \text{when } R < R_0 \\ \lambda_0 \beta R^{-\delta} & \text{otherwise;} \end{cases}$$

Model	λ_0 g cm^{-2}	R_0 GV	δ	V_a $\text{km s}^{-1} \text{kpc}^{-1}$	$\chi^2_{\text{min}}/\text{dof}$
I	54^{+2}_{-2}	$4.2^{+0.3}_{-0.9}$	$0.70^{+0.01}_{-0.01}$	-	3.35
II	26^{+2}_{-2}	-	$0.52^{+0.02}_{-0.02}$	88^{+6}_{-11}	1.43
III	30^{+5}_{-4}	$2.8^{+0.6}_{-0.8}$	$0.58^{+0.01}_{-0.06}$	75^{+10}_{-13}	1.30

2) Antiprotons or the revenge of orthodoxy

Space diffusion dominates in the master equation

$$V_C \partial_z \Psi - K \Delta \Psi + \partial_E \{ b^{\text{loss}}(E) \Psi - K_{EE}(E) \partial_E \Psi \} = Q$$

$$\text{Poisson equation } K \Delta \Psi + Q = 0$$



$$\text{Long range with } G_{\text{p}}^{3\text{D}}(r) = \frac{Q}{4\pi K r}$$

- Evaporation at the vertical boundaries $\pm L$
- Leakage at the radial boundaries $R = 20$ kpc
- Evaporation from convective wind V_C
- Annihilations inside the MW gaseous disk
- Energy losses and mild diffusive reacceleration

BESS 95+97 BESS 98 AMS 98 CAPRICE 98

$\delta = 0.46$ to 0.85

B/C measurements @ high E

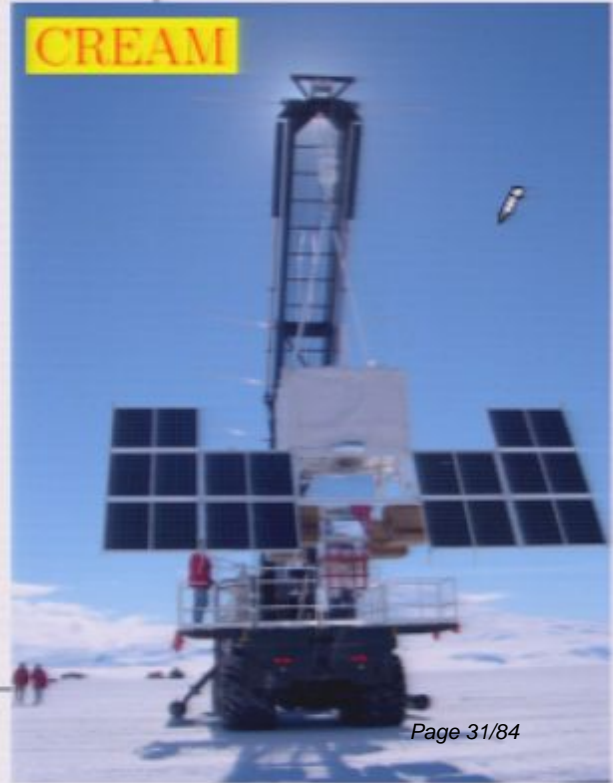
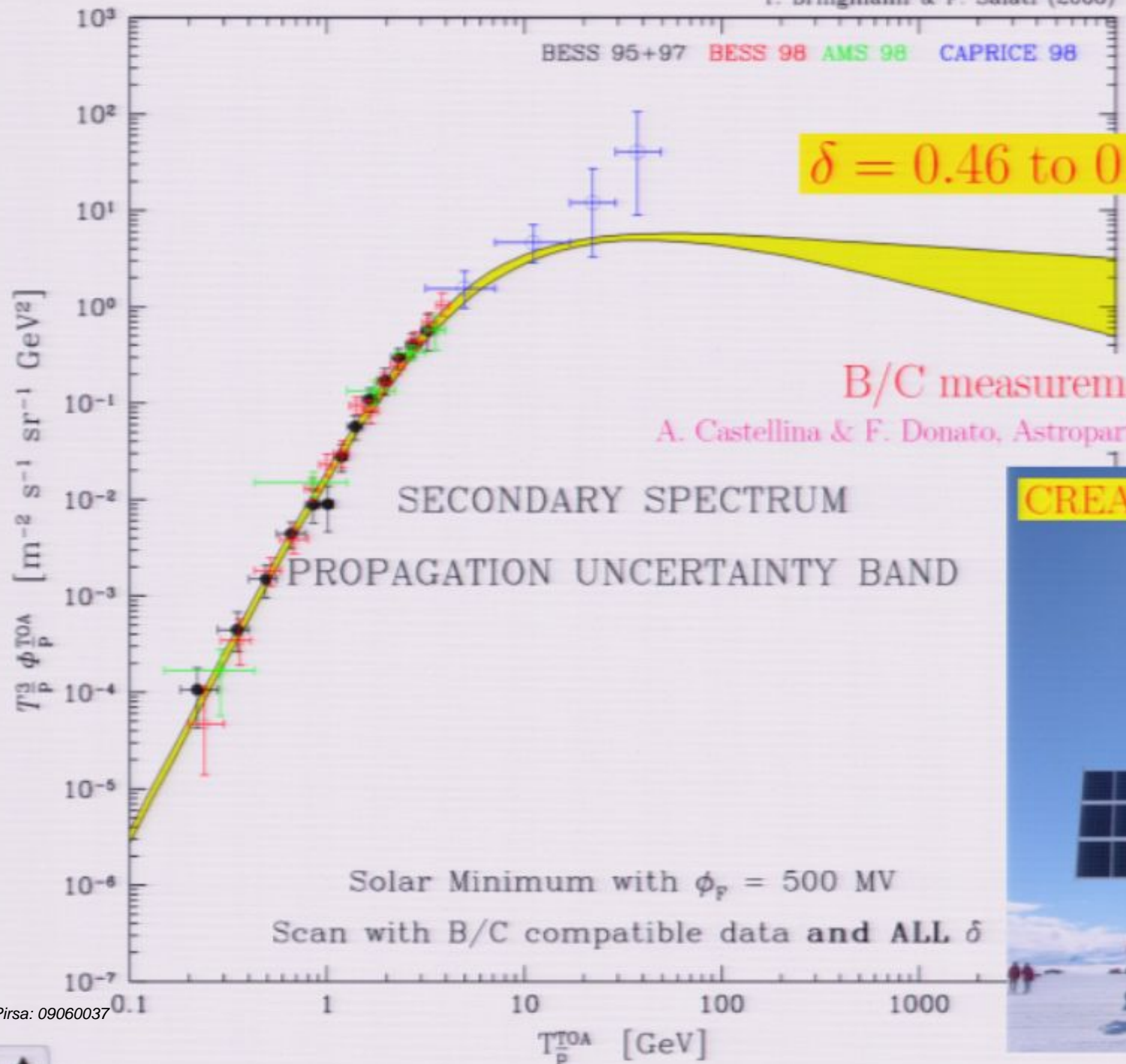
A. Castellina & F. Donato, *Astropart. Phys.* **24** (2005) 146-159

SECONDARY SPECTRUM

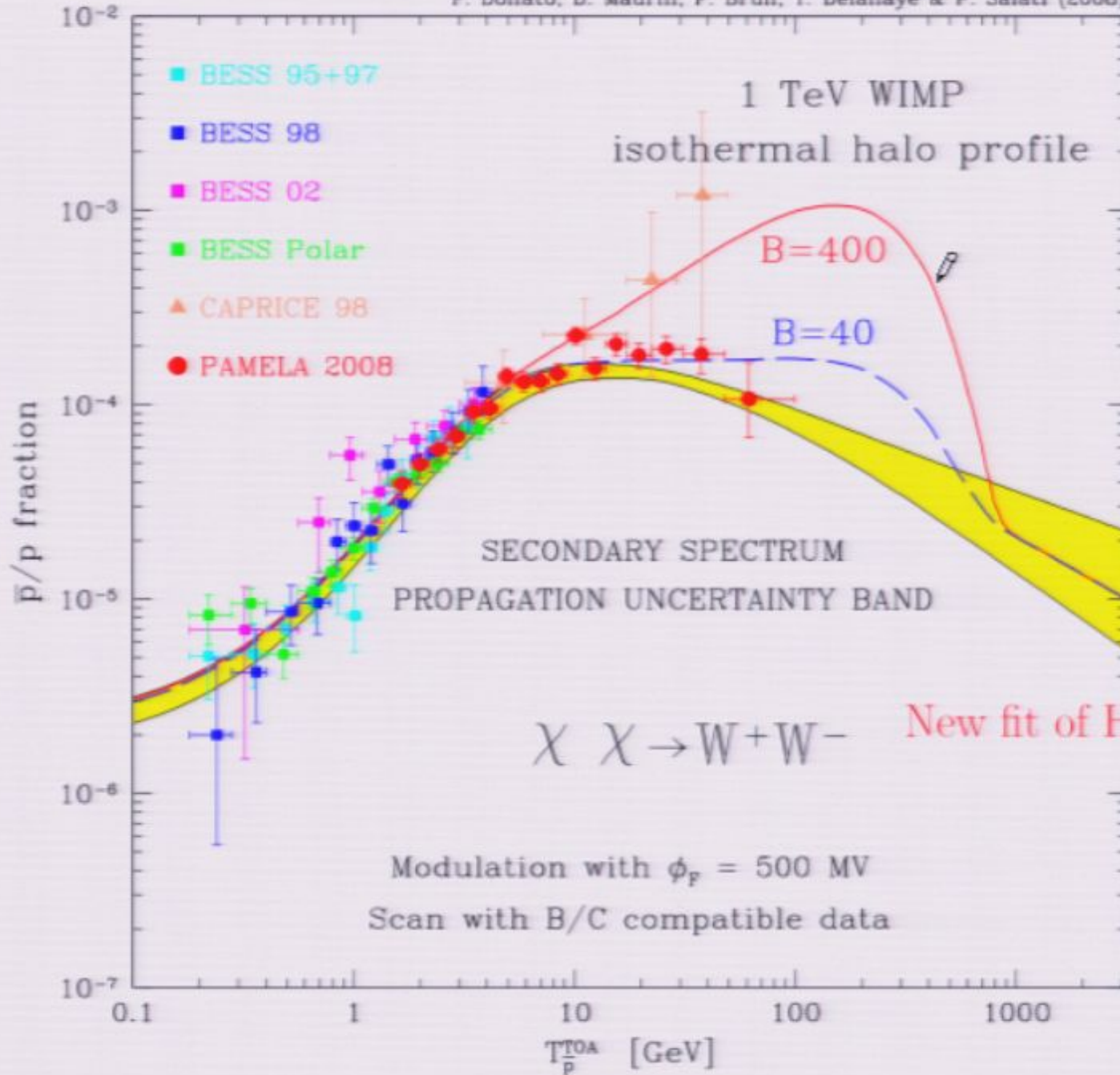
PROPAGATION UNCERTAINTY BAND

Solar Minimum with $\phi_p = 500$ MV

Scan with B/C compatible data and ALL δ

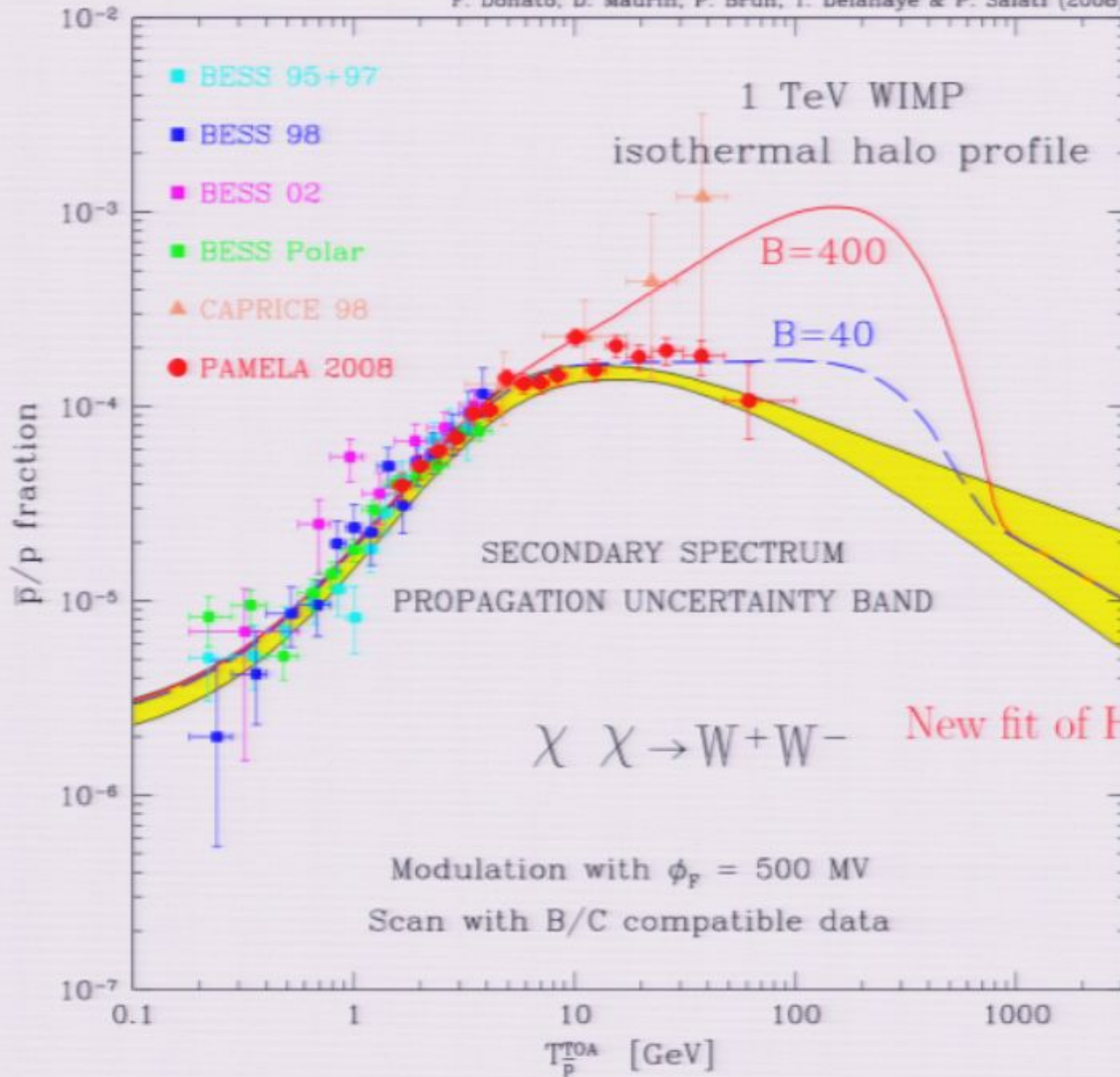


M. Cirelli^a, M. Kadastik^b, M. Raidal^b, A. Strumia^c
F. Donato, D. Maurin, P. Brun, T. Delahaye & P. Salati (2008)



2.839

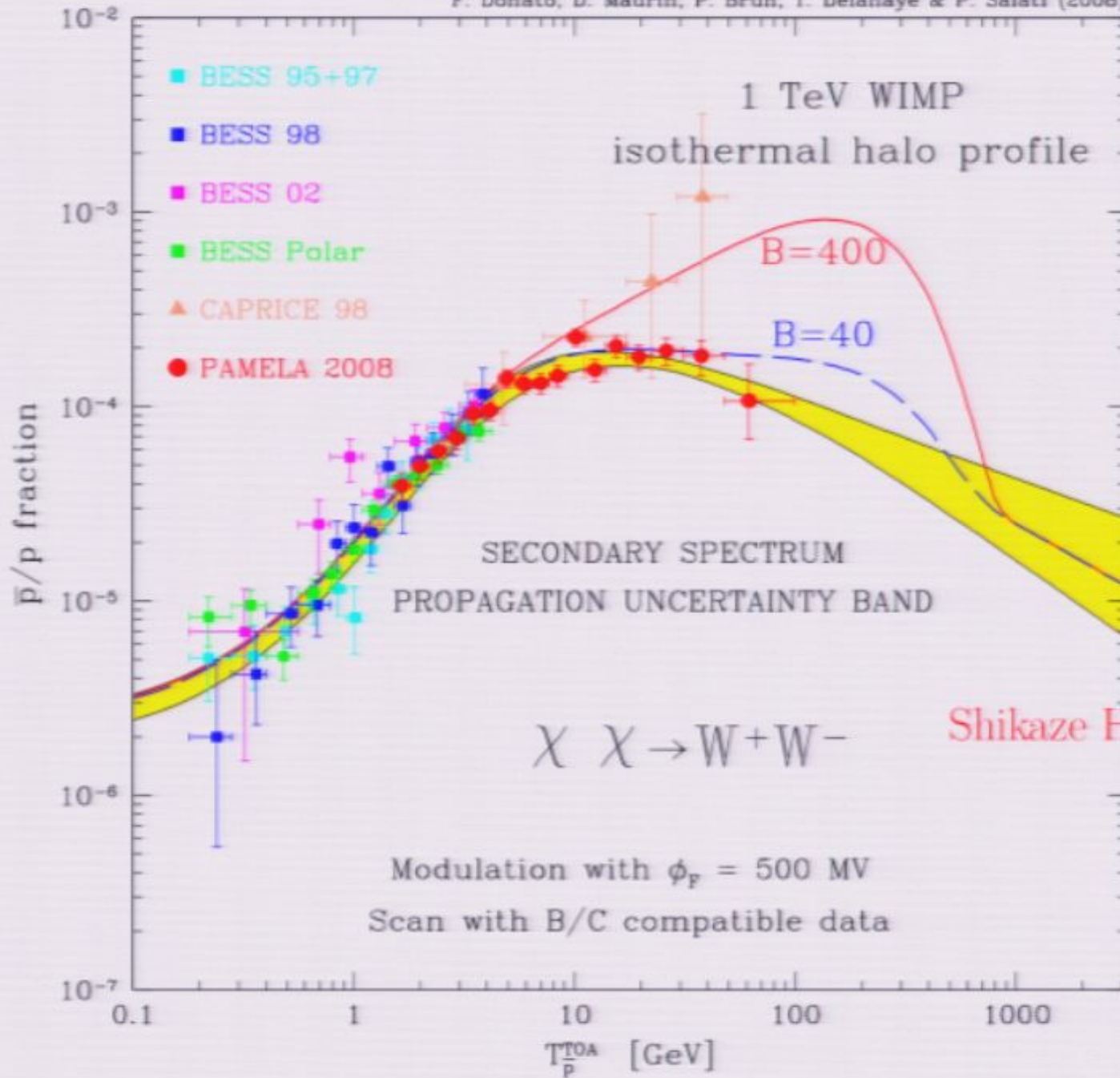
M. Cirelli^a, M. Kadastik^b, M. Raidal^b, A. Strumia^c
F. Donato, D. Maurin, P. Brun, T. Delahaye & P. Salati (2008)



2.839

New fit of H & He spectra

M. Cirelli^a, M. Kadastik^b, M. Raidal^b, A. Strumia^c
F. Donato, D. Maurin, P. Brun, T. Delahaye & P. Salati (2008)



3) Secondary positron uncertainties

Mostly sensitive to the local region

Energy losses dominate

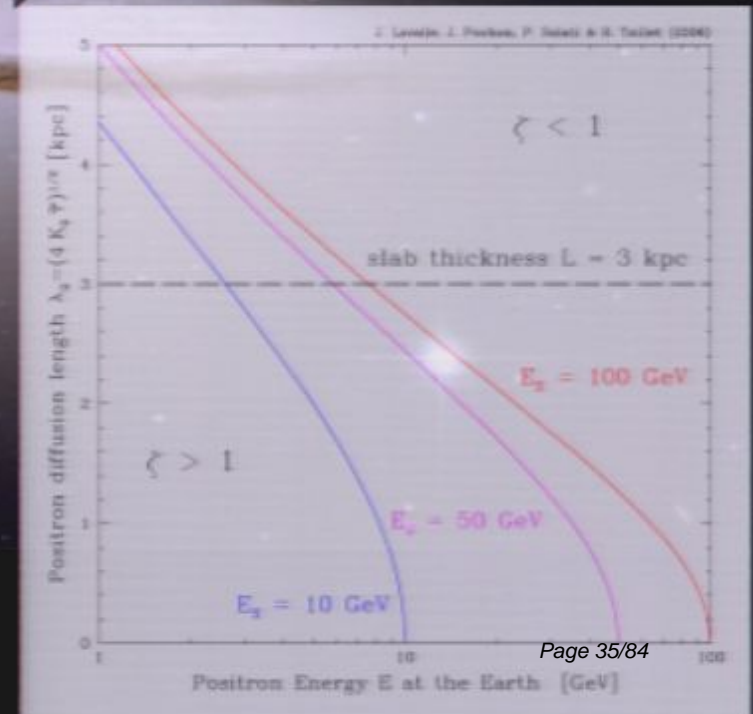
IC on stellar light and CMB – synchrotron

$$E_{\text{obs}} \leq E_S$$

$$G_{e^+}(\vec{x}_{\odot}, E \leftarrow \vec{x}, E_S) = \frac{\tau_E}{E_0 \epsilon^2} \tilde{G}(\vec{x}_{\odot}, \tilde{t} \leftarrow \vec{x}, \tilde{t}_S)$$

$$\tilde{G}(\vec{x}_{\odot}, \tilde{t} \leftarrow \vec{x}, \tilde{t}_S) = \frac{\theta(r_S - r)}{V_S}$$

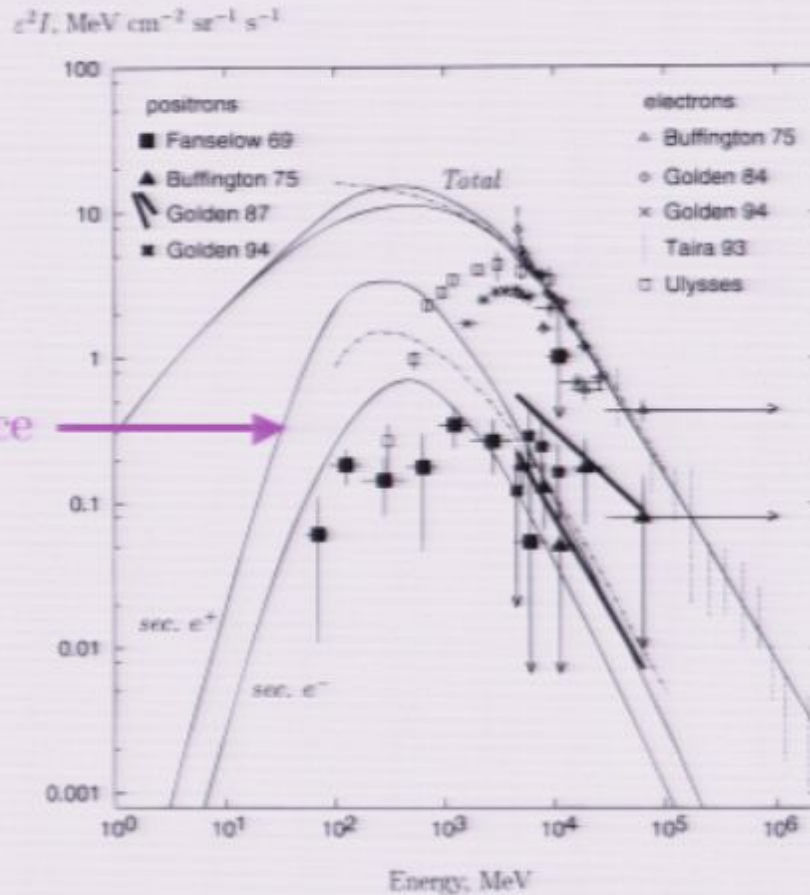
$$V_S = (\sqrt{2\pi} \lambda_D)^3$$



The secondary e^+ spectrum so far used has been computed in 1998

L. V. Moskalenko and A. W. Strong, *Production and propagation of cosmic ray positrons and electrons*, *Astrophys. J.* **493** (1998) 694 [astro-ph/9710124].

E. A. Baltz and J. Edsjö, *Positron propagation and fluxes from neutralino annihilation in the halo*, *Phys. Rev.* **D59** (1999) 023511 [astro-ph/9808243].



e^+ spectral reference

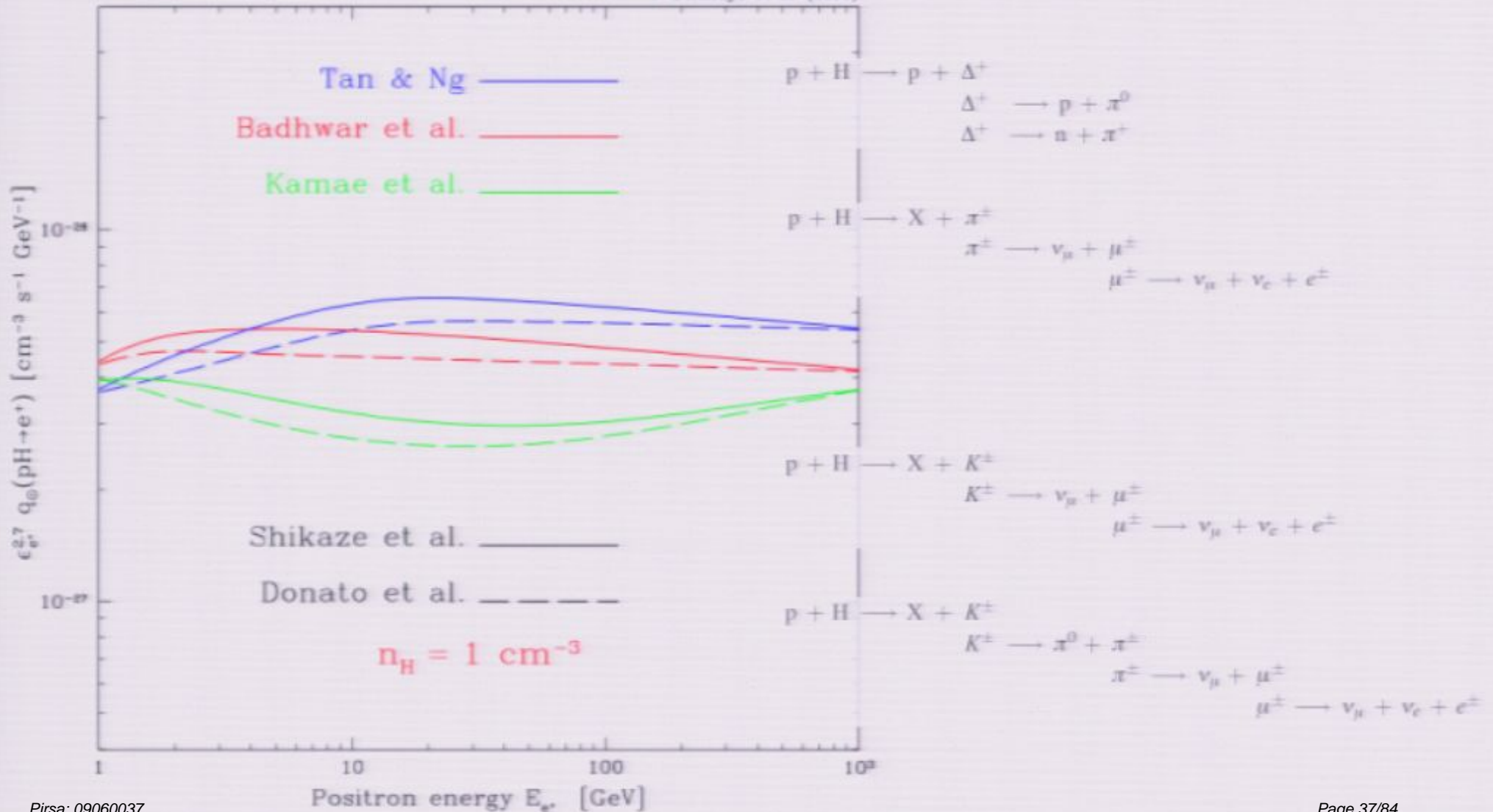
PARAMETERS OF MODELS

Model	z_0 (kpc)	D_{10} ($\text{cm}^2 \text{s}^{-1}$)	p_{10} (MV/c)	β	v_A (km s^{-1})	PROTONS			HELIUM		
						γ	p_0^+	I_0^+	γ	p_0^+	I_0^+
08-005.....	3	2.0×10^{28}	3.0×10^7	0.60	0	2.15	10^6	3×10^{-5}	2.35	4×10^6	4×10^{-5}
08-006.....	3	4.2×10^{28}	3.0×10^7	0.35	20	2.25	10^6	3×10^{-5}	2.45	4×10^6	4×10^{-5}
08-009.....	3	2.0×10^{28}	3.0×10^7	0.60	0	2.00	10^6	3×10^{-5}	2.00	4×10^6	4×10^{-5}

Positron source term

Delahaye T. et al. - arXiv:0809.5268

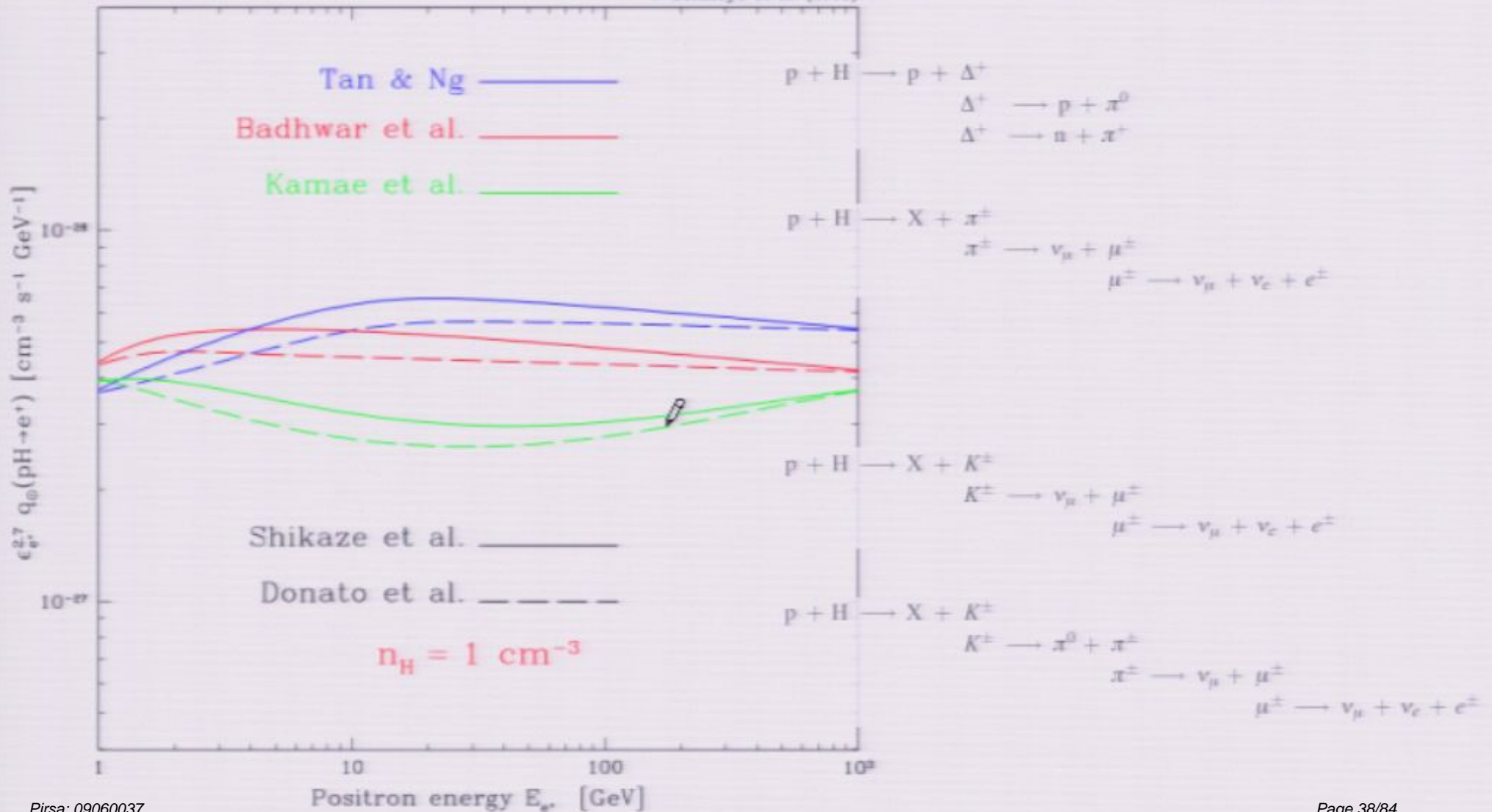
T. Delahaye et al. (2006)



Positron source term

Delahaye T. et al. - arXiv:0809.5268

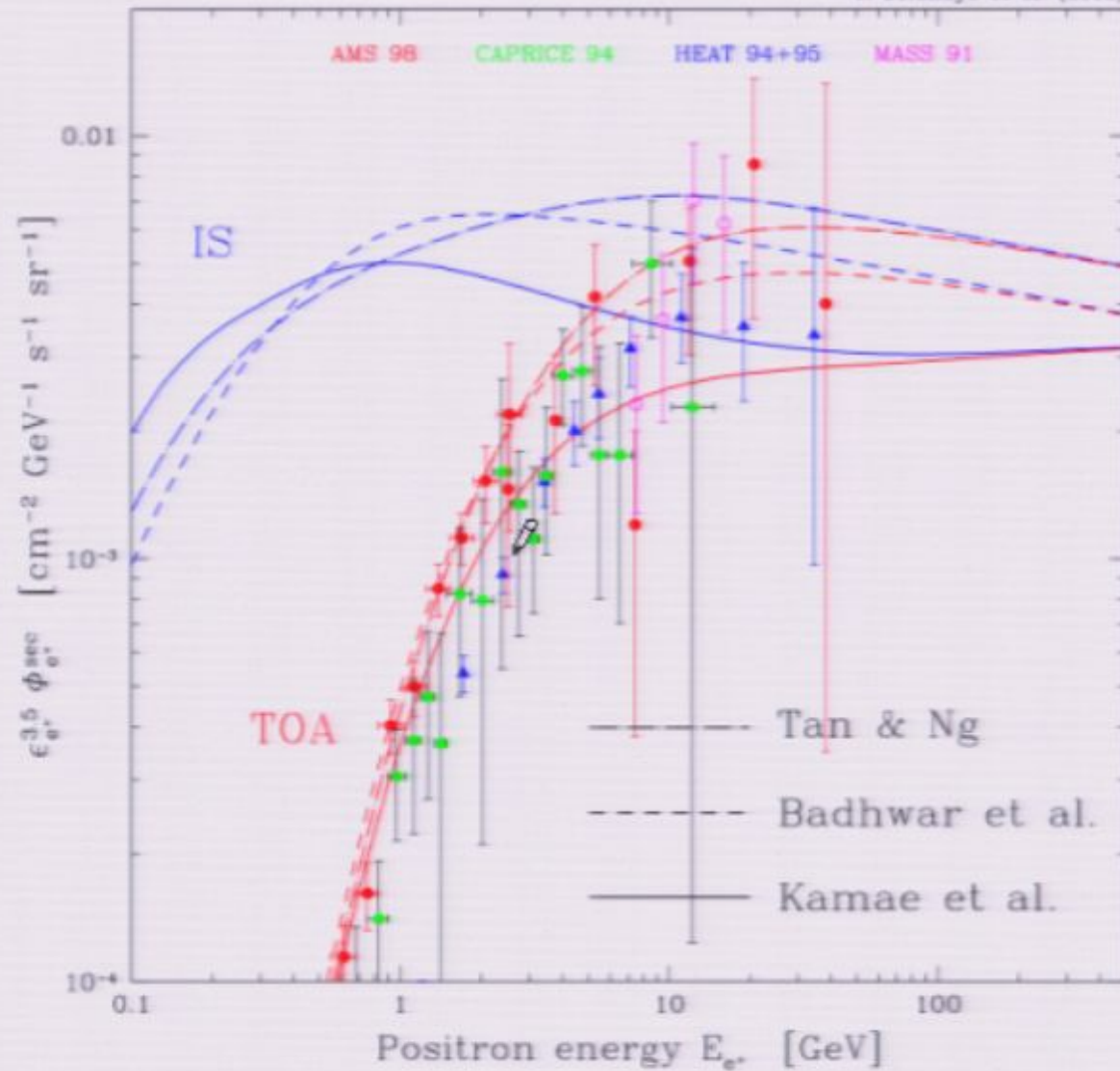
T. Delahaye et al. (2008)



Cross sections

Delahaye T. et al. - arXiv:0809.5268

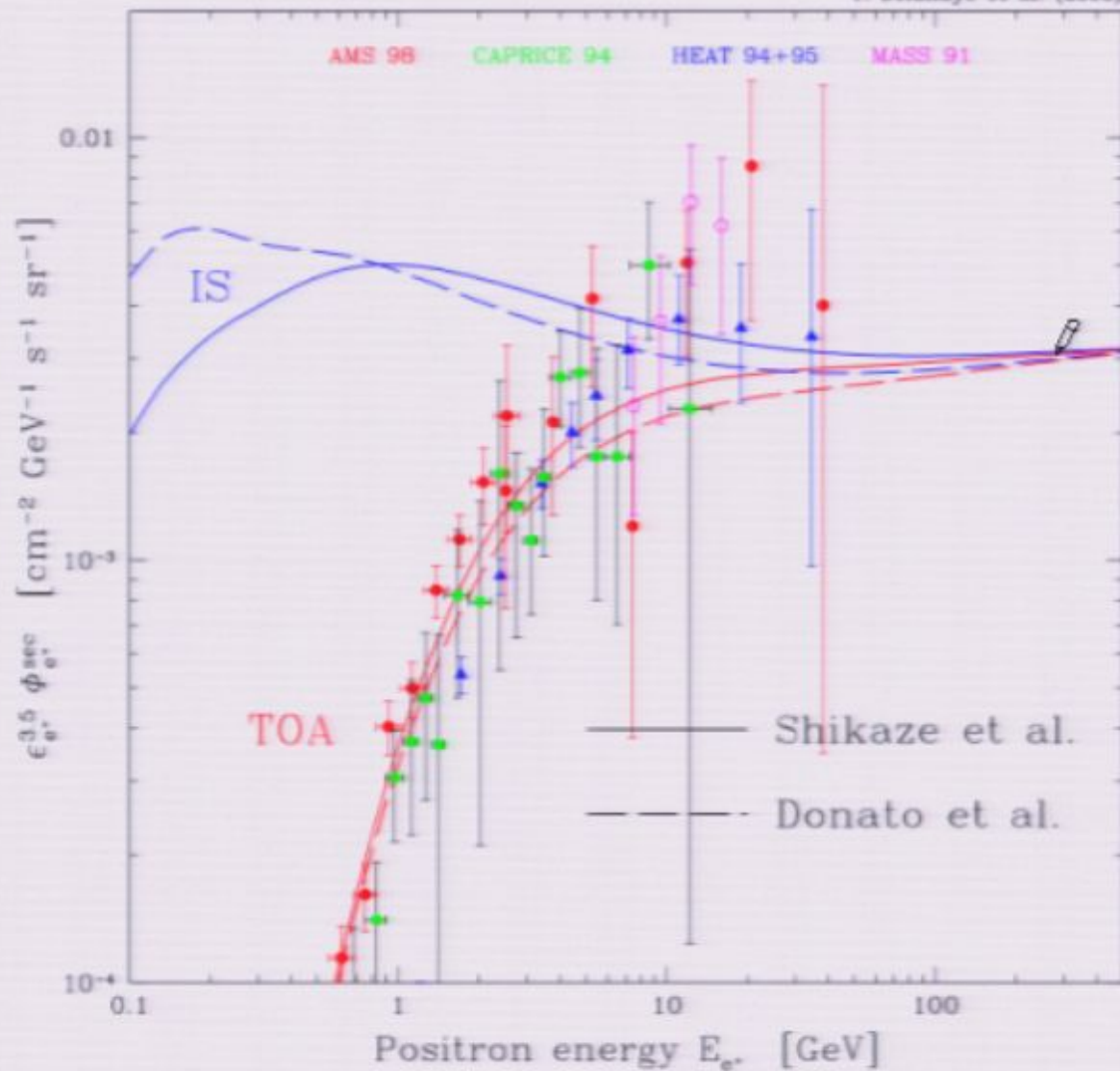
T. Delahaye et al. (2008)



Proton & Helium fluxes

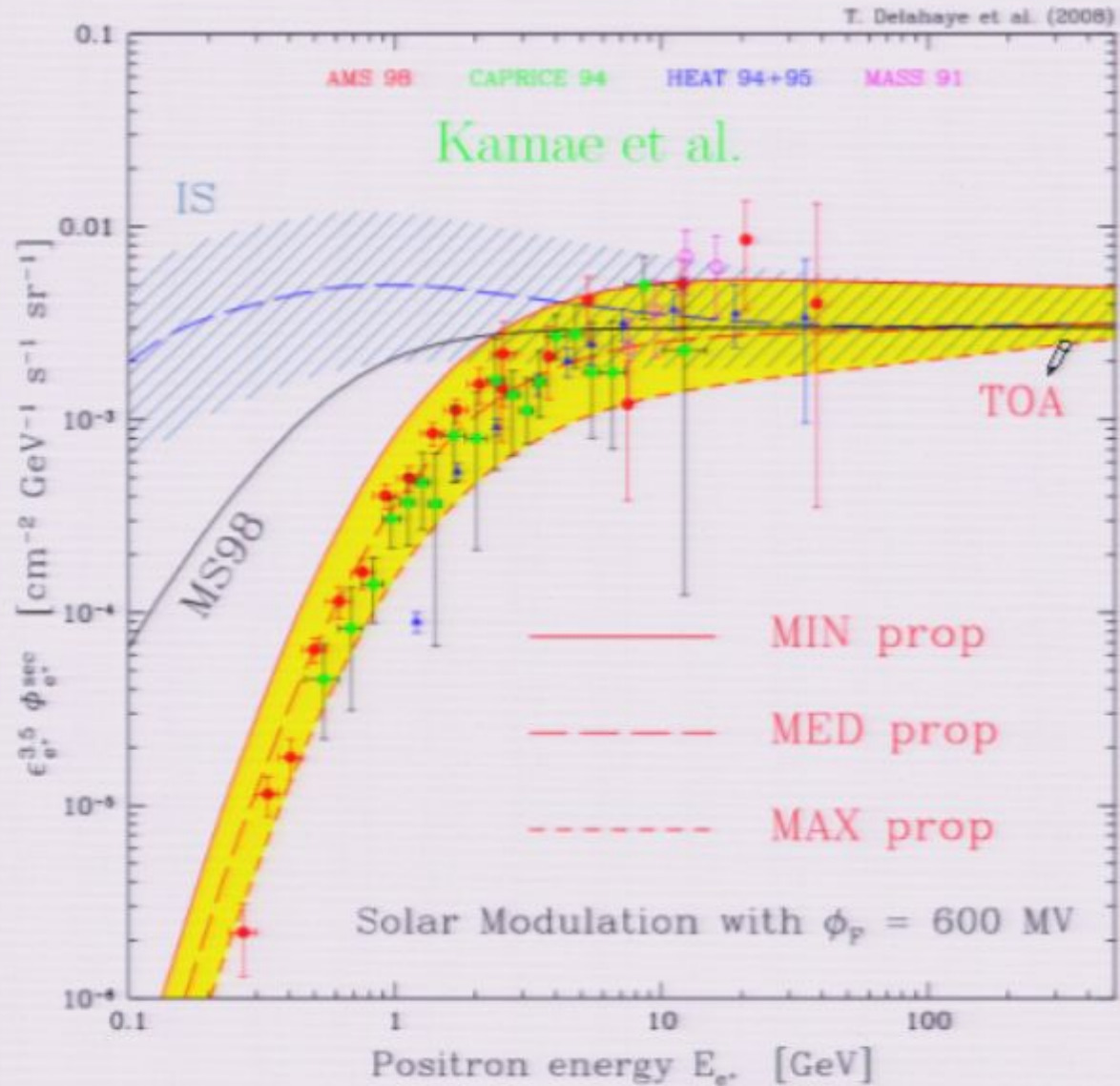
Delahaye T. et al. - arXiv:0809.5268

T. Delahaye et al. (2008)



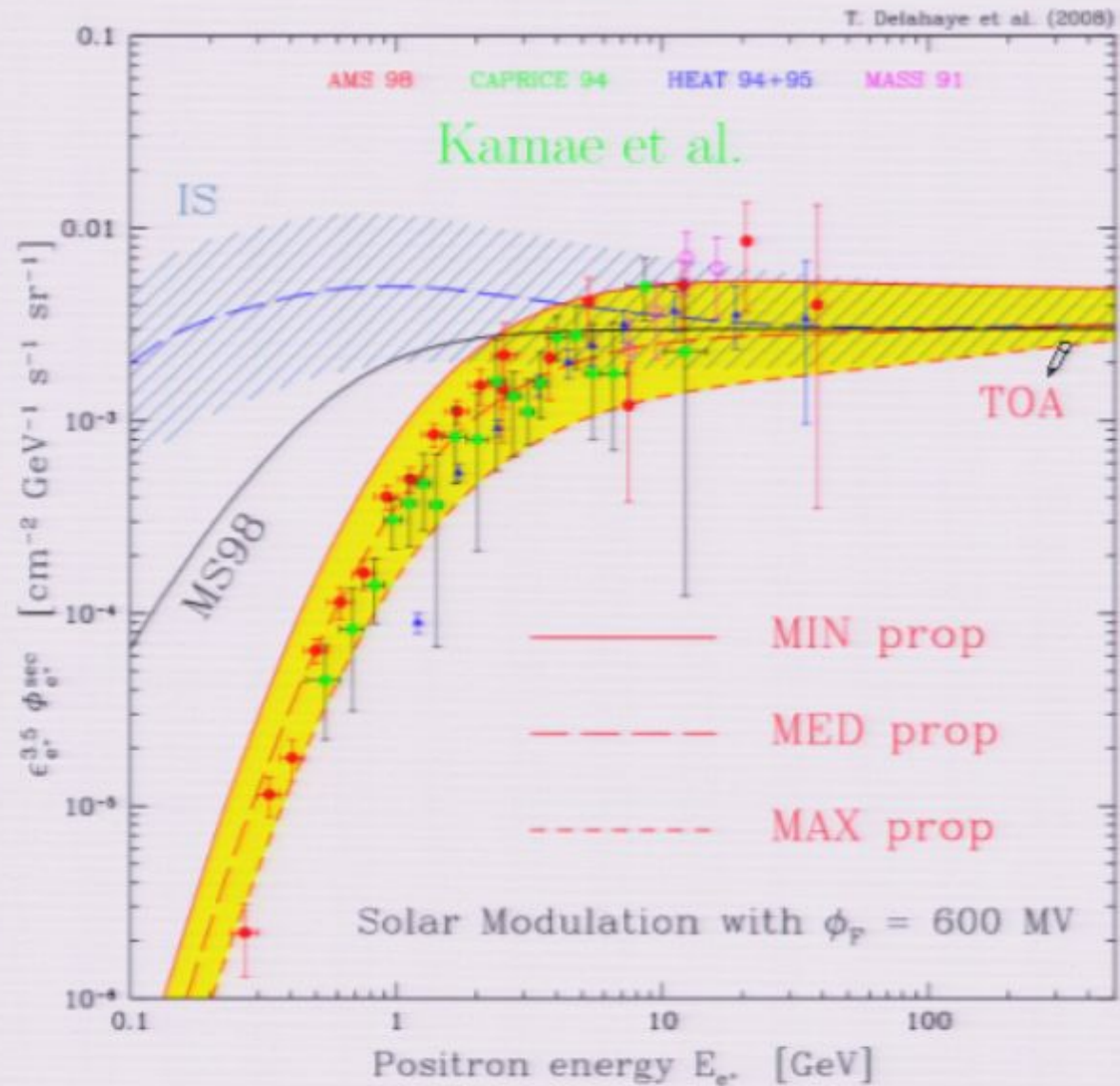
Galactic CR propagation

Delahaye T. et al. - arXiv:0809.5268



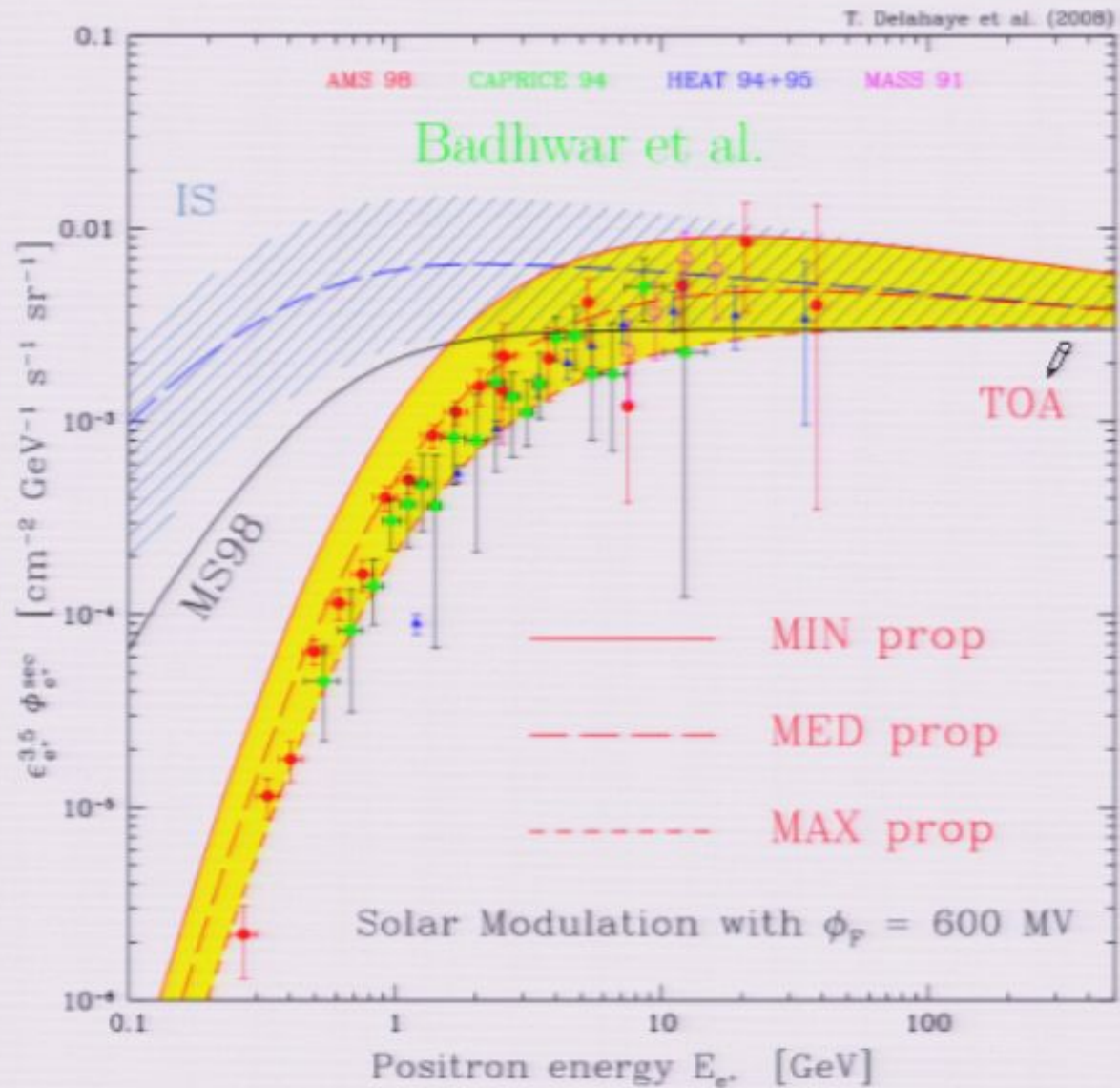
Galactic CR propagation

Delahaye T. et al. - arXiv:0809.5268



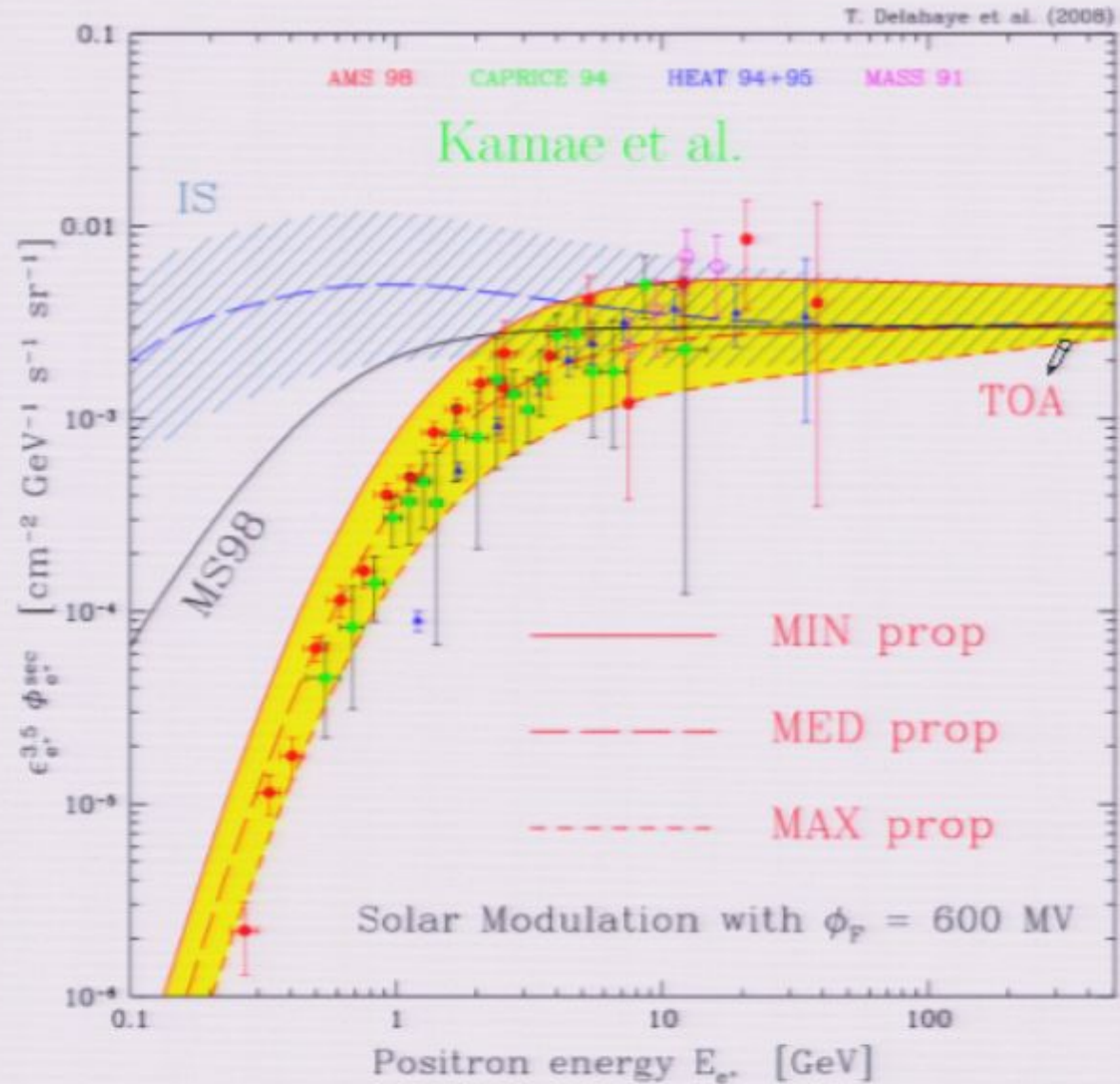
Galactic CR propagation

Delahaye T. et al. – arXiv:0809.5268



Galactic CR propagation

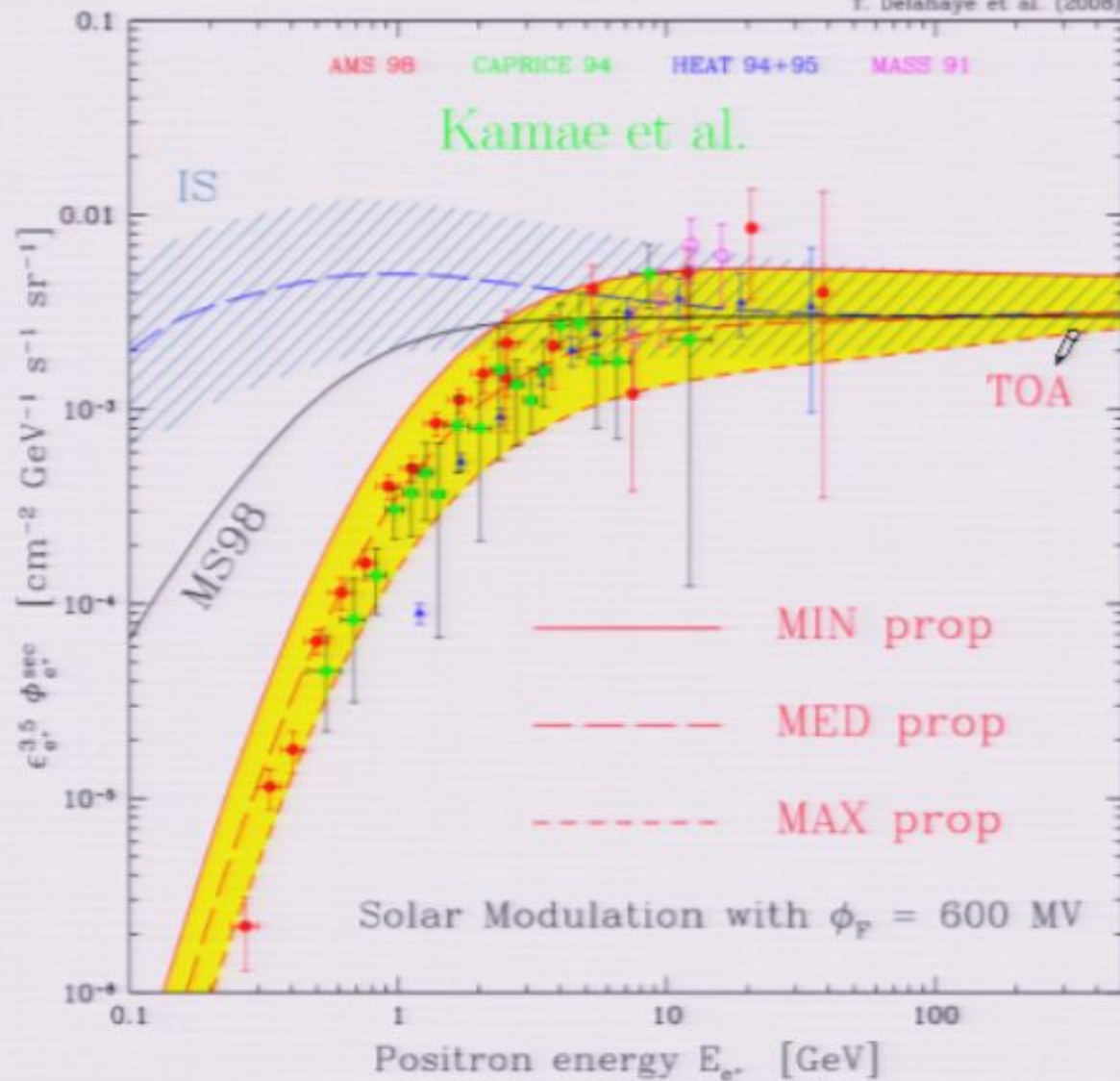
Delahaye T. et al. – arXiv:0809.5268



Galactic CR propagation

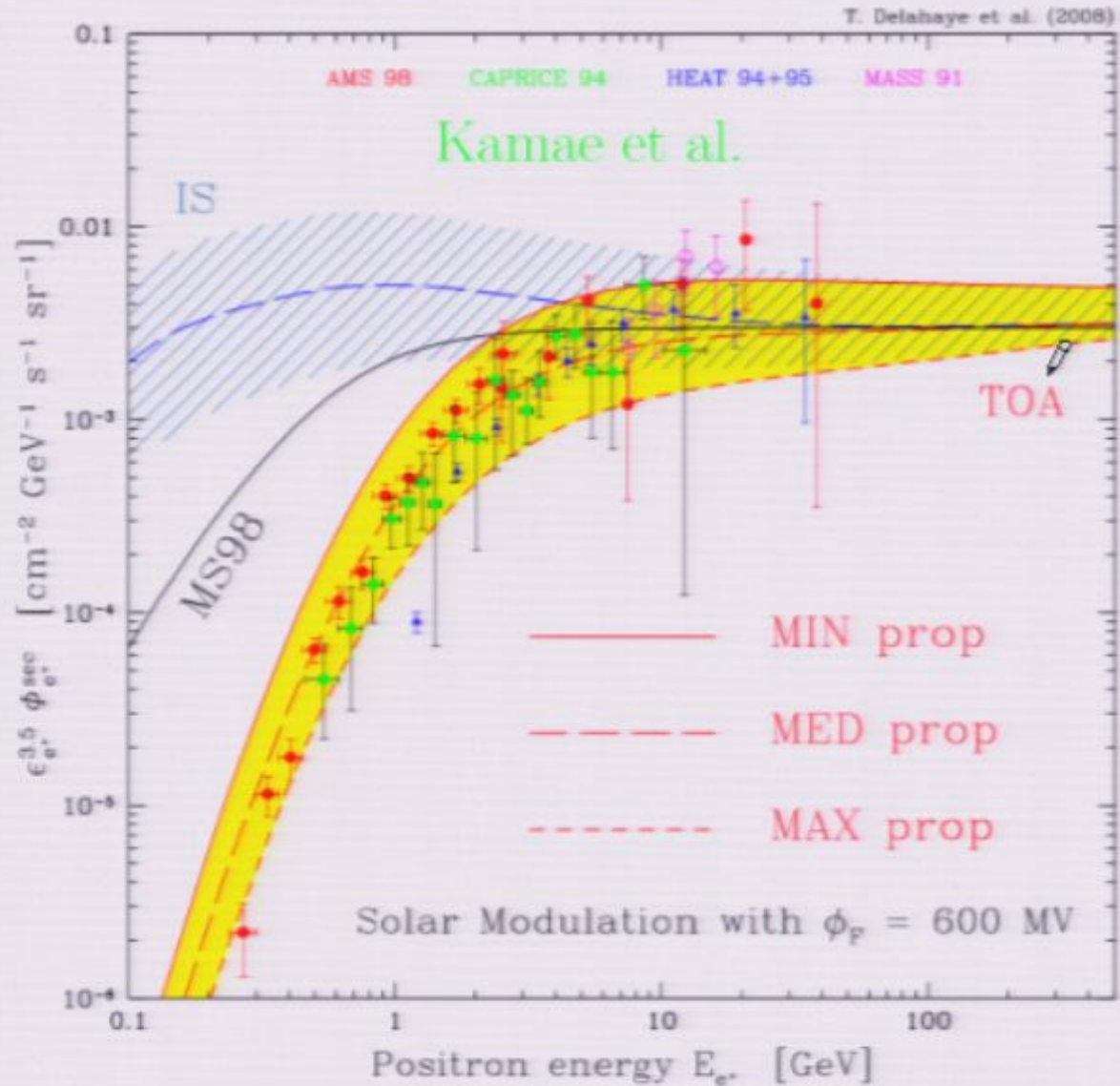
Delahaye T. et al. - arXiv:0809.5268

T. Delahaye et al. (2008)



Galactic CR propagation

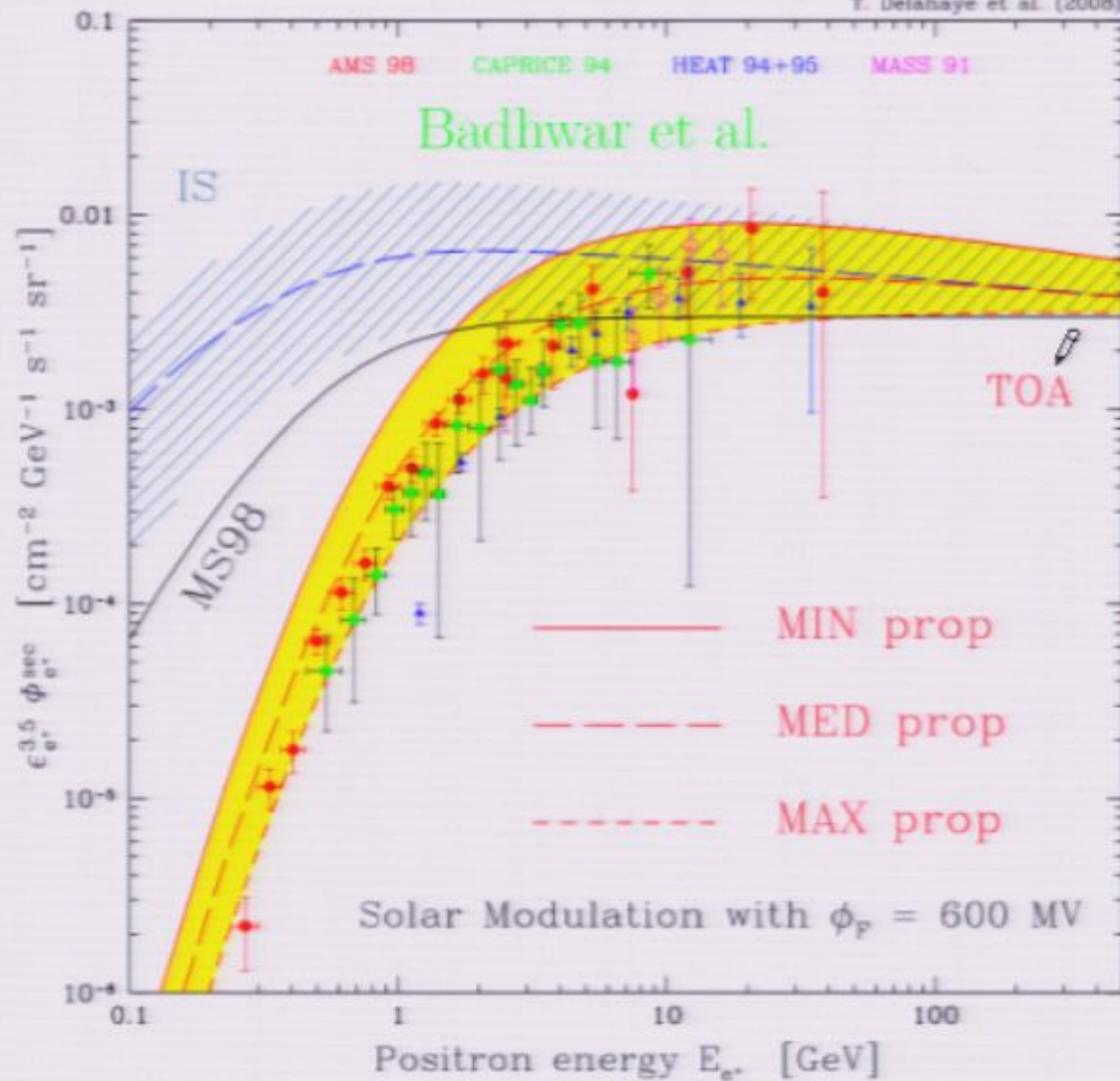
Delahaye T. et al. - arXiv:0809.5268



Galactic CR propagation

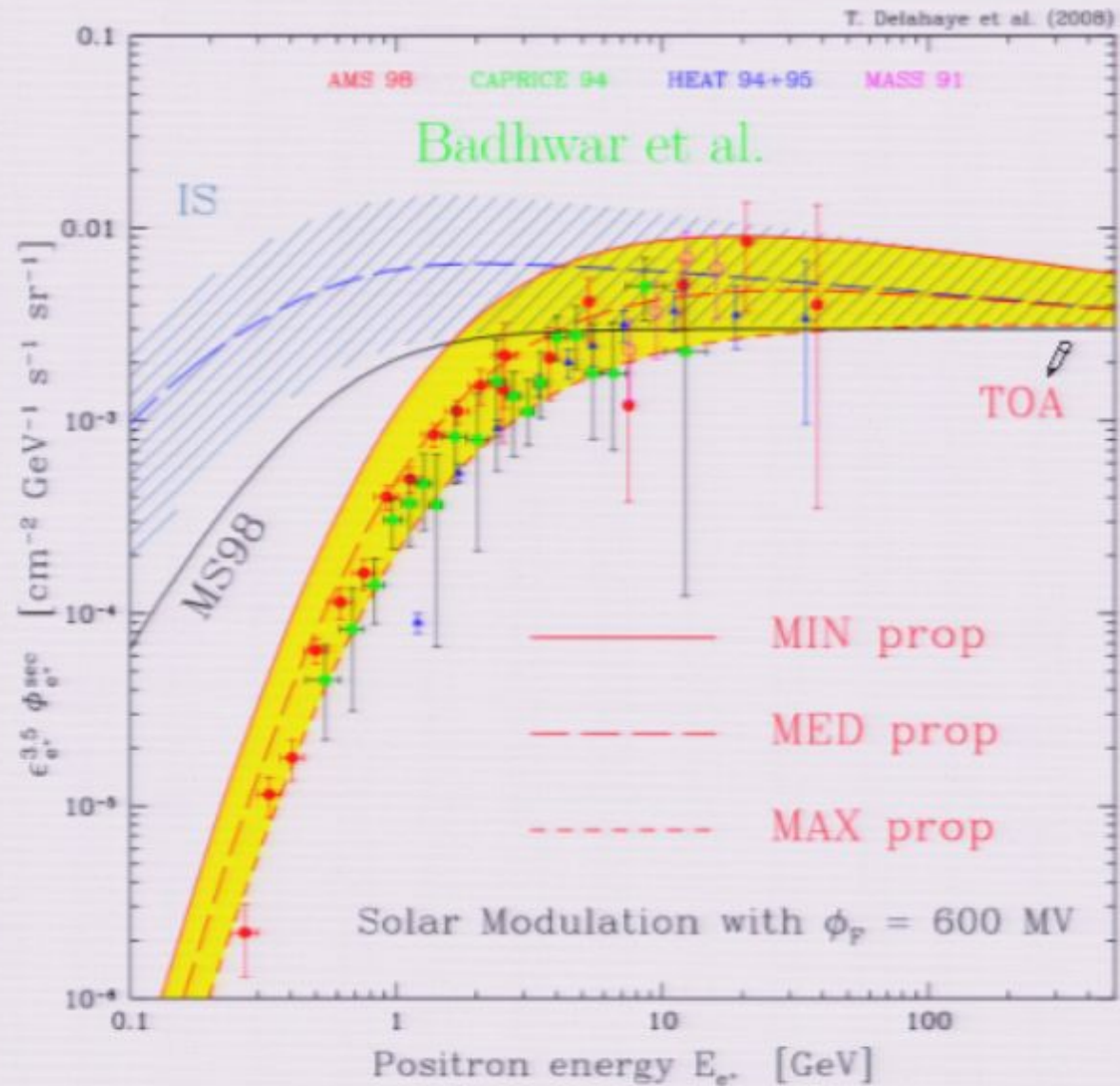
Delahaye T. et al. – arXiv:0809.5268

T. Delahaye et al. (2008)



Galactic CR propagation

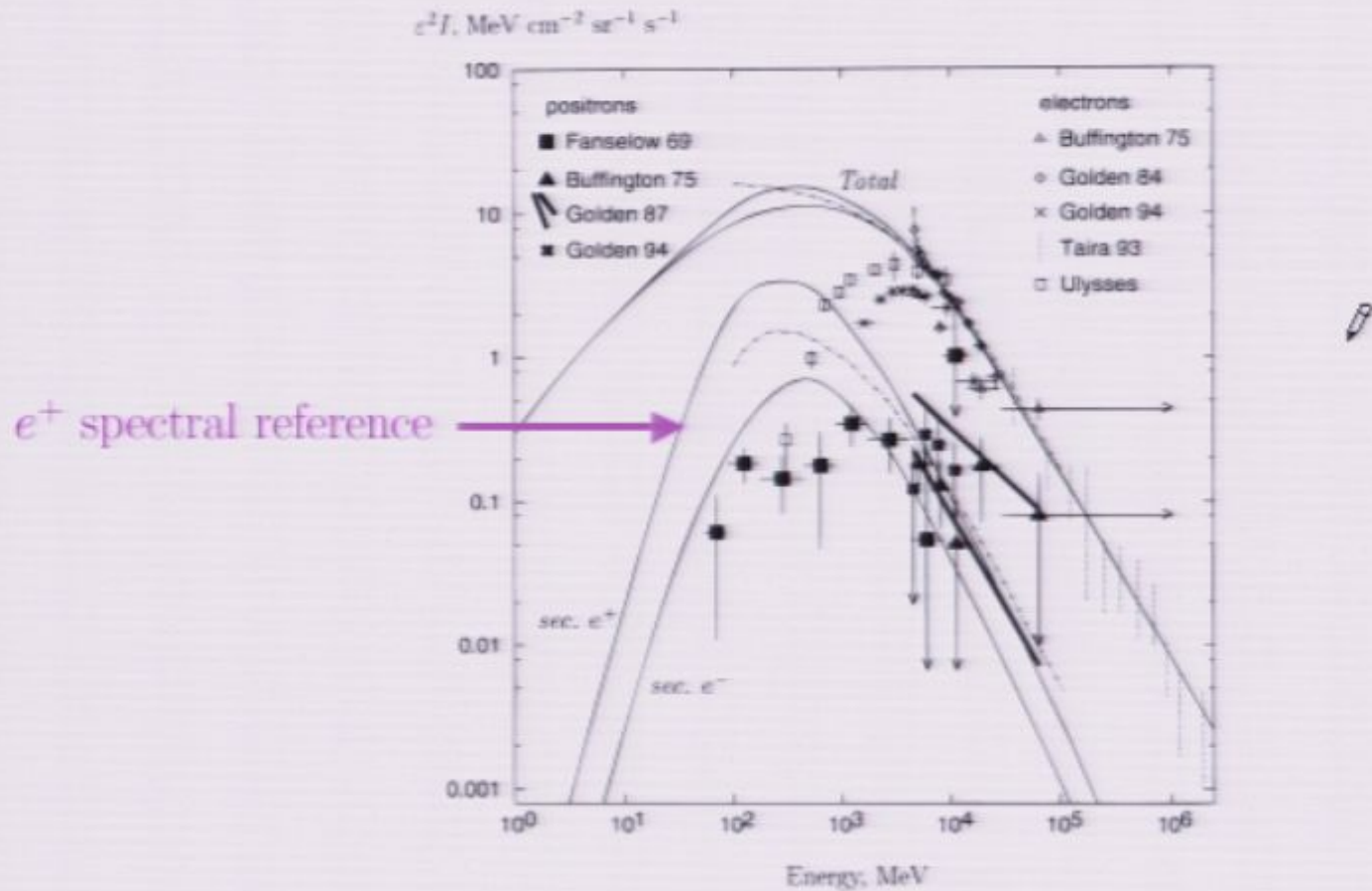
Delahaye T. et al. - arXiv:0809.5268



The secondary e^+ spectrum so far used has been computed in 1998

I. V. Moskalenko and A. W. Strong, *Production and propagation of cosmic ray positrons and electrons*, *Astrophys. J.* **493** (1998) 694 [astro-ph/9710124].

no diffusive reacceleration



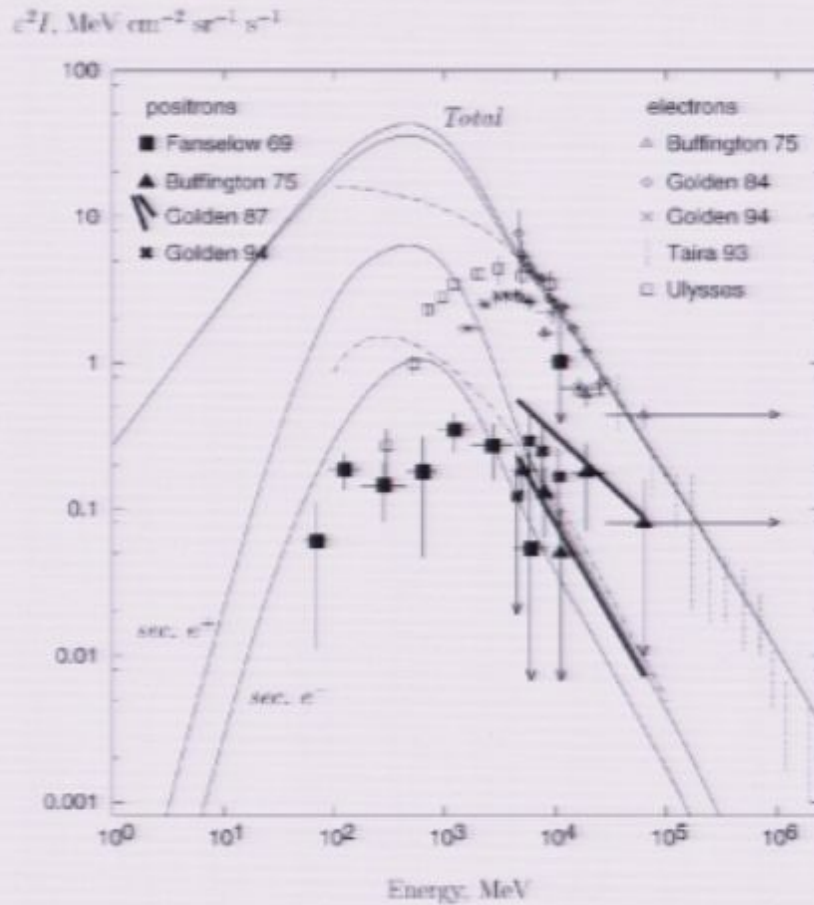
PARAMETERS OF MODELS

Model	z_0 (kpc)	D_0 ($\text{cm}^2 \text{s}^{-1}$)	ρ_0 (MV/c)	δ	v_A (km s^{-1})	PROTONS			HELIUM		
						γ	ρ_0^+	I_0^+	γ	ρ_0^+	I_0^+
08-005.....	3	2.0×10^{28}	3.0×10^5	0.60	0	2.15	10^6	3×10^{-6}	2.35	4×10^6	4×10^{-6}
08-006.....	3	4.2×10^{28}	3.0×10^5	0.33	20	2.25	10^6	3×10^{-6}	2.45	4×10^6	4×10^{-6}
08-009.....	3	2.0×10^{28}	3.0×10^5	0.60	0	2.00	10^6	3×10^{-6}	2.00	4×10^6	4×10^{-6}

The secondary e^+ spectrum so far used has been computed in 1998

I. V. Moskalenko and A. W. Strong, *Production and propagation of cosmic ray positrons and electrons, Astrophys. J.* **493** (1998) 694 [astro-ph/9710124].

diffusive reacceleration



PARAMETERS OF MODELS

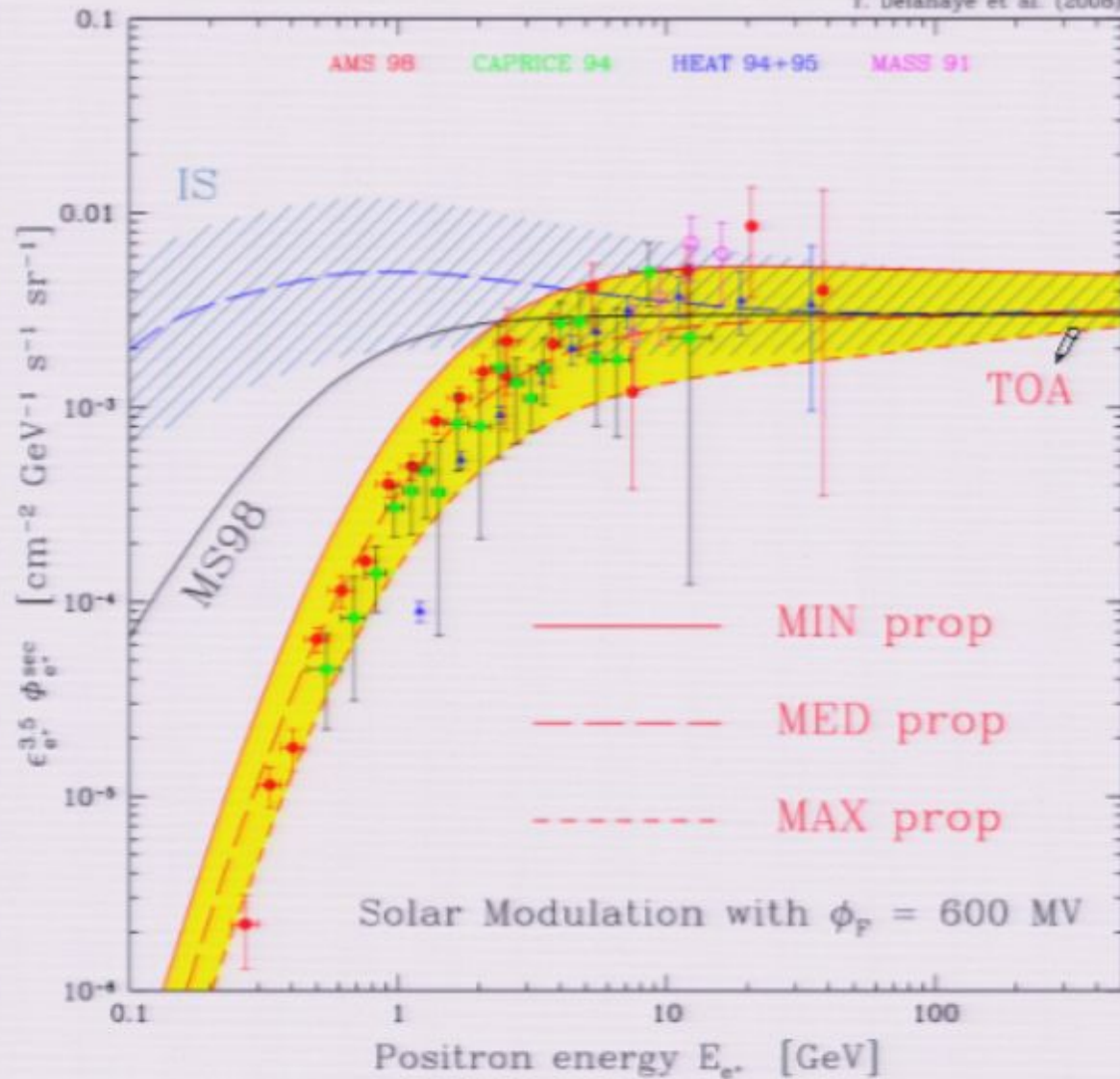
Model	z_0 (kpc)	D_0 ($\text{cm}^2 \text{s}^{-1}$)	ρ_0 (MV/c)	δ	z_0 (km s^{-1})	PROTONS			HELIUM		
						τ	ρ_0^+	I_0^+	τ	ρ_0^+	I_0^+
08-005.....	3	2.0×10^{28}	3.0×10^7	0.60	0	2.15	10^6	3×10^{-6}	2.35	4×10^6	4×10^{-6}
08-006.....	3	4.2×10^{28}	3.0×10^7	0.33	20	2.25	10^6	3×10^{-6}	2.45	4×10^6	4×10^{-6}
08-009.....	3	2.0×10^{28}	3.0×10^7	0.60	0	2.00	10^6	3×10^{-6}	2.00	4×10^6	4×10^{-6}

Absolute e^+ flux

no diffusive reacceleration

Delahaye T. et al. - arXiv:0809.5268

T. Delahaye et al. (2008)

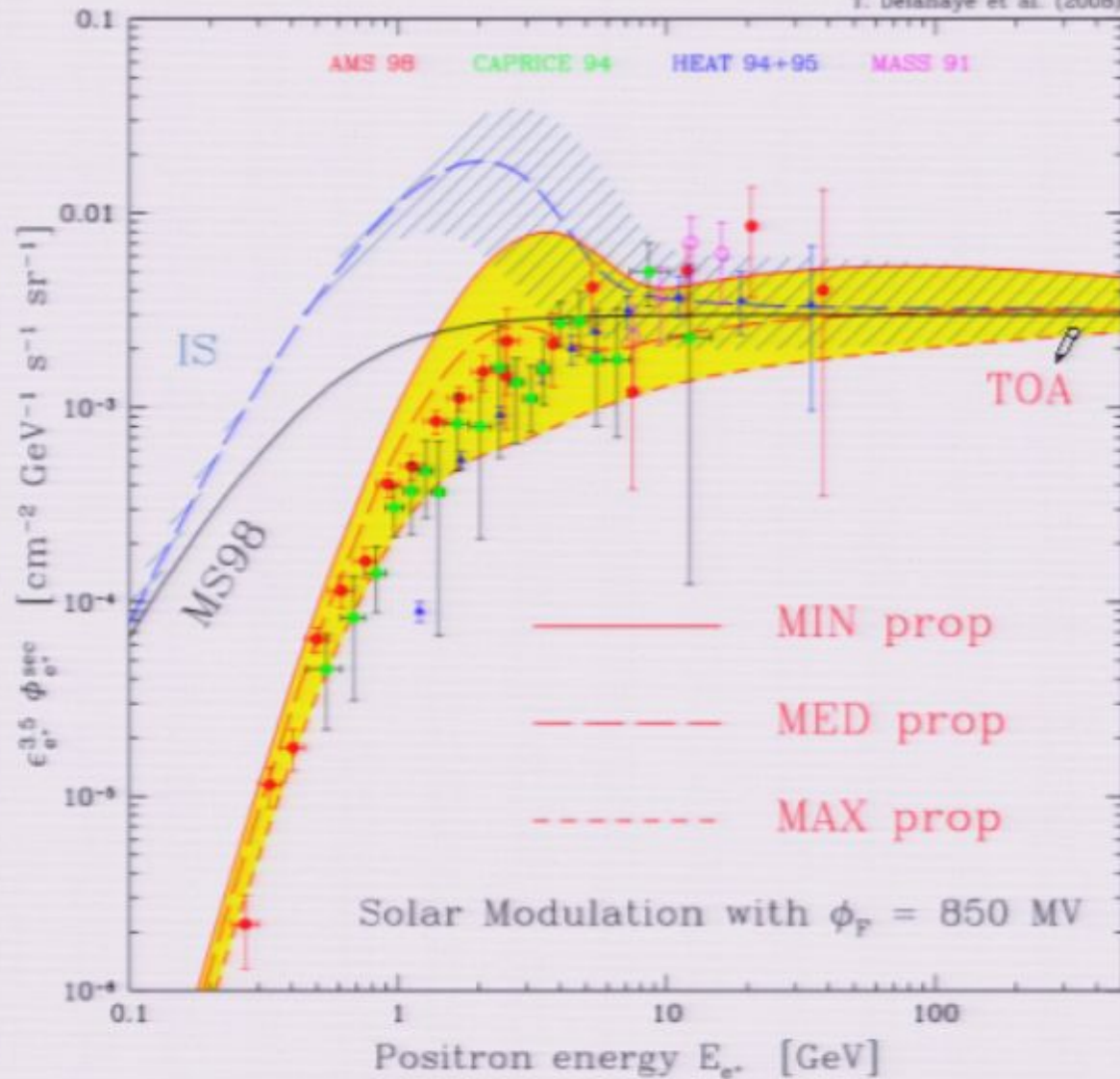


Absolute e^+ flux

diffusive reacceleration

Delahaye T. et al. - arXiv:0809.5268

T. Delahaye et al. (2008)

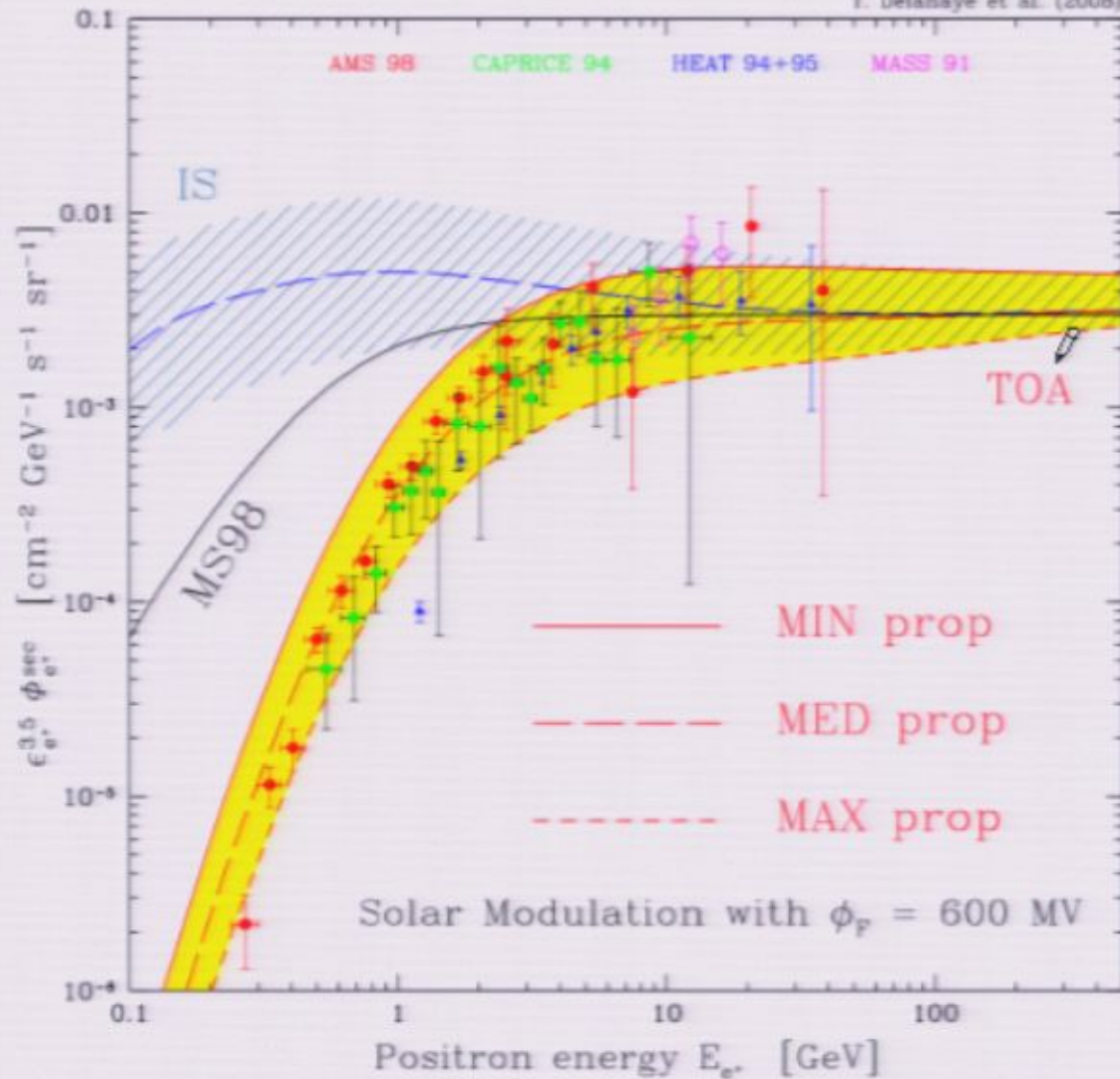


Absolute e^+ flux

no diffusive reacceleration

Delahaye T. et al. - arXiv:0809.5268

T. Delahaye et al. (2008)

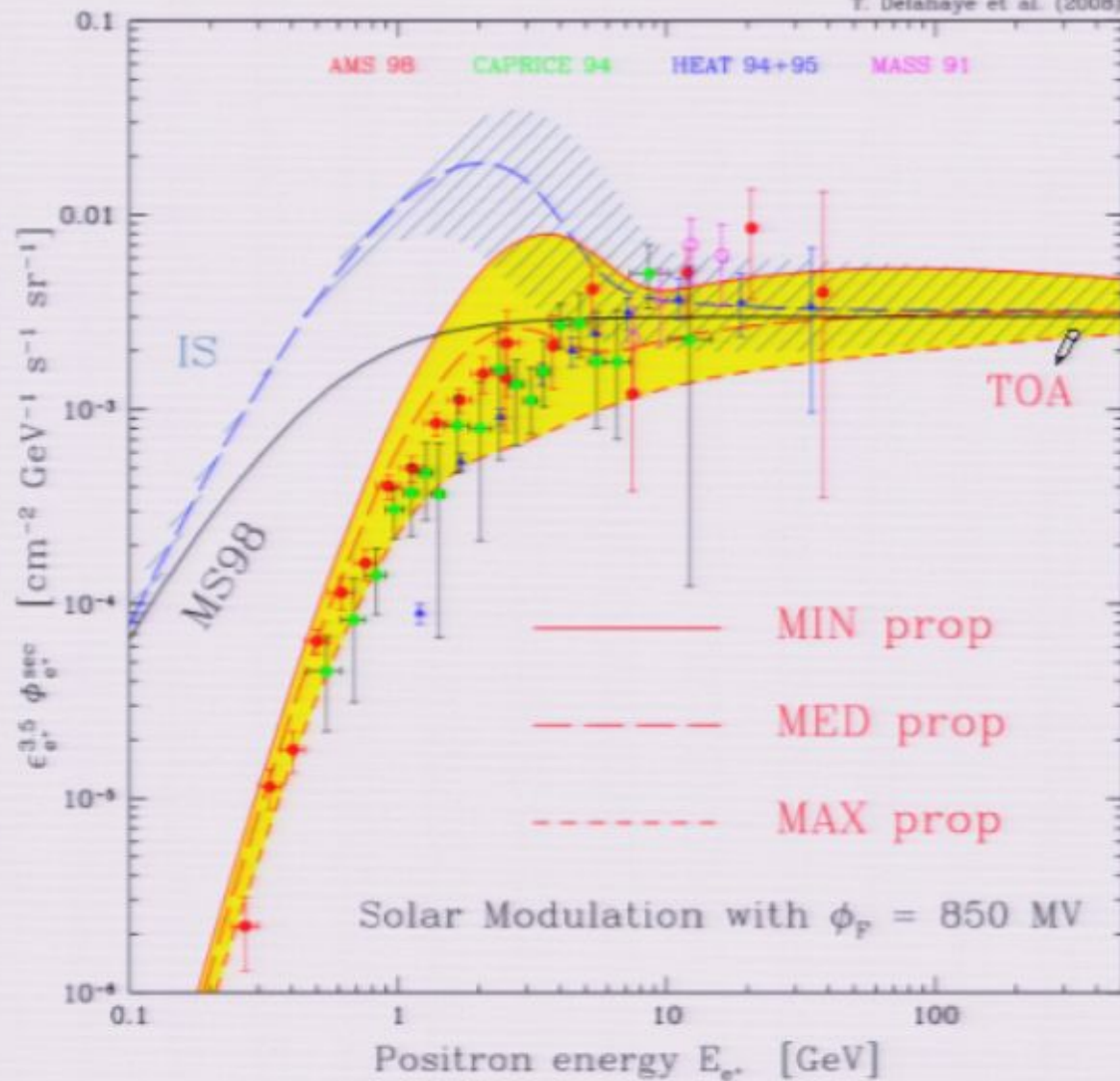


Absolute e^+ flux

diffusive reacceleration

Delahaye T. et al. – arXiv:0809.5268

T. Delahaye et al. (2008)

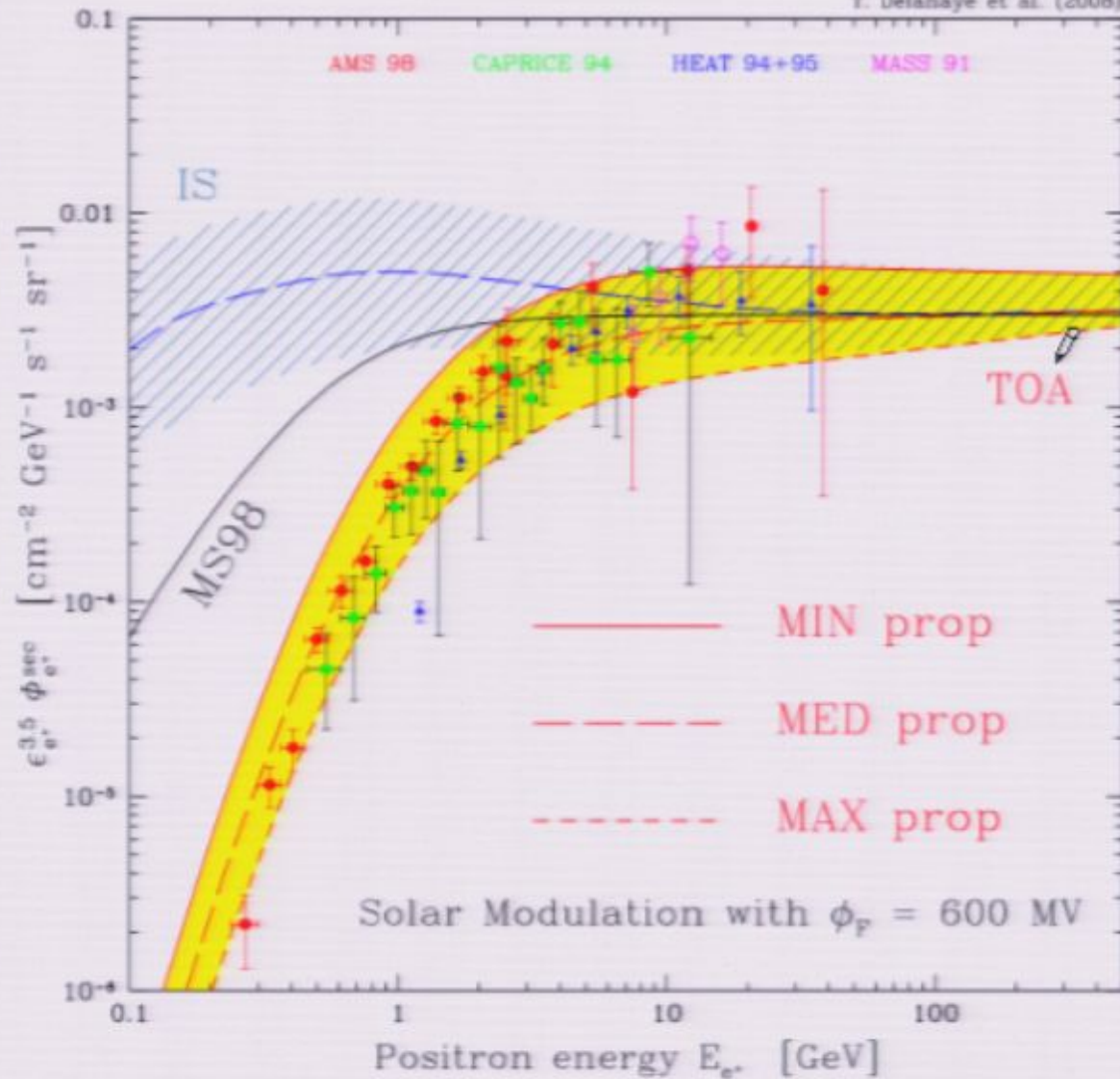


Absolute e^+ flux

no diffusive reacceleration

Delahaye T. et al. - arXiv:0809.5268

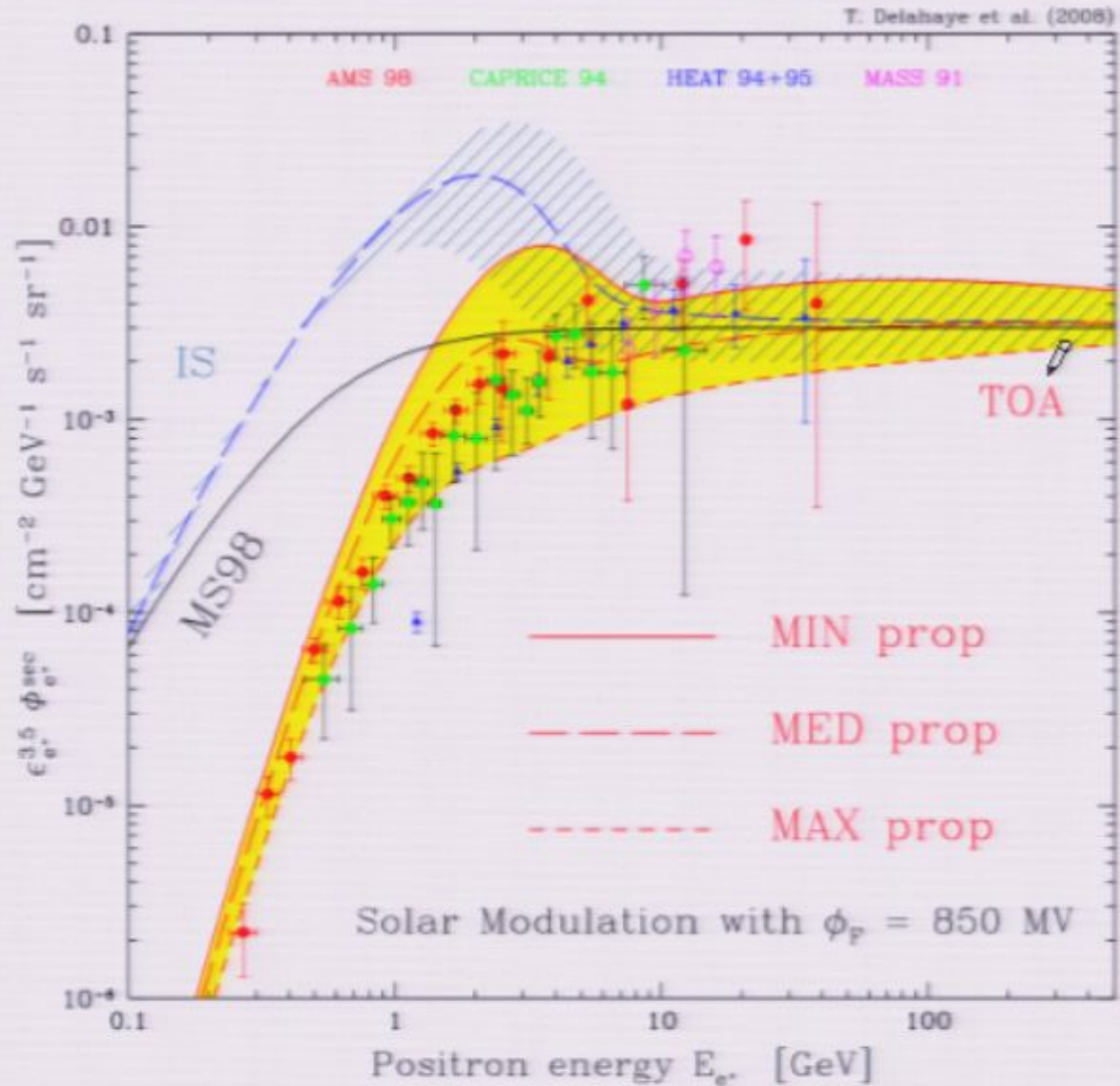
T. Delahaye et al. (2008)



Absolute e^+ flux

diffusive reacceleration

Delahaye T. et al. - arXiv:0809.5268

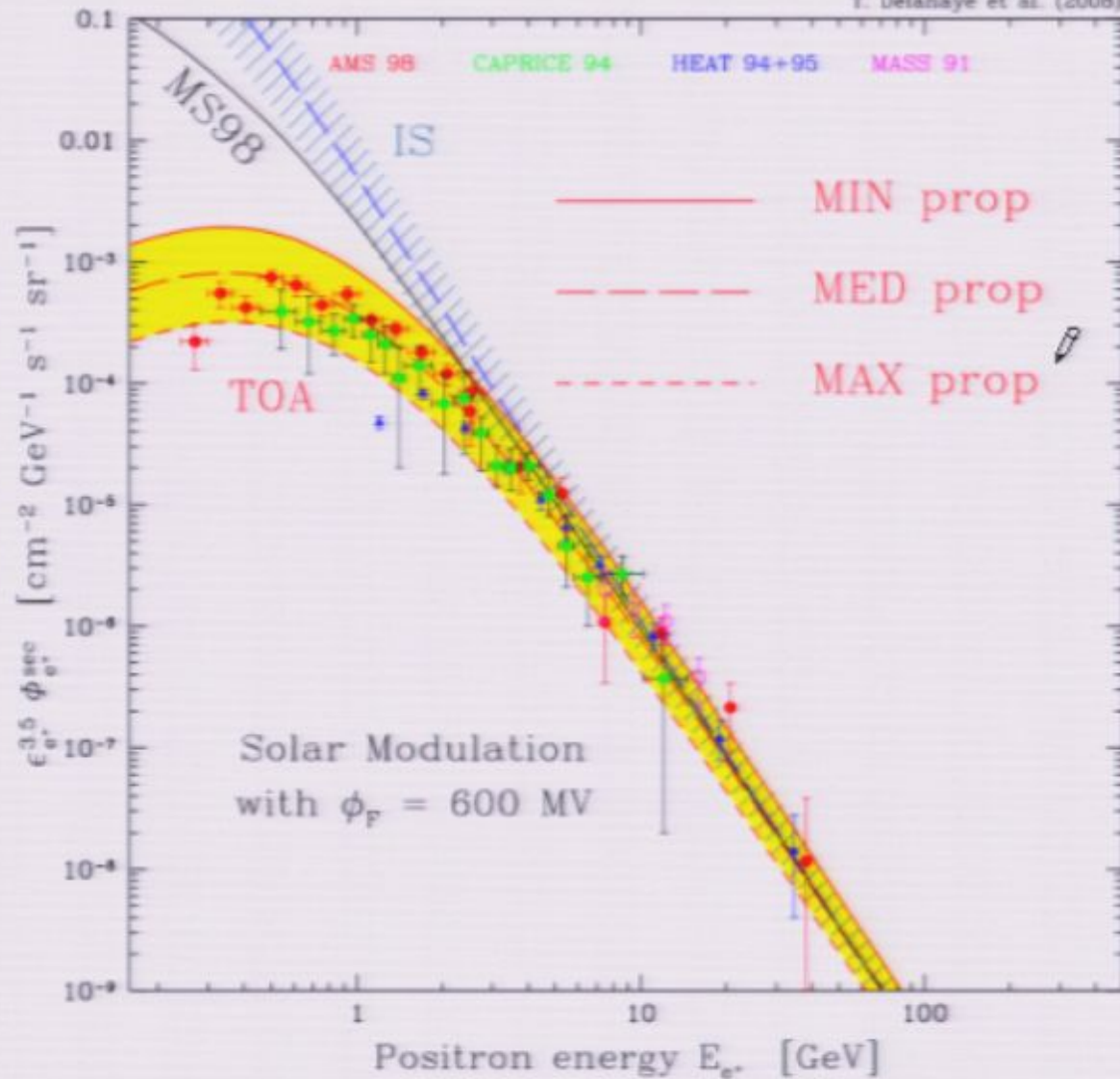


Absolute e^+ flux

no diffusive reacceleration

Delahaye T. et al. – arXiv:0809.5268

T. Delahaye et al. (2008)

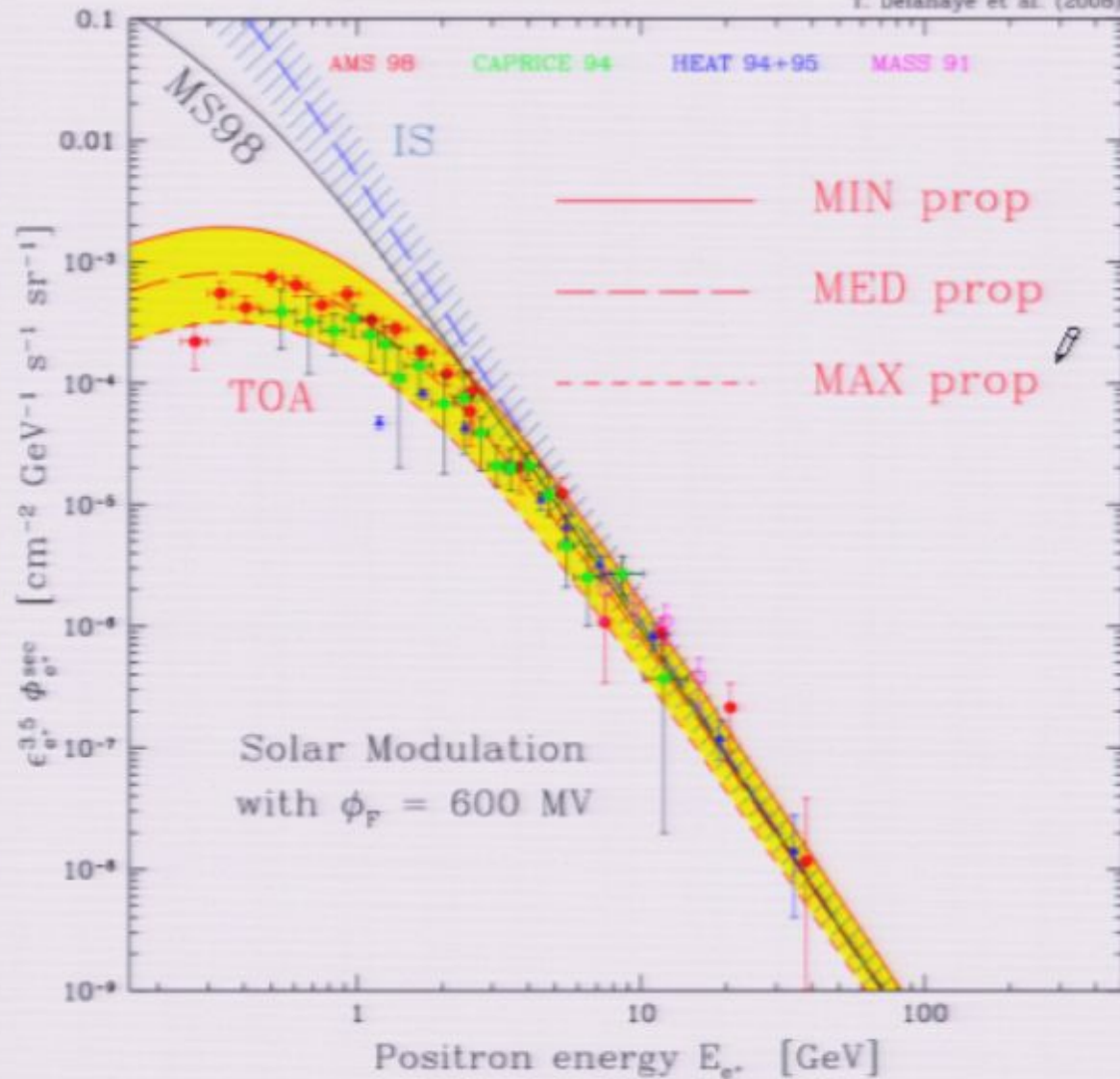


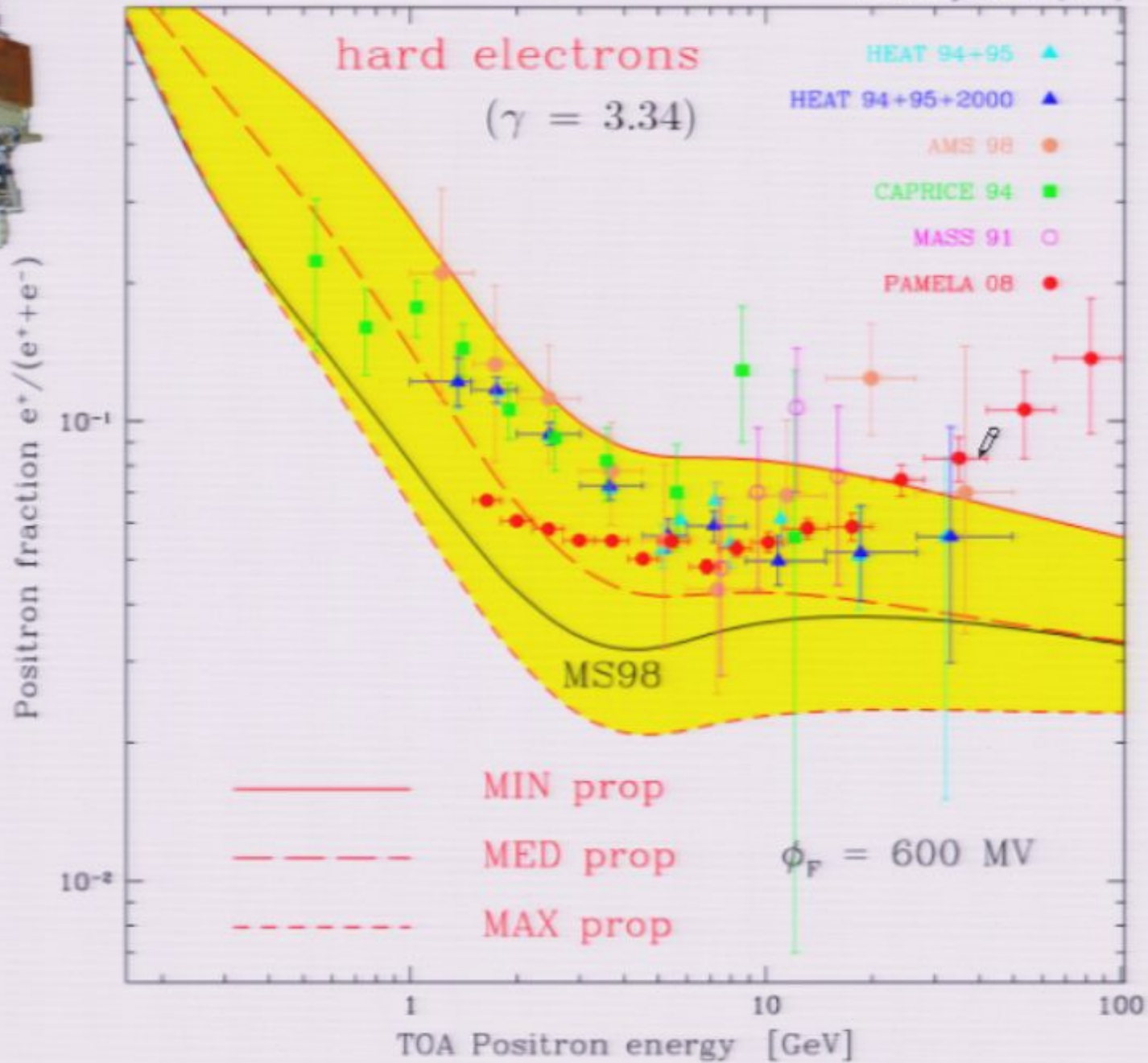
Absolute e^+ flux

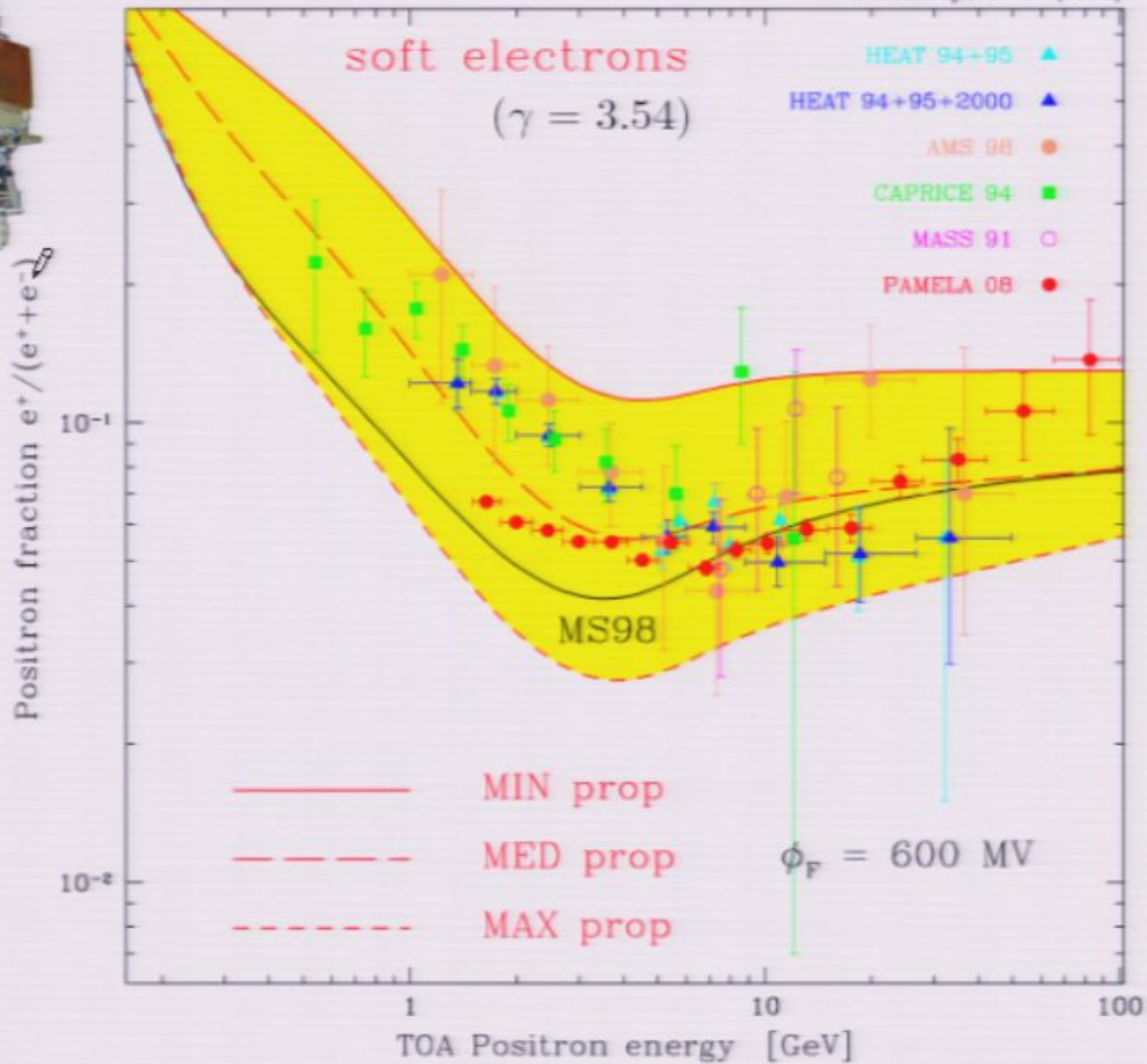
no diffusive reacceleration

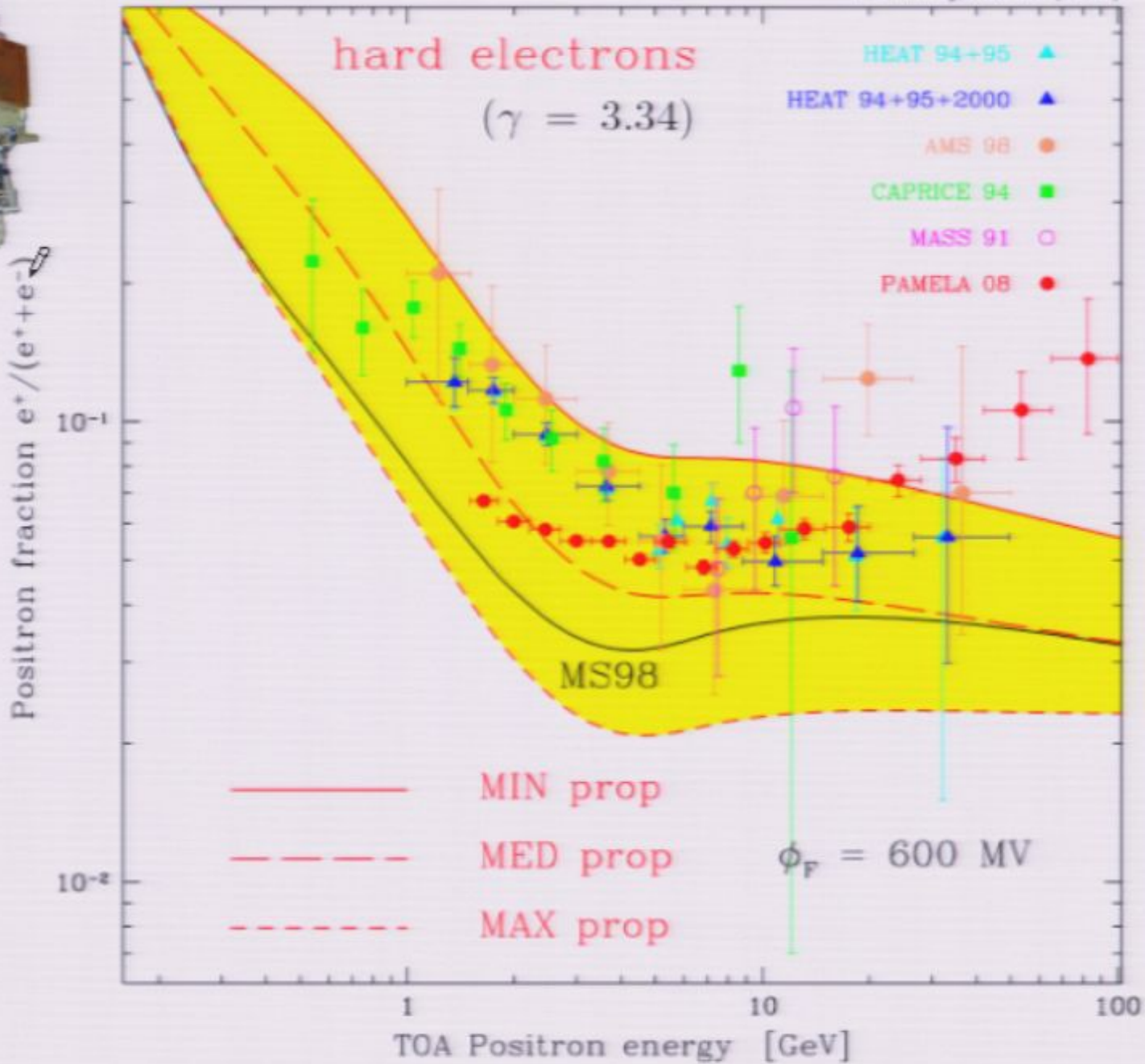
Delahaye T. et al. - arXiv:0809.5268

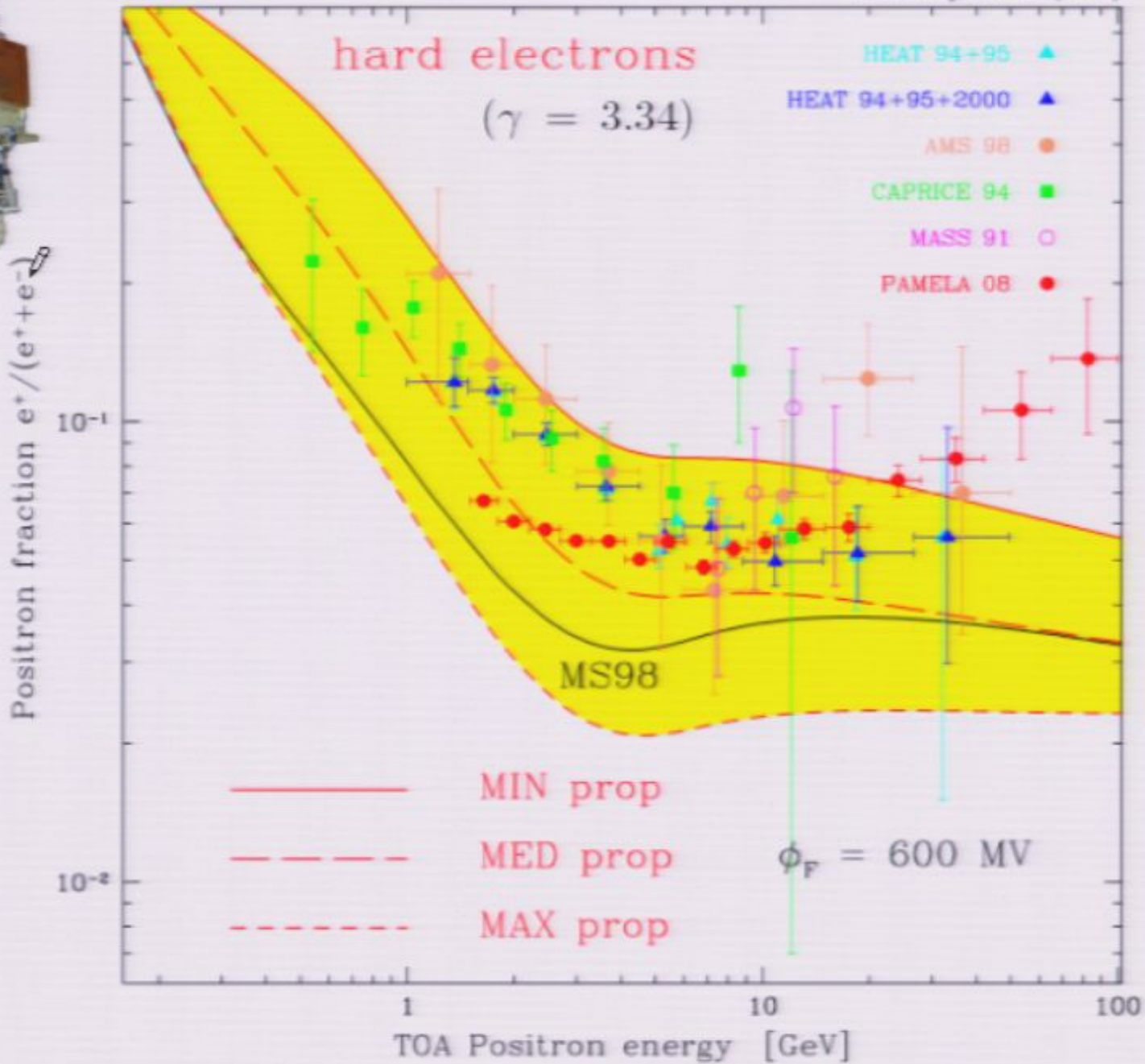
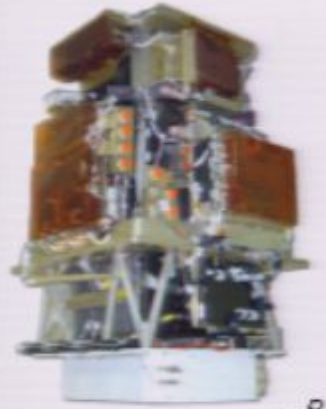
T. Delahaye et al. (2008)

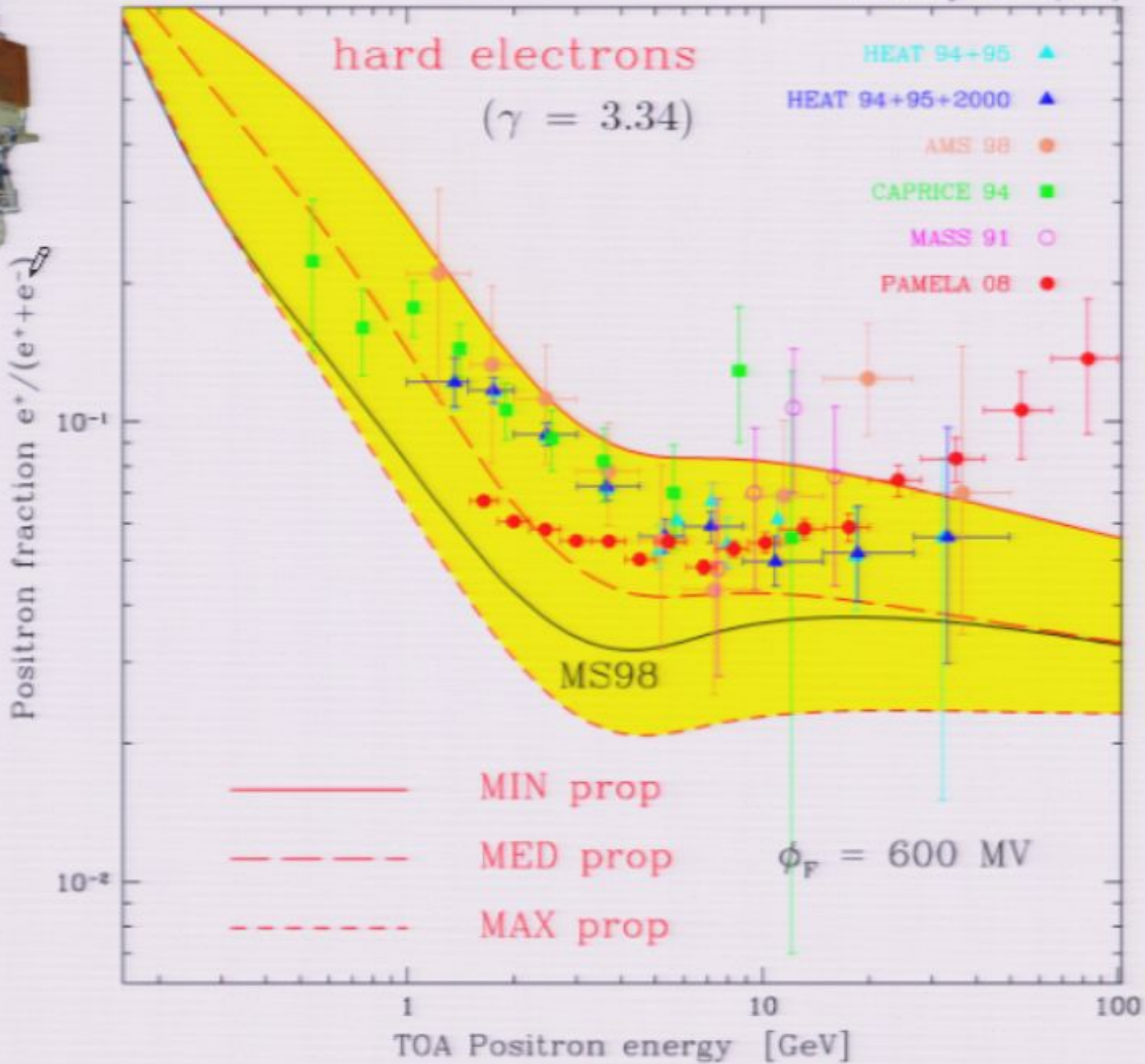


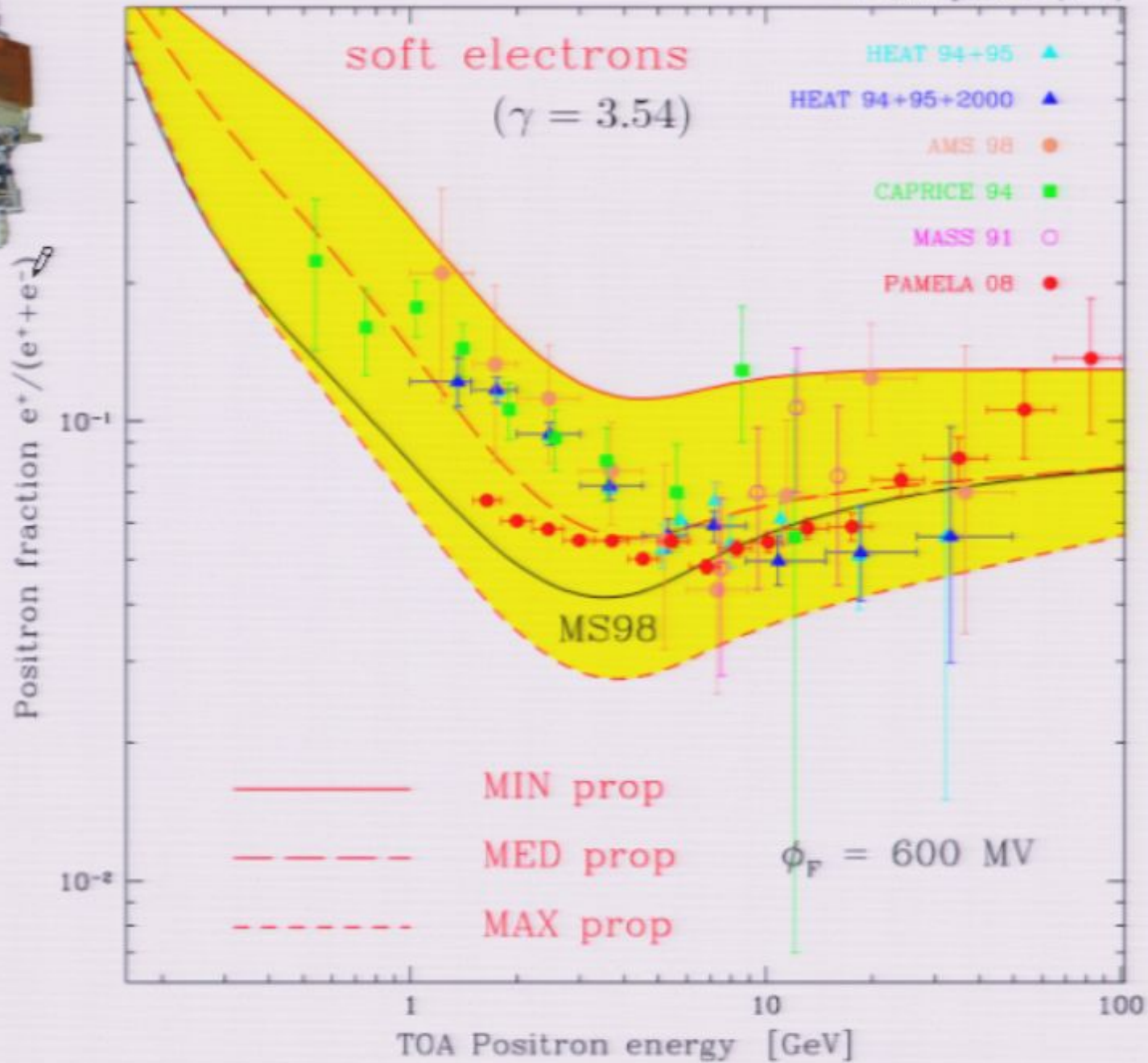






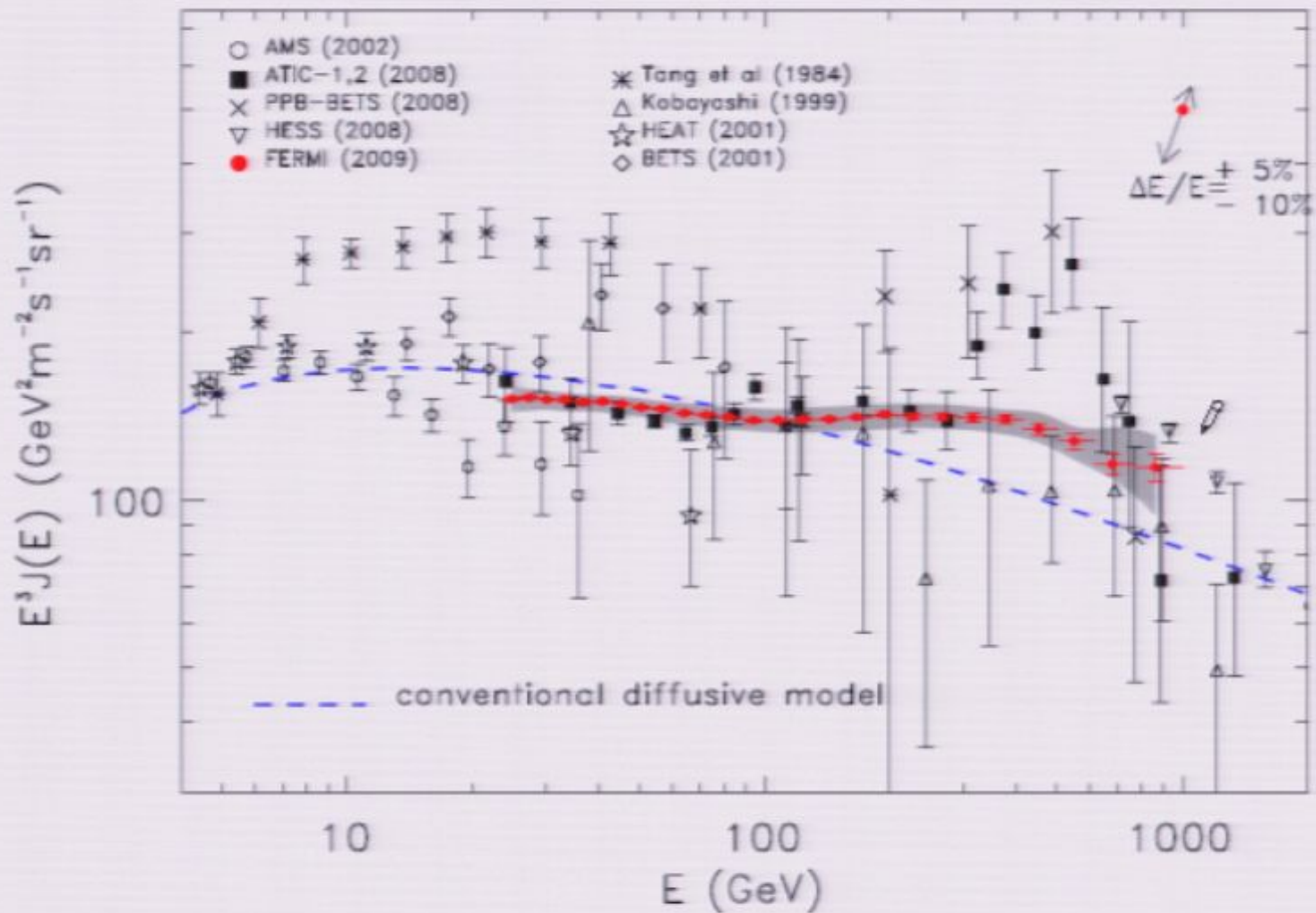


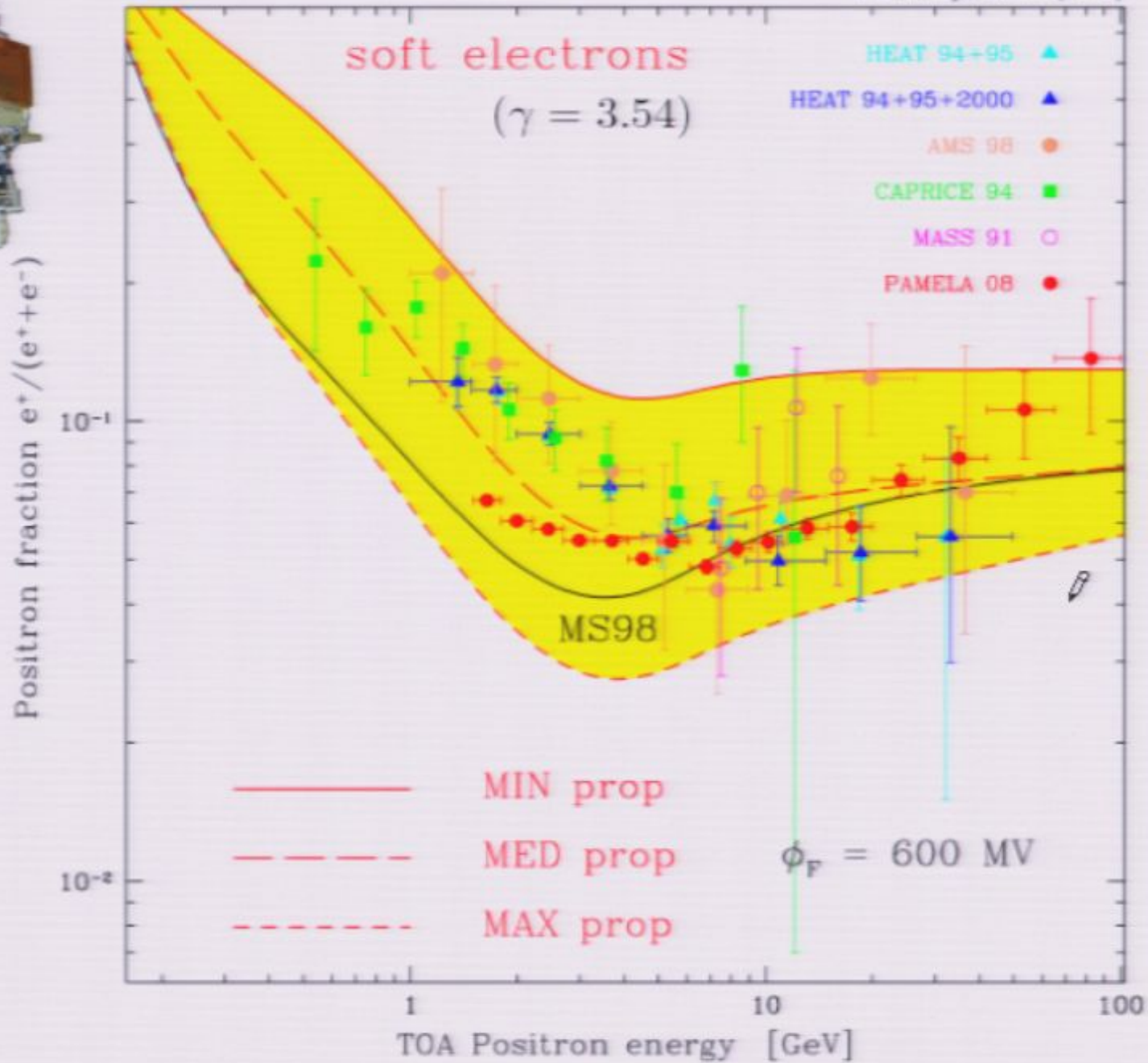




Measurement of the Cosmic Ray $e^+ + e^-$ spectrum from 20 GeV to 1 TeV with the Fermi Large Area Telescope

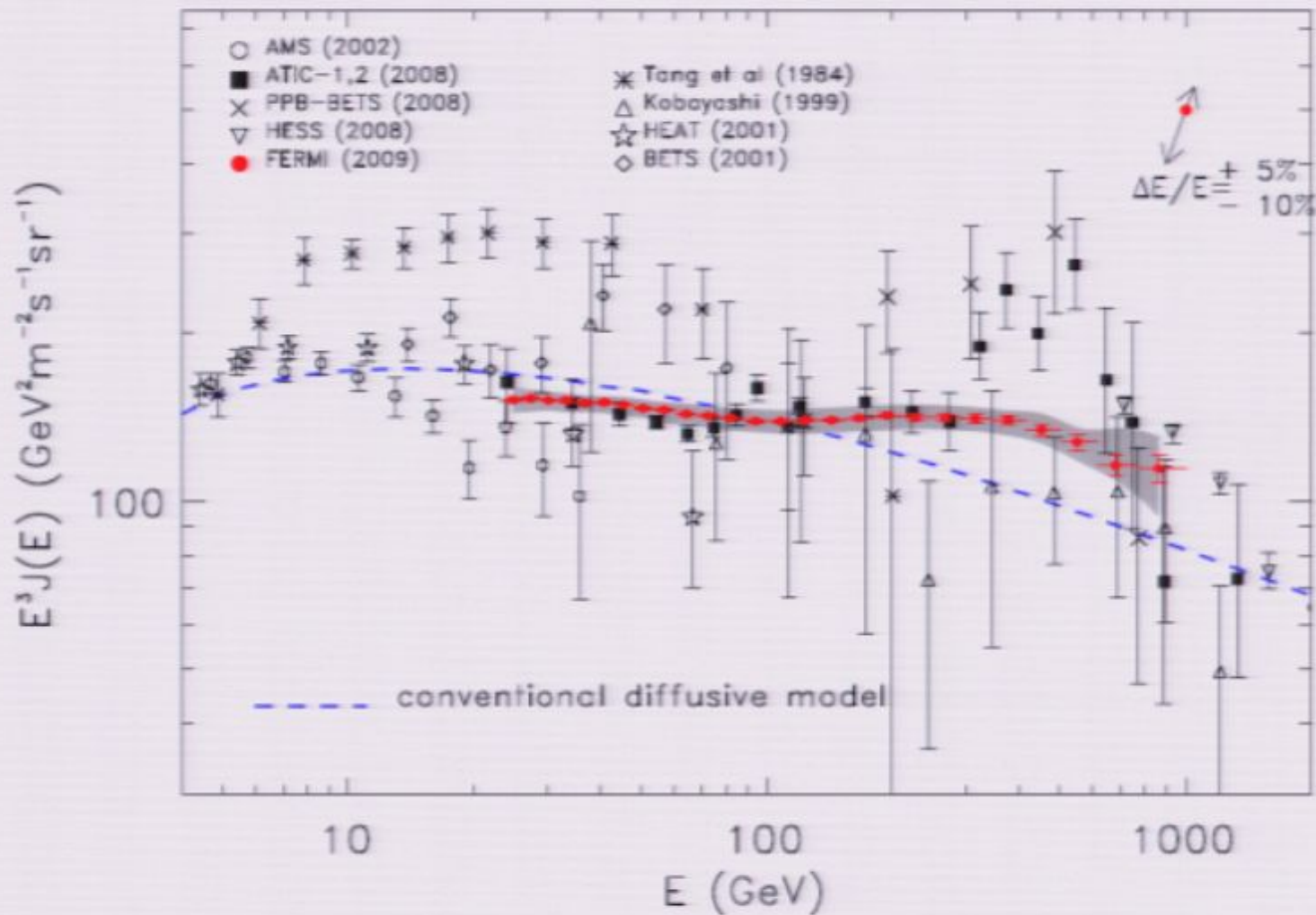
arXiv:0905.0025v1 [astro-ph.HE] 30 Apr 2009





Measurement of the Cosmic Ray $e^+ + e^-$ spectrum from 20 GeV to 1 TeV with the Fermi Large Area Telescope

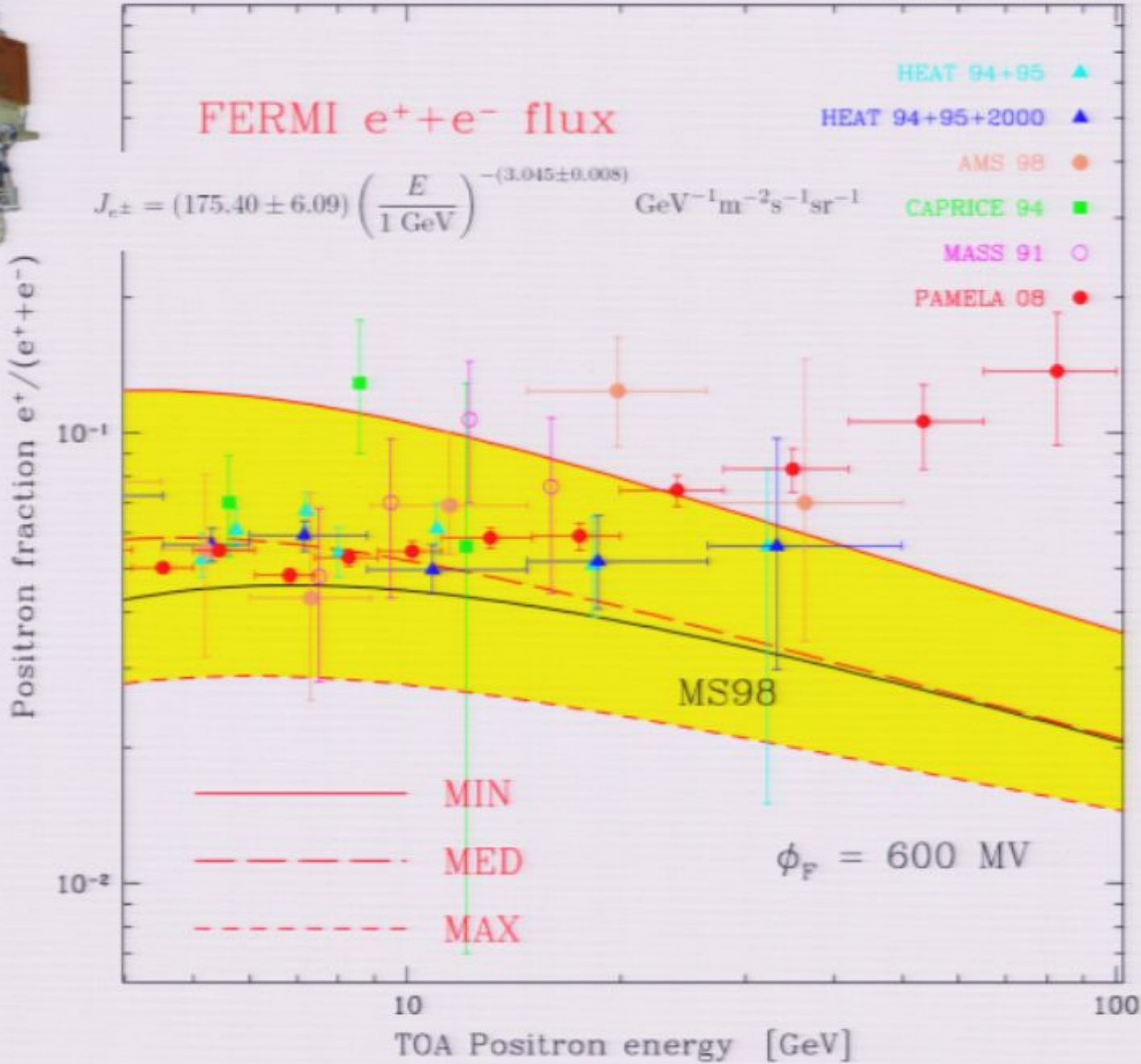
arXiv:0905.0025v1 [astro-ph.HE] 30 Apr 2009



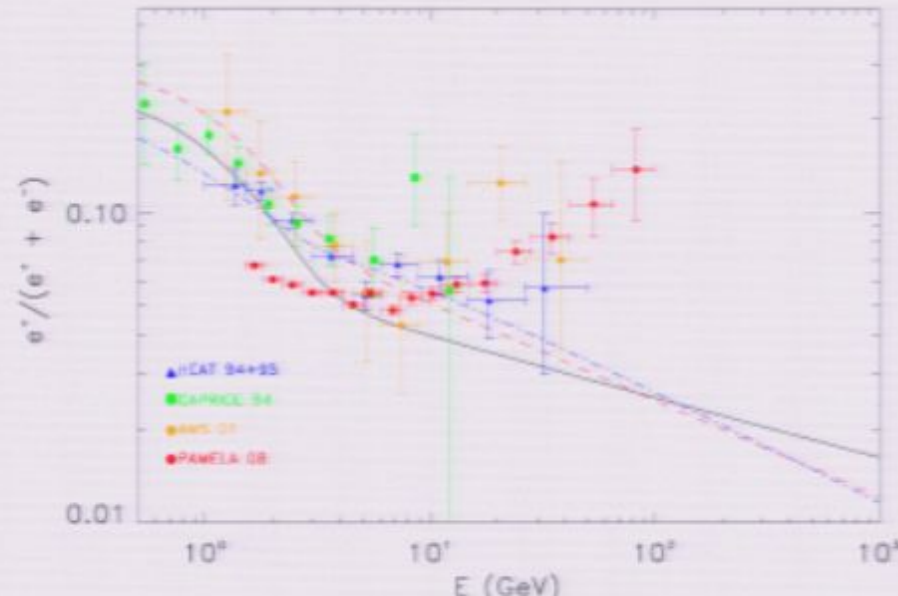
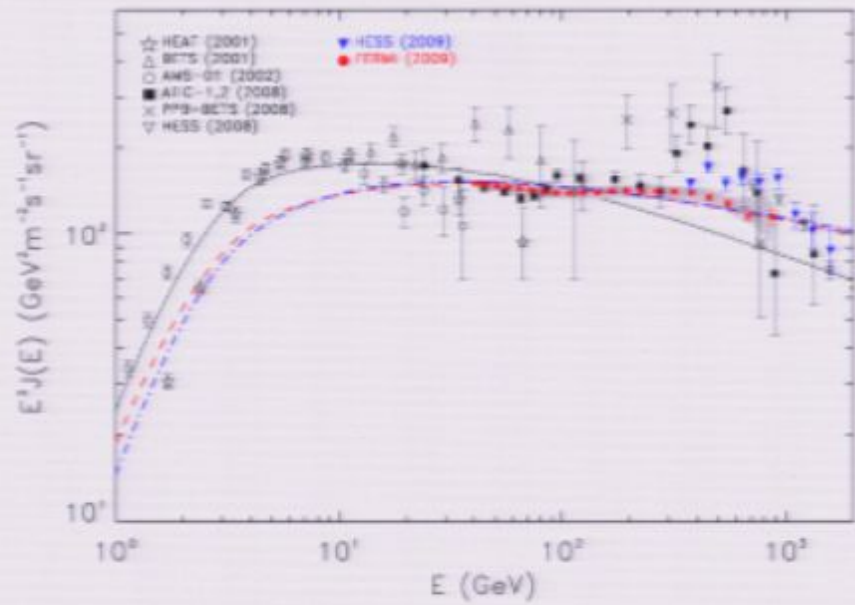


FERMI $e^+ + e^-$ flux

$$J_{e^\pm} = (175.40 \pm 6.09) \left(\frac{E}{1 \text{ GeV}} \right)^{-(3.045 \pm 0.008)} \text{ GeV}^{-1} \text{ m}^{-2} \text{ s}^{-1} \text{ sr}^{-1}$$

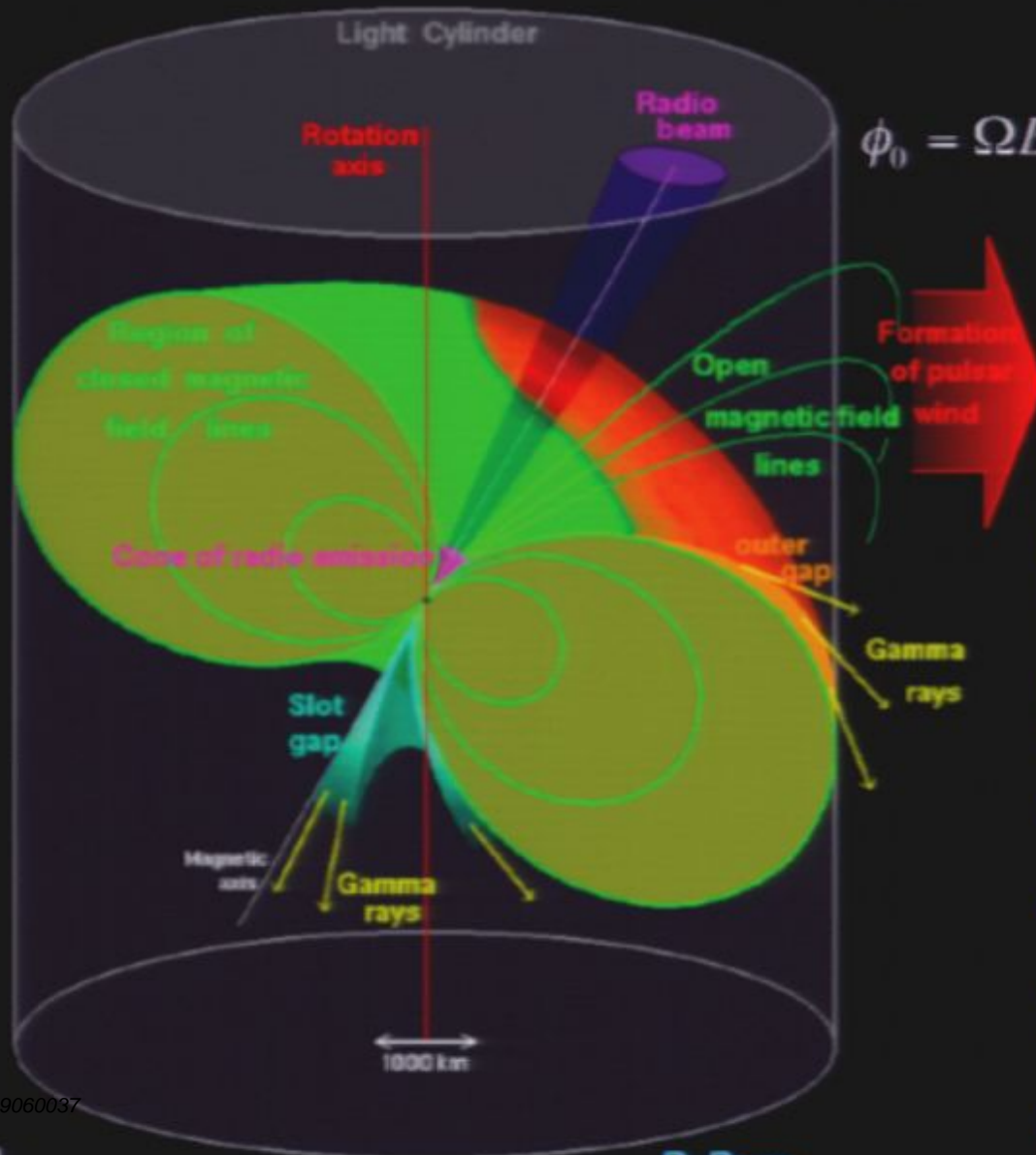


Model #	D_0 ($cm^2 s^{-1}$)	δ	z_h (kpc)	γ_0	N_{e^-} ($m^{-2} s^{-1} sr^{-1} GeV^{-1}$)	γ_0^p
0	3.6×10^{28}	0.33	4	2.54	1.3×10^{-4}	2.42
1	3.6×10^{28}	0.33	4	2.42	1.3×10^{-4}	2.42
2	1.3×10^{28}	0.60	4	2.33	1.3×10^{-4}	2.1

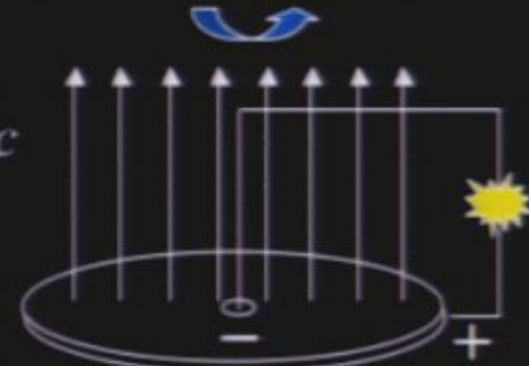


4) Astrophysical explanations of the PAMELA excess

Courtesy of Anatoly Spitkovsky – Princeton



$$\phi_0 = \Omega B a^2 / c$$



Faraday disk: unipolar induction

- *but pulsars are not in vacuum!*
- *Equator-pole potential difference ($10^{15}V$ for Crab)*
- *Charge extraction from the surface (E field \gg gravity)*
- *Currents, strong magnetization*
- *Corotating zone; Light cylinder*
- *Throwing away toroidal field – energy loss (Poynting flux)*
- *Plasma currents modify field. How can we model this?*

Galactic and local pulsars

D. Hooper, P. Blasi & P. D. Serpico, [arXiv:0810.1527](https://arxiv.org/abs/0810.1527)

S. Profumo, [arXiv:0812.4457](https://arxiv.org/abs/0812.4457)

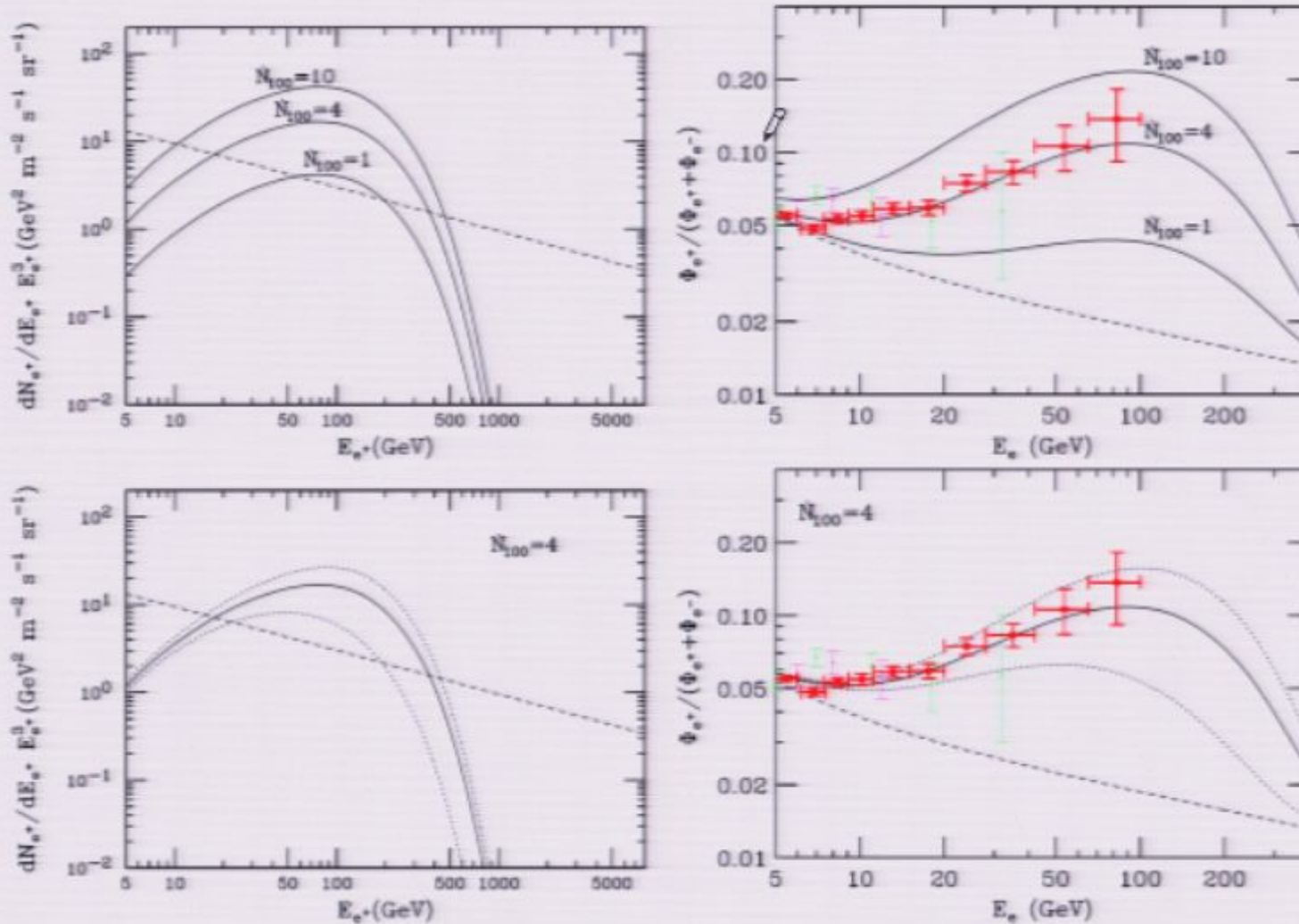
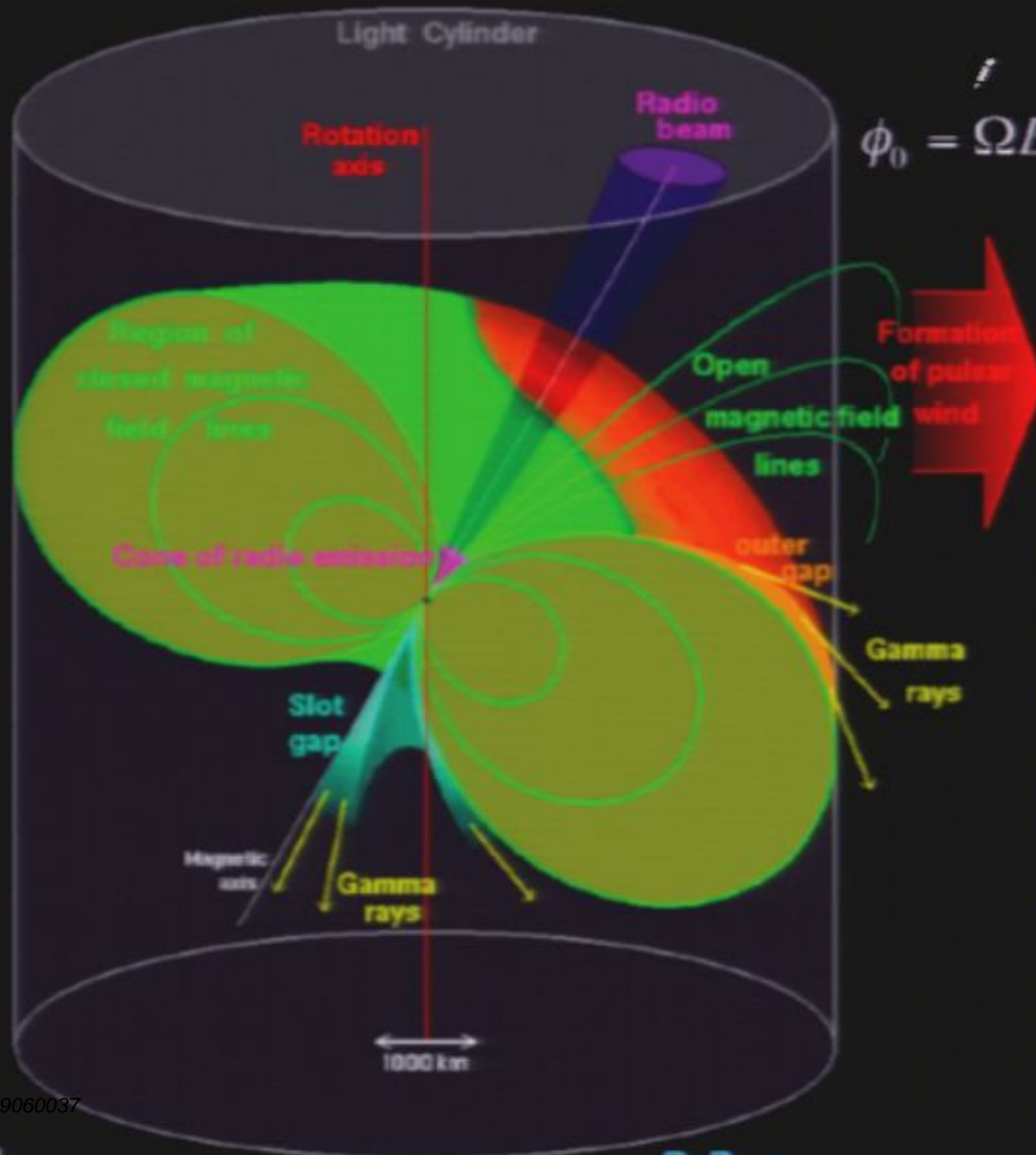


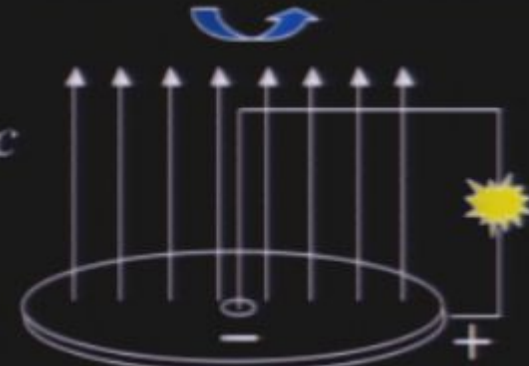
FIG. 1: The spectrum of cosmic ray positrons (left) and the positron fraction (right) resulting from the sum of all pulsars throughout the Milky Way. Also shown as a dashed line is the prediction for secondary positrons (and primary and secondary electrons in the right frames) as calculated in Ref. [27]. In the right frames, the measurements of HEAT [3] (light green and magenta) and measurements of PAMELA [2] (dark red) are also shown. We have used the injected spectrum reported in Eq. (7). In the lower frames, the upper (lower) dotted line represents the case in which the injection rate within 500 parsecs of the Solar System is doubled (neglected), providing an estimate the variance resulting from the small number of nearby pulsars contributing to the spectrum.

4) Astrophysical explanations of the PAMELA excess

Courtesy of Anatoly Spitkovsky – Princeton



$$\phi_0 = \Omega B a^2 / c$$



Faraday disk: unipolar induction

- *but pulsars are not in vacuum!*
- *Equator-pole potential difference ($10^{15}V$ for Crab)*
- *Charge extraction from the surface (E field \gg gravity)*
- *Currents, strong magnetization*
- *Corotating zone; Light cylinder*
- *Throwing away toroidal field – energy loss (Poynting flux)*

• *Plasma currents modify field. How can we model this?*

Galactic and local pulsars

D. Hooper, P. Blasi & P. D. Serpico, [arXiv:0810.1527](https://arxiv.org/abs/0810.1527)

S. Profumo, [arXiv:0812.4457](https://arxiv.org/abs/0812.4457)

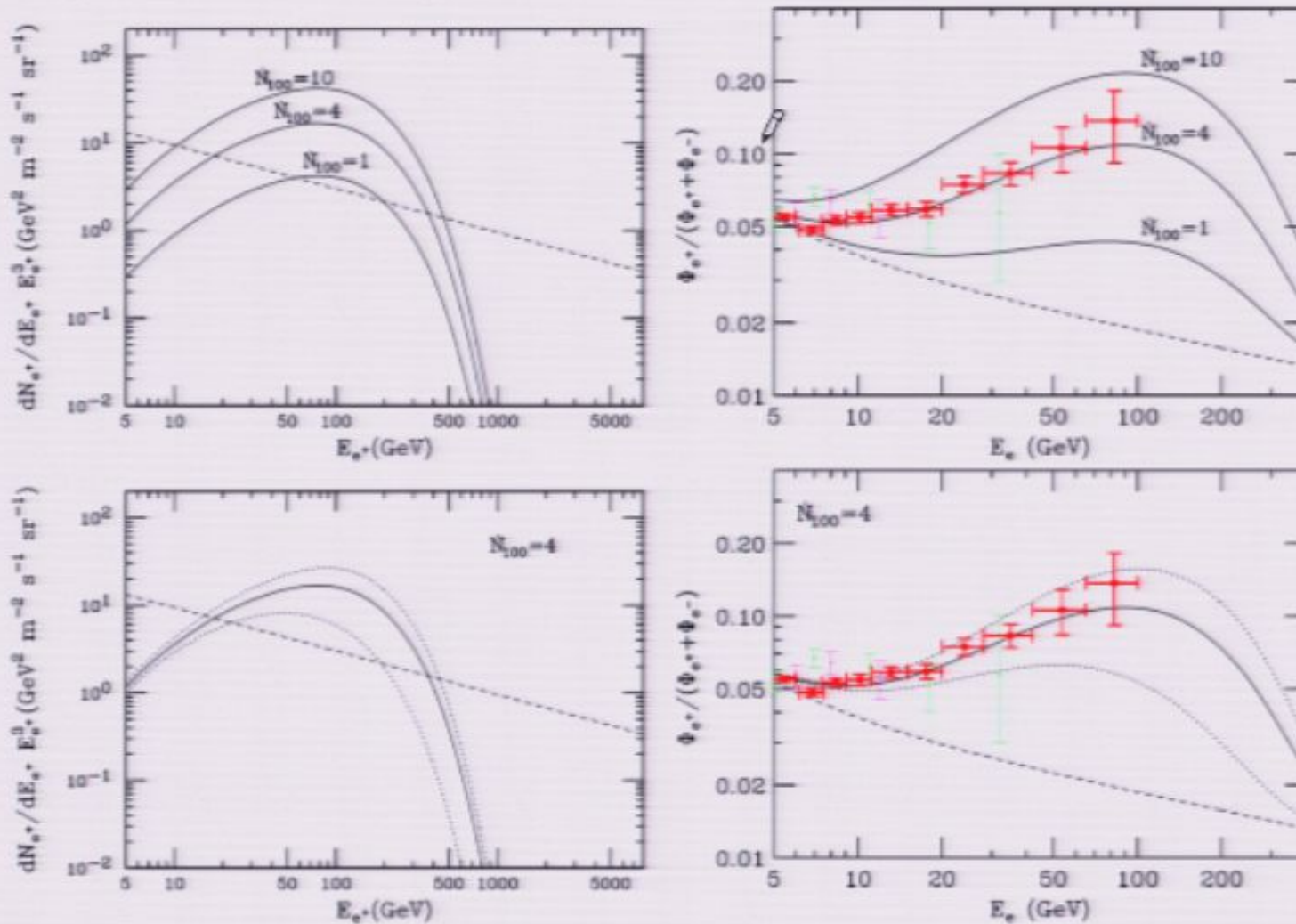


FIG. 1: The spectrum of cosmic ray positrons (left) and the positron fraction (right) resulting from the sum of all pulsars throughout the Milky Way. Also shown as a dashed line is the prediction for secondary positrons (and primary and secondary electrons in the right frames) as calculated in Ref. [27]. In the right frames, the measurements of HEAT [3] (light green and magenta) and measurements of PAMELA [2] (dark red) are also shown. We have used the injected spectrum reported in Eq. (7). In the lower frames, the upper (lower) dotted line represents the case in which the injection rate within 500 parsecs of the Solar System is doubled (neglected), providing an estimate of the variance resulting from the small number of nearby pulsars contributing to the spectrum.

Galactic and local pulsars

D. Hooper, P. Blasi & P. D. Serpico, [arXiv:0810.1527](https://arxiv.org/abs/0810.1527)

S. Profumo, [arXiv:0812.4457](https://arxiv.org/abs/0812.4457)

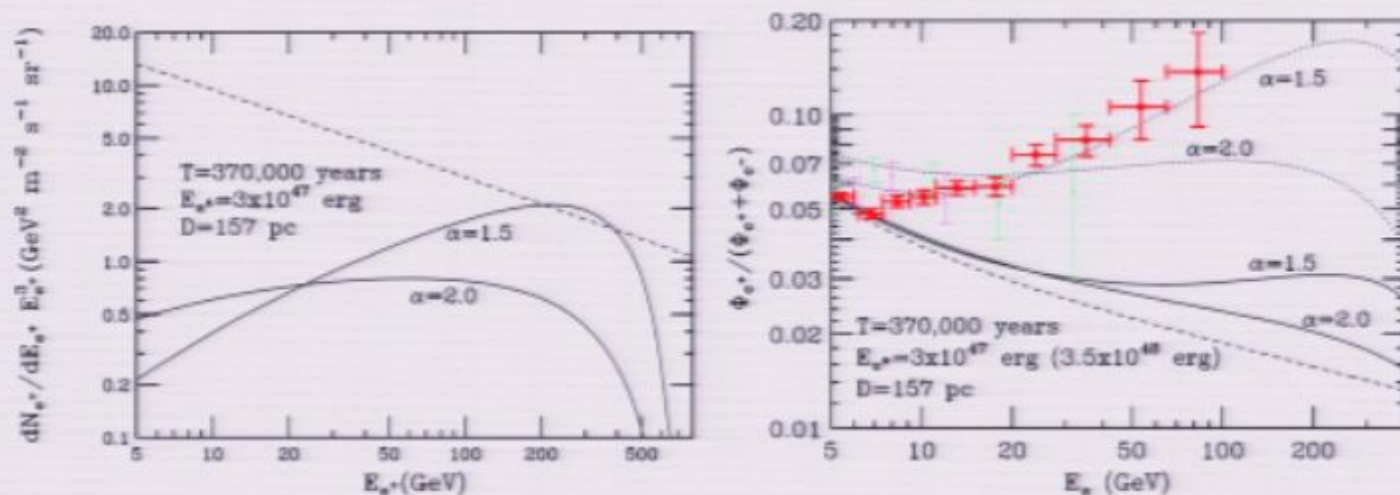


FIG. 2: The spectrum of positrons (left) and ratio of positrons to electrons plus positrons (right) from the pulsar Geminga, with the dashed lines as in Fig. 1. In the right frames, the measurements of HEAT [3] (light green and magenta) and measurements of PAMELA [2] (dark red) are also shown. Here we have used an injected spectrum such that $dN_{e^+}/dE_{e^+} \propto E_{e^+}^{-\alpha} \exp(-E_{e^+}/600 \text{ GeV})$, with $\alpha = 1.5$ and 2.2 . The solid lines correspond to an energy in pairs given by 3.5×10^{47} erg, while the dotted lines require an output of 3×10^{48} erg.

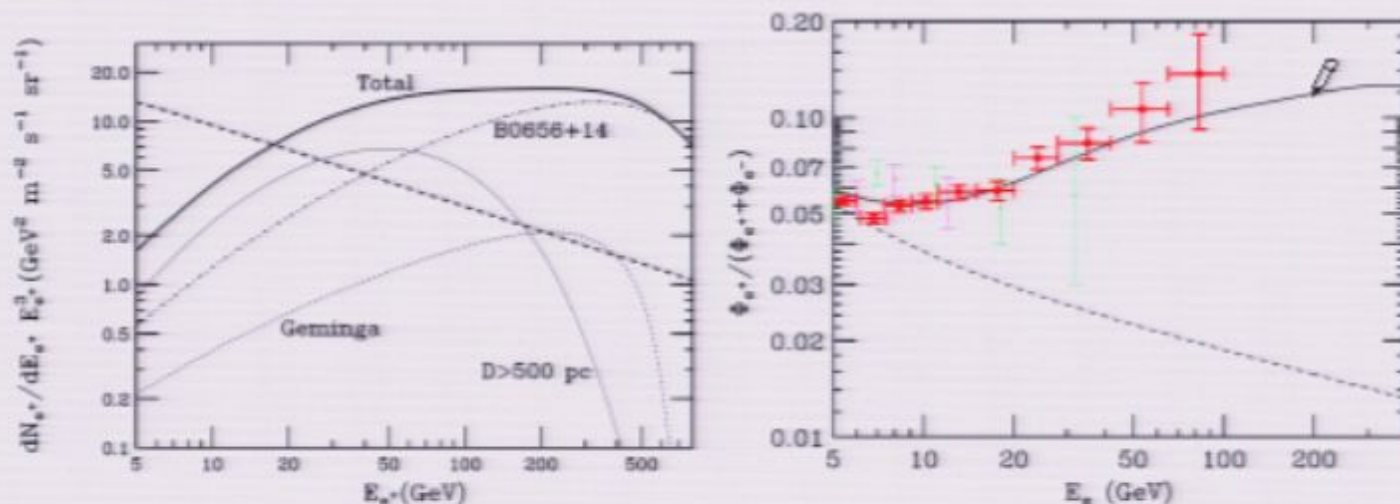


FIG. 4: The positron spectrum and positron fraction from the sum of contributions from B0656+14, Geminga, and all pulsars farther than 500 parsecs from the Solar System.

Galactic and local pulsars

D. Hooper, P. Blasi & P. D. Serpico, [arXiv:0810.1527](https://arxiv.org/abs/0810.1527)

S. Profumo, [arXiv:0812.4457](https://arxiv.org/abs/0812.4457)

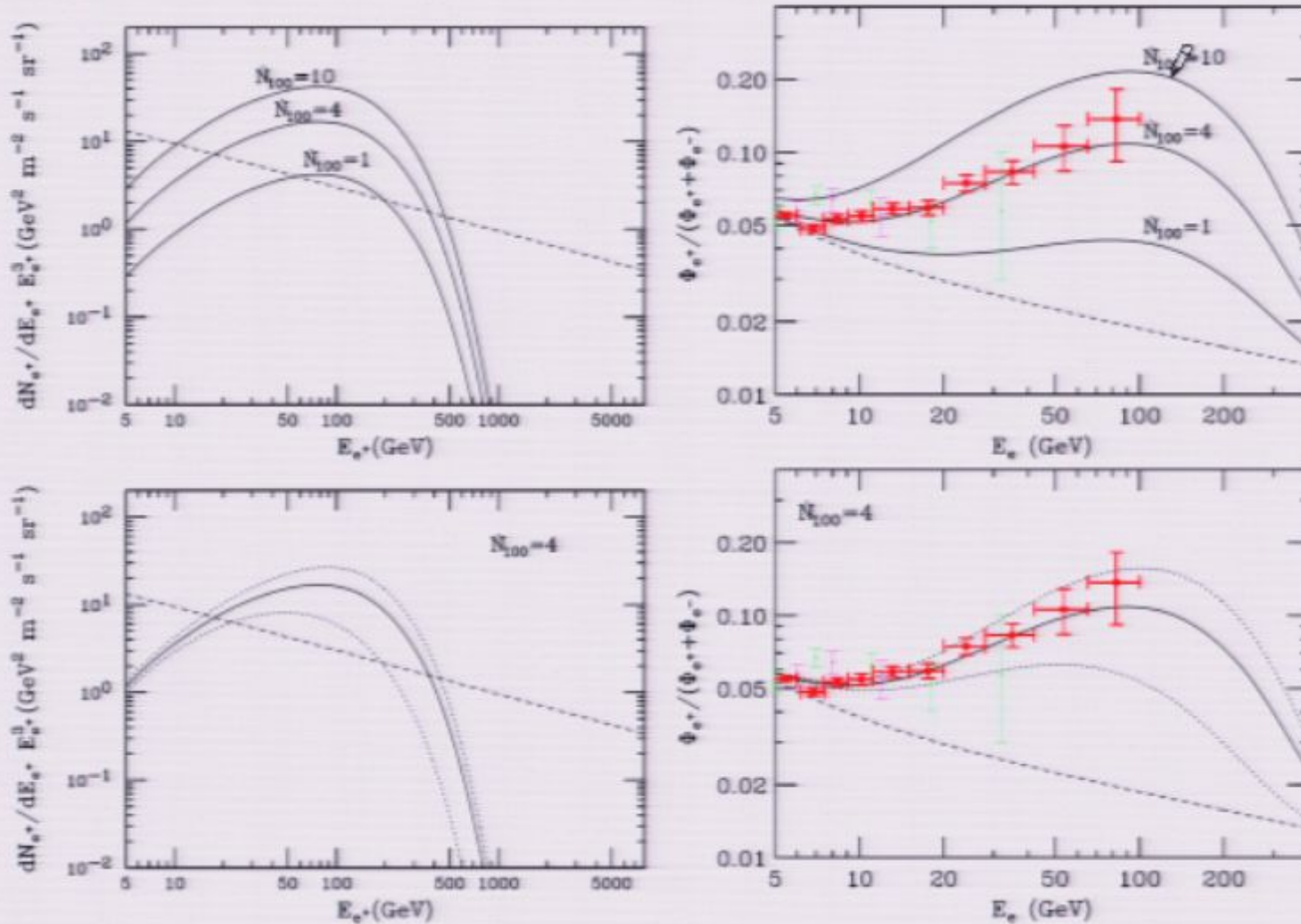
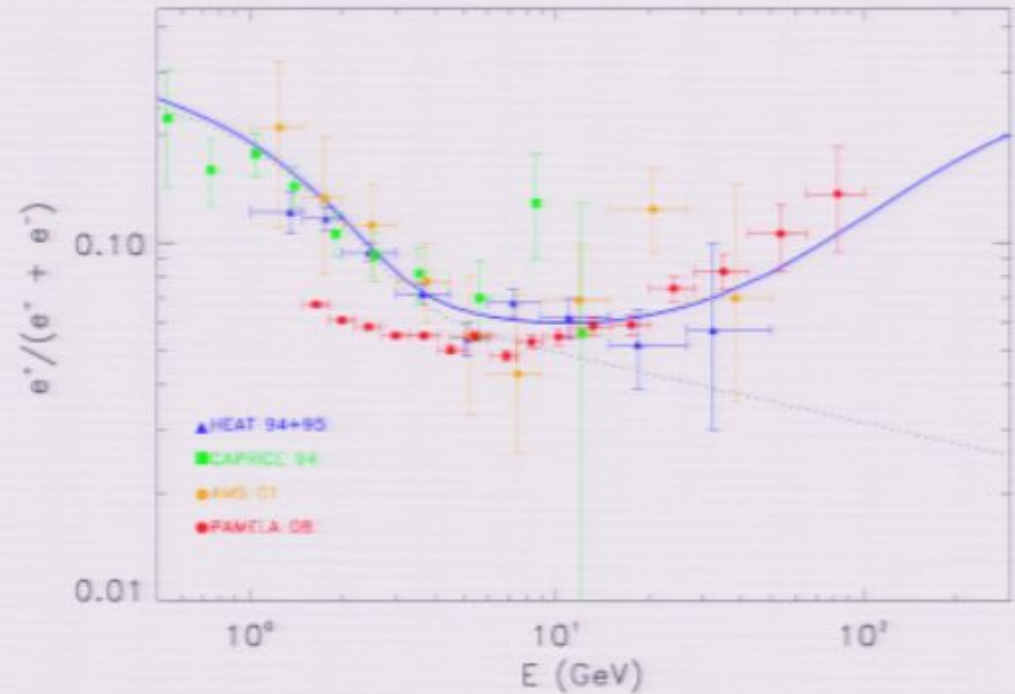
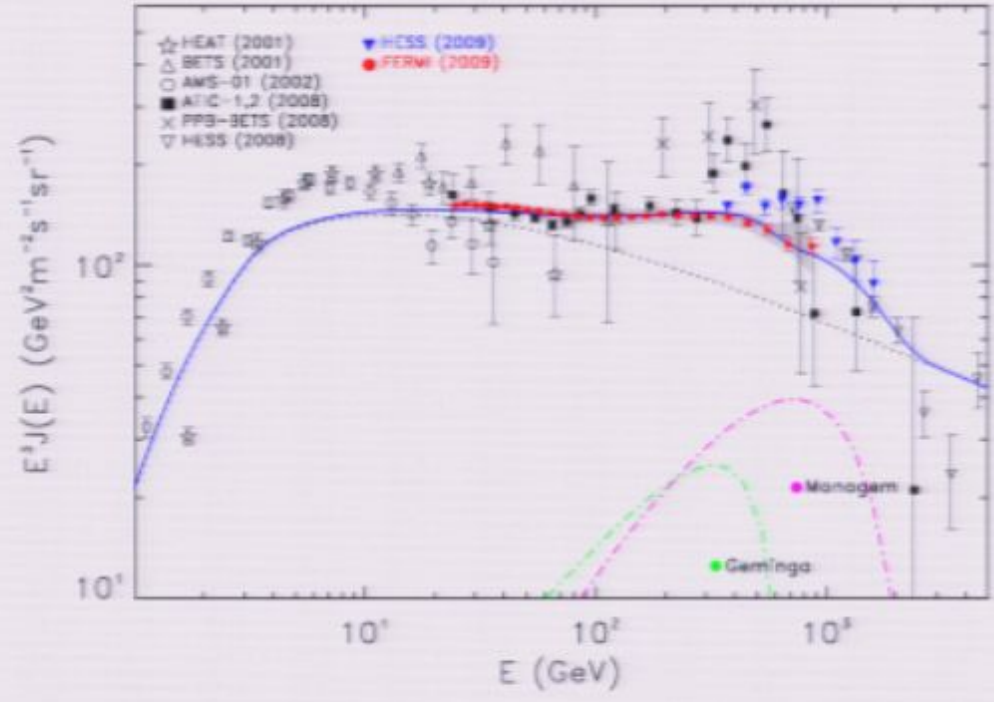


FIG. 1: The spectrum of cosmic ray positrons (left) and the positron fraction (right) resulting from the sum of all pulsars throughout the Milky Way. Also shown as a dashed line is the prediction for secondary positrons (and primary and secondary electrons in the right frames) as calculated in Ref. [27]. In the right frames, the measurements of HEAT [3] (light green and magenta) and measurements of PAMELA [2] (dark red) are also shown. We have used the injected spectrum reported in Eq. (7). In the lower frames, the upper (lower) dotted line represents the case in which the injection rate within 500 parsecs of the Solar System is doubled (neglected), providing an estimate the variance resulting from the small number of nearby pulsars contributing to the spectrum.



Galactic and local pulsars

D. Hooper, P. Blasi & P. D. Serpico, [arXiv:0810.1527](https://arxiv.org/abs/0810.1527)

S. Profumo, [arXiv:0812.4457](https://arxiv.org/abs/0812.4457)

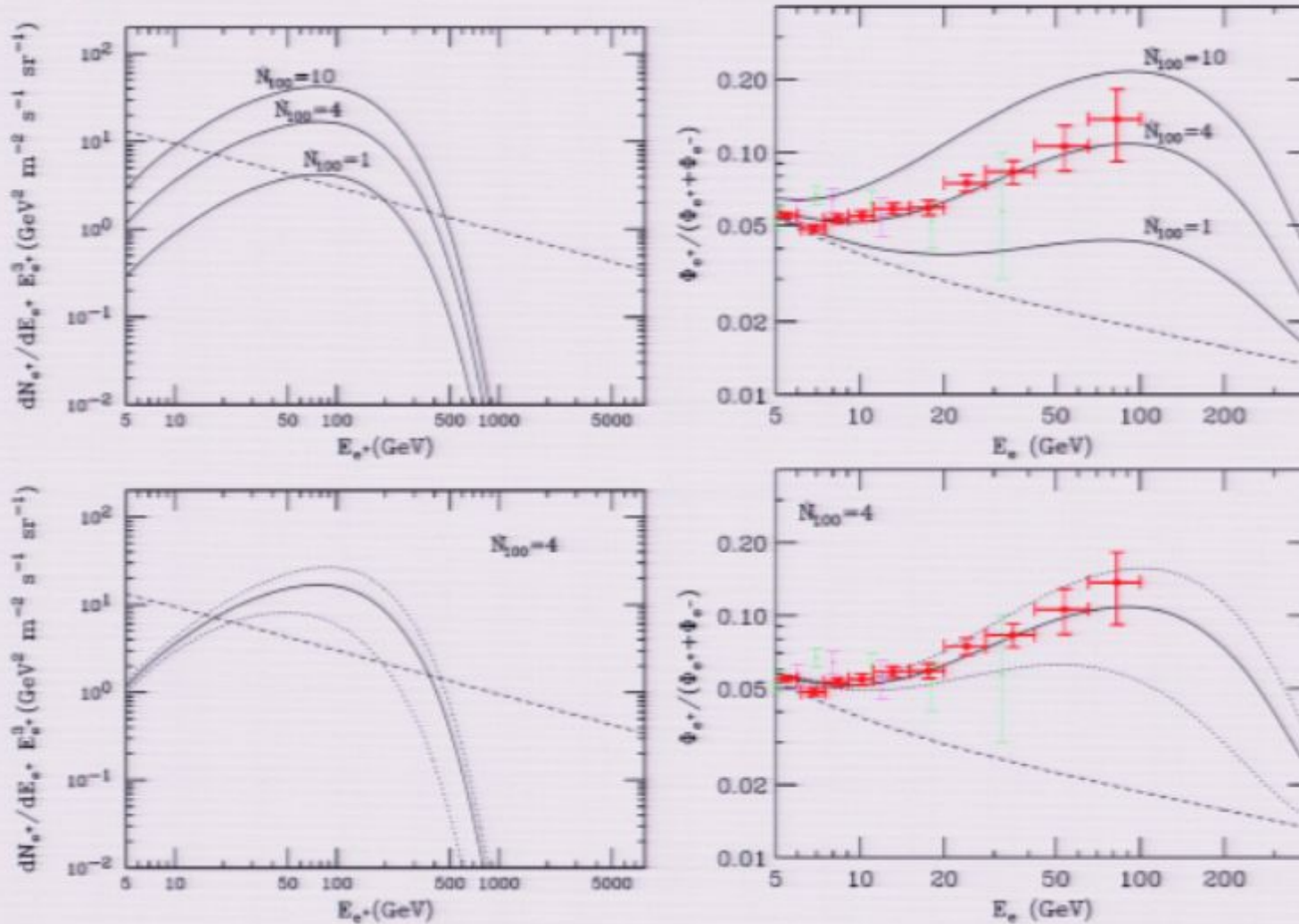
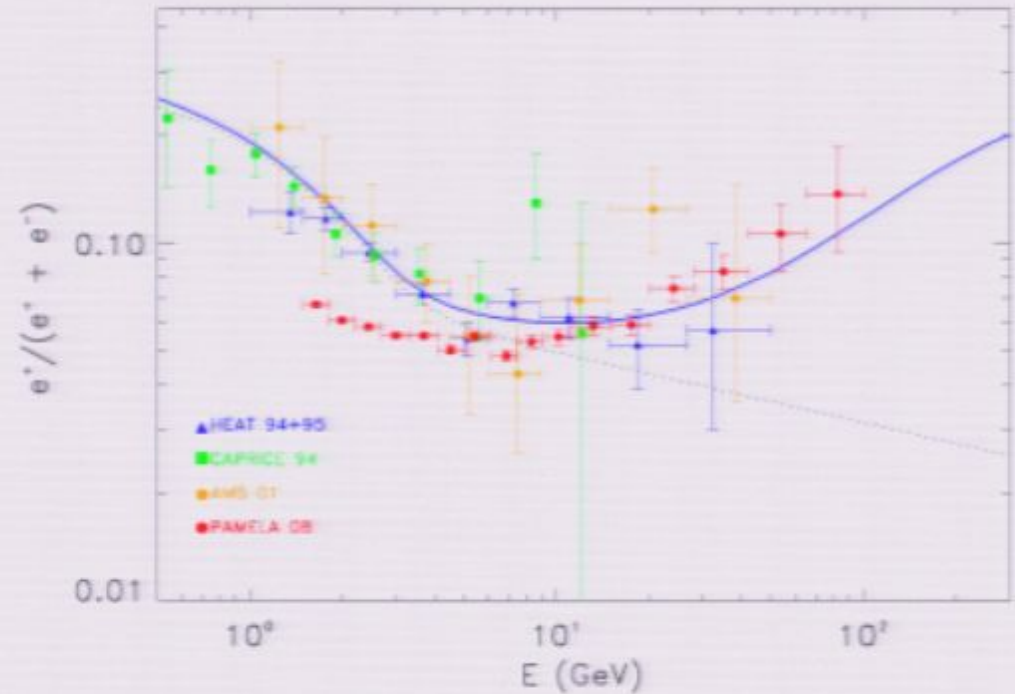
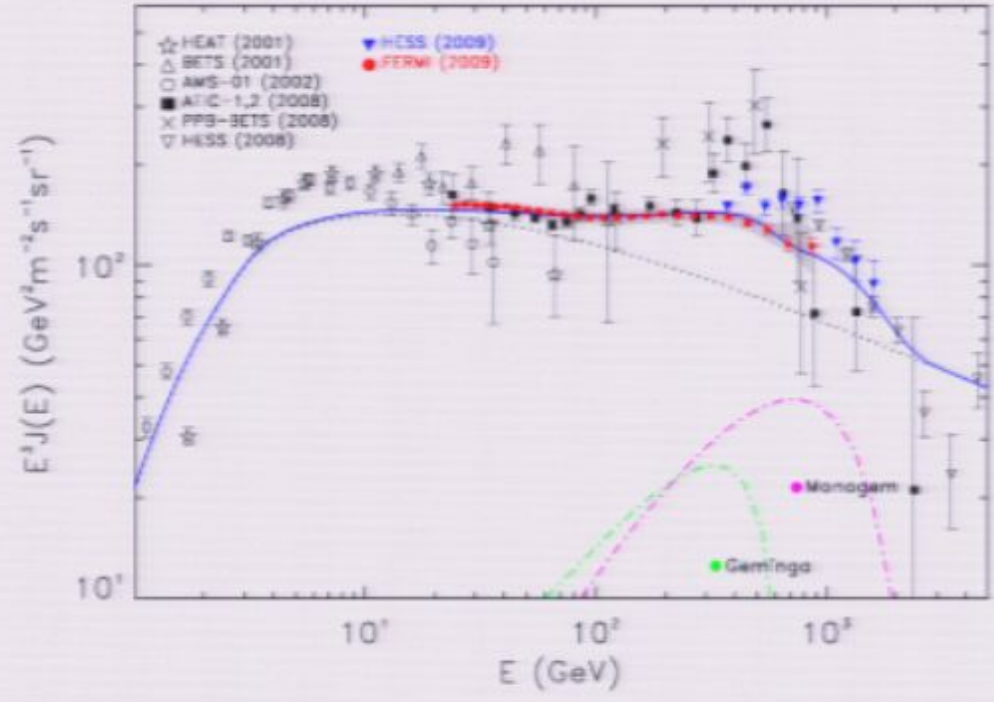
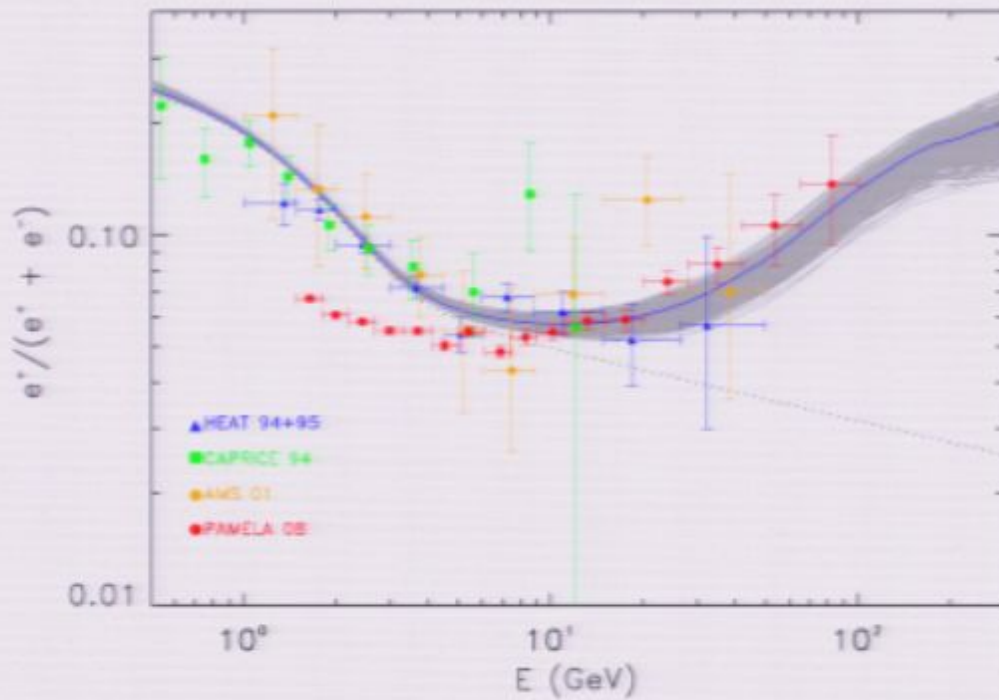
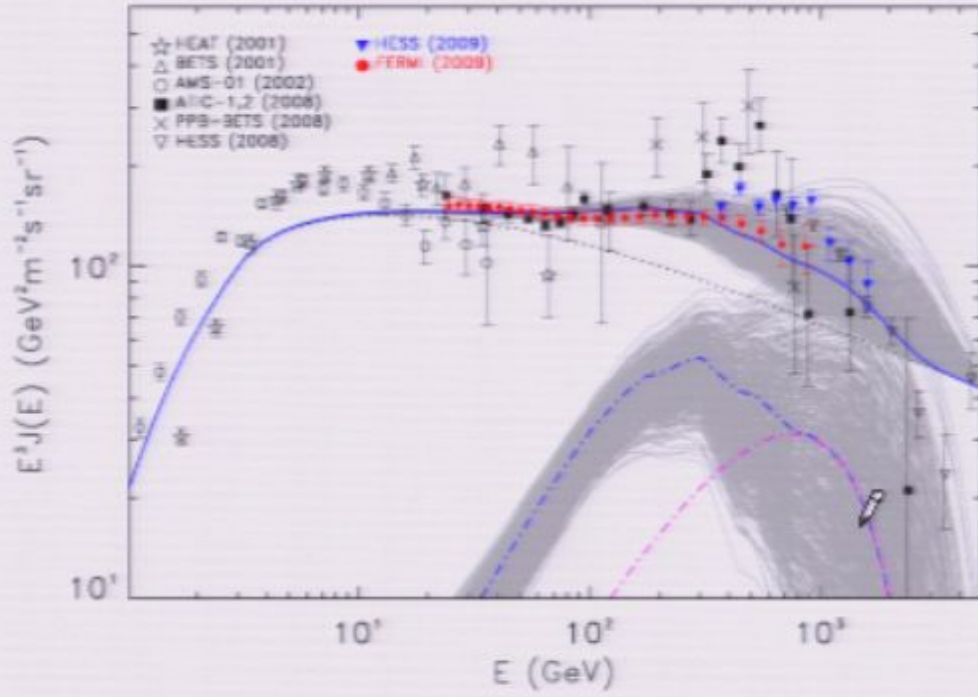


FIG. 1: The spectrum of cosmic ray positrons (left) and the positron fraction (right) resulting from the sum of all pulsars throughout the Milky Way. Also shown as a dashed line is the prediction for secondary positrons (and primary and secondary electrons in the right frames) as calculated in Ref. [27]. In the right frames, the measurements of HEAT [3] (light green and magenta) and measurements of PAMELA [2] (dark red) are also shown. We have used the injected spectrum reported in Eq. (7). In the lower frames, the upper (lower) dotted line represents the case in which the injection rate within 500 parsecs of the Solar System is doubled (neglected), providing an estimate the variance resulting from the small number of nearby pulsars contributing to the spectrum.

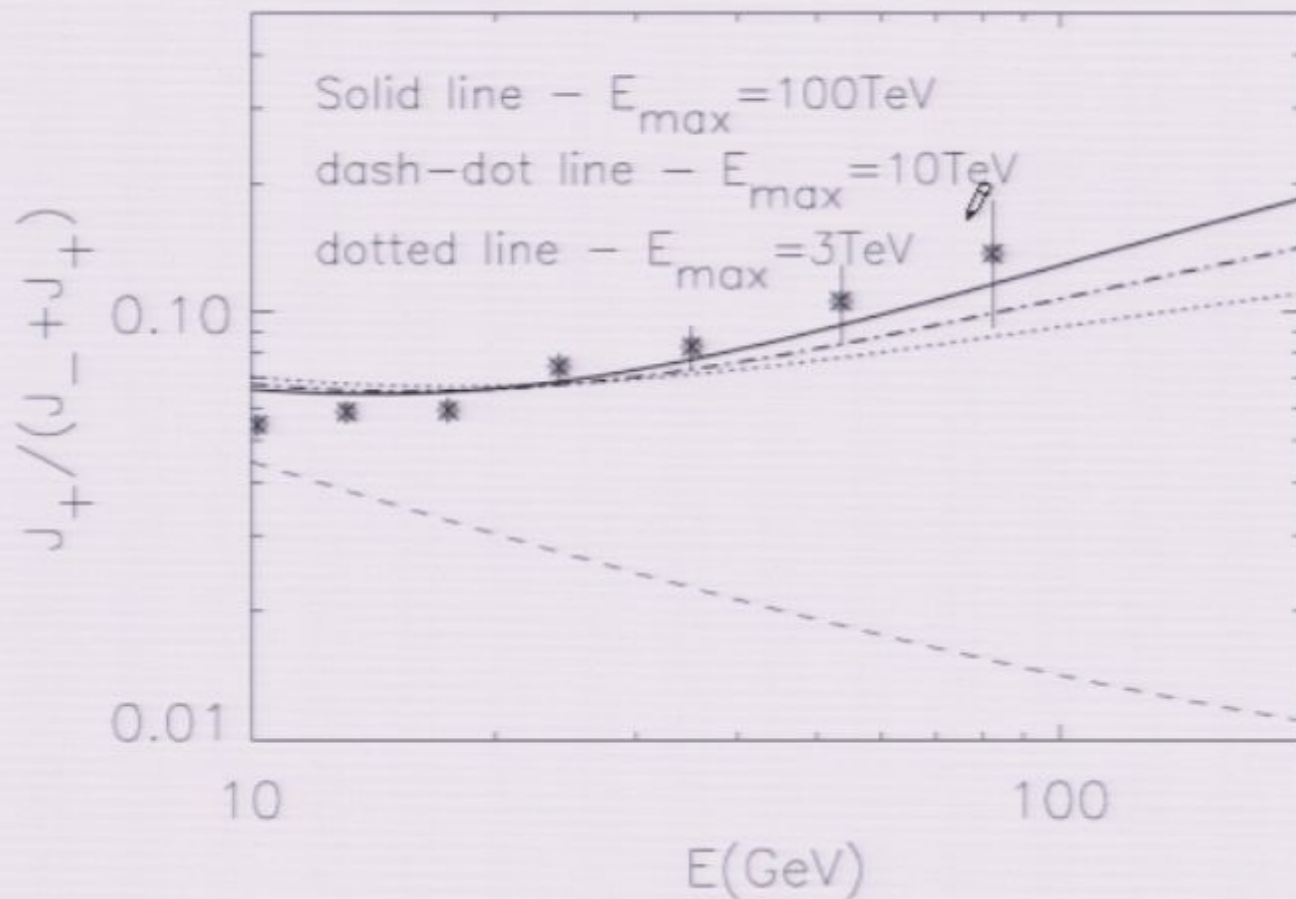




The origin of the positron excess in cosmic rays

Pasquale Blasi

Acceleration **and** spallation in SN shock waves



B/C and \bar{p}/p should increase at high E

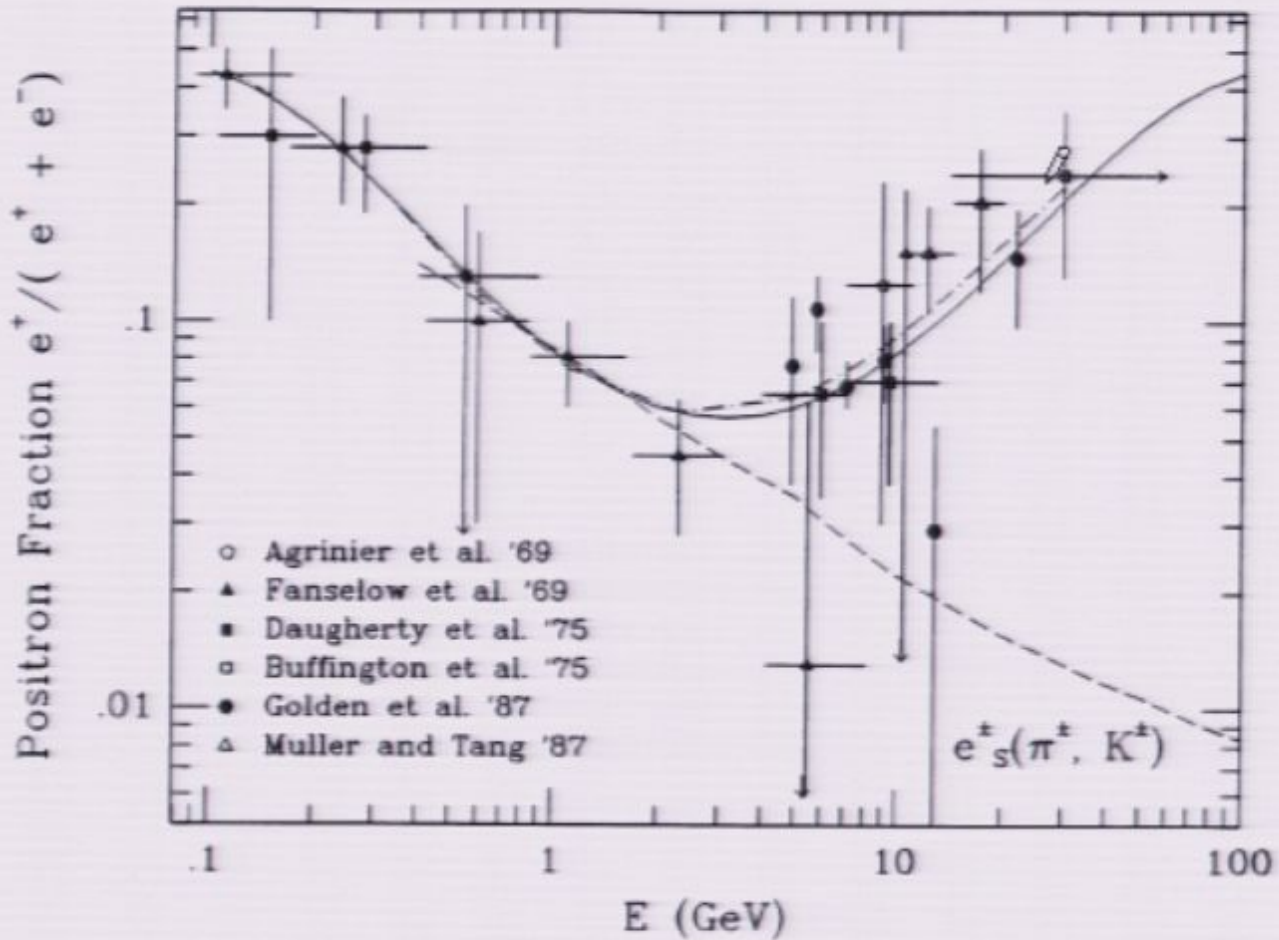
THE NATURE OF THE COSMIC-RAY ELECTRON SPECTRUM, AND SUPERNOVA REMNANT CONTRIBUTIONS

AHMED BOULARES

Physics Department, Space Physics Laboratory, University of Wisconsin-Madison

Received 1988 October 24; accepted 1988 December 29

THE ASTROPHYSICAL JOURNAL, 342:807-813, 1989 July 15





PI_090611.ppt

28	29	30
31		33
34	35	36
37	38	39

Palette de mise en forme

Présentation

Diapositive en cours

Mise en page : Vide

Transition : Sans transition

Thème

Modèles : Nouvelle présentat

Couleurs :

sar_9912.pdf	IB_torsten_C
989ApJ_342_807.pdf	cirelli_080
tu_9902162.pdf	cirelli_080
	barger_080
mp_0812_3202.pdf	hooper_080
tu_0901_1520v1.pdf	huh_0809
	sommerfeld_10_0
ma_radio_0811_3744.pdf	silk_sommer

T. Bringmann & P. Salati (2006)

BESS 95+97 BESS 98 AMS 98 CAPRICE 98

$\delta = 0.46$ to 0.85

B/C measurements @ high E

A. Castellina & F. Donato, *Astropart. Phys.* **24** (2005) 146-159

SECONDARY SPECTRUM

PROPAGATION UNCERTAINTY BAND

Solar Minimum with $\phi_p = 500$ MV

Scan with B/C compatible data and ALL δ

